Formulation of Phytochemicals in Lipid-Based Nanoparticles for Melanoma Treatment

by

Ahmed Abdullah Al Saqr

A dissertation submitted to the Graduate Faculty of
Auburn University
in partial fulfillment of the
requirements for the Degree of
Doctor of Philosophy
Auburn, Alabama
May 6, 2019

Keyword: Microemulsion, Proniosome, Liposome, Melanoma, Cancer treatment

Approved by

Jayachandra Babu Ramapuram, Chair,
Professor of Drug Discovery and Development
Robert D Arnold,
Professor of Drug Discovery and Development
William R Ravis ,
Professor of Drug Discovery and Development
Daniel L Parsons,
Professor of Drug Discovery and Development
Satyanarayana R. Pondugula,
Associate Professor of Anatomy, Physiology and Pharmacology

Abstract

Melanoma is one of the most common and aggressive types of cancer with high mortality. Current treatment is ineffective in preventing relapse of cancer. It also suffers from serious systemic side effects because of the non-selective action on normal cells. Lipid-based nanoparticles are a promising drug delivery system for chemotherapy due to their easy preparation and modification, biocompatibility, enhanced permeability and retention, and reduced toxicity. In this dissertation, different lipid-based nanoparticles that include proniosomes, microemulsions and liposomes were developed for treatment of melanoma.

Topical/transdermal drug delivery for treatment of melanoma represents an attractive alternative to conventional systemic delivery methods because of lack invasiveness, easy targeted administration, good drug distribution and biostability with controlled drug release. One problem with topical delivery, however, is that the skin is highly impermeable membrane barrier which limits the number of drugs that could be delivered through the skin. In the past few decades, various approaches have been used to improve drug permeation across the skin with use of techniques such as microneedles, iontophoresis, sonophoresis, thermal ablation, chemical penetration enhancers, and special formulations. Formulation approaches such as microemulsions and proniosomes have been used to improve skin permeation for several drugs.

In this work, we developed pharmacological formulations for three antioxidant compounds that include hydroxytyrosol, DAB, and hispolon. We also investigated the anticancer effects of these formulations in cell culture. Further, we investigated the

anticancer effects of a formulation that involved a combination of hispolon and doxorubicin, a chemotherapeutic drug widely used in treatment of several common epithelial cancers.

Hydroxytyrosol is a well-known anti-oxidant effective in melanoma. Proniosomes were prepared as transdermal delivery system for hydroxytyrosol by a coacervation method. The optimized formulation of 1% (w/w) hydroxytyrosol, 45% (w/w) span 60, 5% (w/w) cholesterol, 40% (w/w) ethanol and 9% (w/w) PBS showed the highest skin permeation compared to control. These proniosome formulations could be a promising system for transdermal delivery of hydroxytyrosol.

Next, microemulsions were developed for enhanced transdermal delivery of DAB compound. Microemulsion formulations were selected based on the pseudo-ternary phase diagram and the pH of the selected formulations ranged from 5.26 to 6.5. Optimized formulations showed globule size of <50 nm and a polydispersity index of 0.31. There was a significant decrease in melanoma cell proliferation with all DAB microemulsions compared to the control. The IC50 for all the microemulsion formulations were 50-60-fold lower than free drug.

The anti-cancer activity of hispolon has been reported in different types of cancer but not in melanoma. The cytotoxicity study of hispolon formulation in this study showed effective suppression of cell proliferation. We also showed that hispolon is a potent inducer of reactive oxygen species and modulator of several apoptotic genes. Hispolon treatments inhibited the expression of bcl-2 gene, an anti-apoptotic factor, and promoted the expression of Bax gene, a pro-apoptatic factor. It also enhanced expression of caspase enzymes (markers for apoptosis induction). It also inhibited complex I and IV.

Complex I is required for cell survival while complex IV (or cytochrome c oxidase), catalyzes the final step in mitochondrial electron transfer chain, and is considered as one of the major regulation sites for oxidative phosphorylation. Hispolon also stimulated nitrite content and lipid peroxidation levels. All these processes are associated with cell death or apoptosis.

The therapeutic use of doxorubicin is limited due to chronic doxorubicin induced cardiac toxicity and development of multidrug resistance in melanoma cells. To overcome these problems, we developed a combination therapy of doxorubicin and hispolon liposomes. The liposome formulations provided a mean diameter less than 100 nm with a narrow size distribution and 90% recovery for both drugs. Combination of doxorubicin liposomes with hispolon liposomes enhanced cell cytotoxicity and apoptosis more than either single treatment. The study of the doxorubicin and hispolon liposome combination provides a strong evidence for future potential use of this formulation for effective treatment of patients with melanoma.

Acknowledgments

I am very grateful for my dissertation committee members, Dr. Jay Ramapuram (Major Advisor), Dr. Robert Arnold, Dr. William Ravis, Dr. Daniel Parsons and Dr. Satyanarayana Pondugula. They were very kind and supportive in many ways. I have learned a great deal from their knowledge, I appreciate their extensive efforts to help students. I would like to express my gratitude to Dr. Jay Ramapuram for his support in related work, for his patience, motivation, and knowledge. His guidance helped me through my research work as well as the writing of this dissertation. Also, I would like to thank Dr. Mahmoud Mansour for serving as an outside reader of my dissertation. Special thanks to Jennifer Johnson for her substantial help and guidance. I would like to express appreciation to my parents for their support and help throughout the time pursuing my doctoral degree. They have helped me to get over many challenges especially through tough times either financially or emotionally. Also, I would like to extend the appreciation to my wife and kids for providing me with unfailing support and continuous encouragement. I would like to thank my friends and laboratory mates Mohammad Aldawsari, Hamad Alrbyawi, Haley Shelley, Manjusha Annaji, Ishwor Poudel for being kind, honest and helpful. Finally, I would like to thank Saudi government and Prince Sattam bin Abdulaziz University for their financial support through my scholarship assistance.

Table of Contents

List of Figures

List of Tables

Chapter 1 : Introduction to Skin Delivery and Lipid-Based Nanoparticle for Melanoma Treatment

1.1. Introduction to skin delivery

Skin is the largest organ covering the whole body which can protect the body from foreign injury and infection, maintaining fluid retention and controlling body temperature. It has a surface area of 1.8 cm^2 and composes 8% of the total body mass of an adult (Cevc & Vierl, 2010). It is composed of three distinct layers: the epidermis, dermis and subcutaneous fat. The epidermis is the outer most impermeable layer (Figure 1.1). The epidermis is composed of five layers which are the stratum germinativum, stratum basale and stratum spinosum, stratum granulosum, stratum lucidum in thick skin and stratum corneum. The stratum corneum is the outer layer of the skin and is composed of large, flat, polyhedral, plate-like envelopes filled with keratin. Although the stratum corneum is only 20 to 25 μm thick, it provides the major barrier for drug absorption. Thus, it is the rate limiting step in transdermal drug delivery (Morrow, McCarron, Woolfson, & Donnelly, 2007).

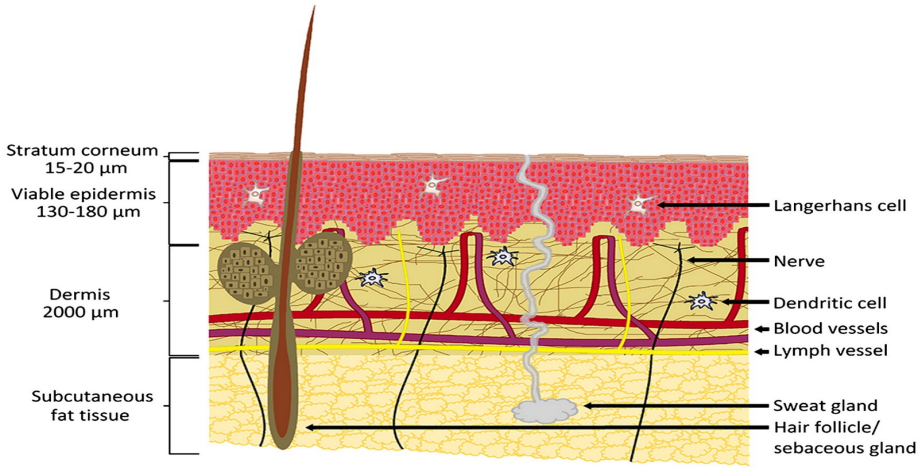

Figure 1-1 Anatomy of the skin. Reproduced with permission from (van Der Maaden, Jiskoot, & Bouwstra, 2012)

There are a number of pathways by which drugs can cross the stratum corneum. These include the intercellular pathway, transcellular pathway and trans-appendage pathway (Figure 1.2). The intercellular pathway is a more common way in which drug molecules overcome the stratum corneum by passing between keratinocytes. The transcellular pathway is a more direct method in which the drug passes through keratinocytes. This route is shorter, but offers significant permeation resistance exit because molecules have to cross both lipophilic and hydrophilic barriers. The trans-appendage pathway is a minor pathway where drug molecules pass through the hair follicles, sweat ducts, sebaceous glands which occupy only 1% of the total surface area of the skin (Ali, Shabbir, & Shahid, 2015; Desai, Patlolla, & Singh, 2010).

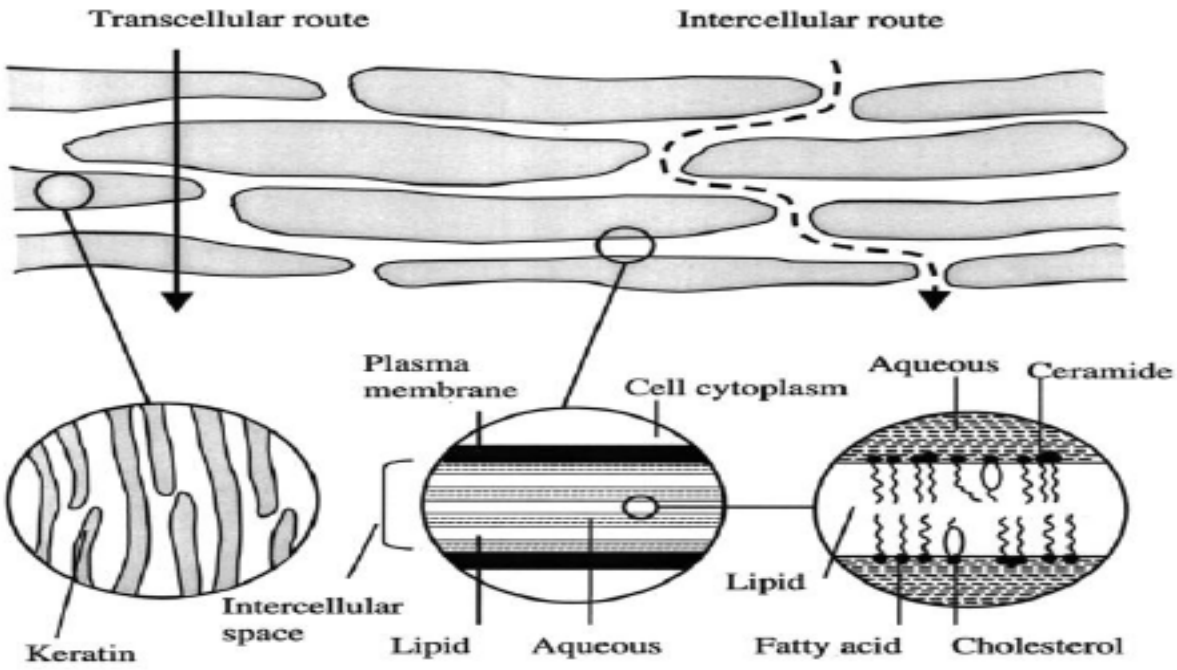

Figure 1-2 Possible drug penetration routes across human skin.
Reproduced with permission from (Moghimi, Williams, & Barry, 1996)

1.2. Transdermal drug delivery

Transdermal drug delivery is one of the oldest methods used to deliver drugs to treat various diseases. The delivery of drugs through the skin offers many advantages such as the avoidance of first past metabolism and GI tract degradation and metabolism. It provids constant blood level for drug with a narrow therapeutic window which will minimize the risk of toxic effects. It is suitable for patients who have difficulty swallowing or are unconscious. It is noninvasive alternative to parenteral injections (Alkilani, McCrudden, & Donnelly, 2015; Isaac & Holvey, 2012). For effective transdermal delivery, the drug molecular weight should be below 500 Da, with balanced lipophilicity and hydrophilicity (log p between 1 and 3). The drug should also have a melting point less than 200ºC (Bos & Meinardi, 2000; Xie et al., 2016). There are a limited number of transdermal products on the market such as fentanyl, nitroglycerin, estradiol, ethinyl estradiol, norethindrone acetate, testosterone, clonidine, nicotine, lidocaine, prilocaine, scopolamine, norelgestromin and oxybutynin (Prausnitz & Langer, 2008).

Topical and transdermal drug delivery is limited to drugs that are potent and require smaller doses, preferably less than 20 mg. There are many methods that can be used to modify the barrier properties of the stratum corneum. These can be divided into passive or active methods.

The active methods include ultrasound, electrical assisted methods (electroporation and iontophoresis), thermal methods (laser), and mechanical methods (microneedle and tape stripping) (Xie et al., 2016). All the active methods improve the drug permeation by physically disrupting the stratum corneum or forcing the drug molecules to pass through skin. The main advantage of active method is that it expands

the range of drugs that can be delivered through the skin. Furthermore, these methods provide more reproducible and controlled drug delivery since the lag time would be minimal to achieve an effective plasma concentration (Alkilani et al., 2015).

One of the most used passive methods is the use of chemical penetration enhancers that facilitate drug permeation across the skin by increasing drug partitioning into the stratum corneum. Penetration enhancers can help drug cross the skin by either increasing stratum corneum lipid bilayers fluidity, interaction with intercellular proteins, disruption of the intercellular lipids, or increase in stratum corneum hydration (Desai et al., 2010). The ideal chemical penetration enhancer should be safe and non-toxic, nonirritant and pharmacologically inert (Raut, Chougule, Dongare, Nemade, & Devmore, 2014). There are many penetration enhancers such as ethanol, surfactants, fatty acids, fatty acid esters, fatty alcohols, pyrrolidines, phospholipids, and terpenes (Lopes, J Garcia, & LB Bentley, 2015). In addition to chemical penetration enhancers, colloidal carriers such as microemulsions and vesicular particulate carriers such as proniosomes have been used for topical and transdermal delivery (Heuschkel, Goebel, & Neubert, 2008; Indira & Shankar; Singh, Chaudhari, Singh, & Kunwarpuriya, 2015).

1.2.1. Proniosomes for enhanced transdermal delivery

Proniosomes are non-ionic based surfactant vesicles which have the ability to entrap both hydrophilic and lipophilic drugs. Proniosomes can be converted to niosomes by water addition (Radha, Rani, & Sarvani, 2013). Proniosomes overcome problems of niosome physical stability such as aggregation, fusion and leaking. They are also more convenient in transportation, distribution, storage and dosing (Yasam, Jakki, Natarajan, & Kuppusamy, 2014). Proniosomes are becoming promising skin delivery systems due

to their ability to enhance drug penetration, provide sustained drug release, increase drug stability, and their ability to carry both hydrophilic and lipophilic drugs (Singla, Hari Kumar, & Aggarwal, 2012).

The proniosomes may require hydration before drug release and permeation through the skin. There are several mechanisms by which proniosomes can improve the drug permeation across the skin as described in Figure 1.3. The permeation enhancer effect and direct vesicle fusion with stratum corneum may play a major role in the enhanced permeation of drugs loaded in proniosomes.

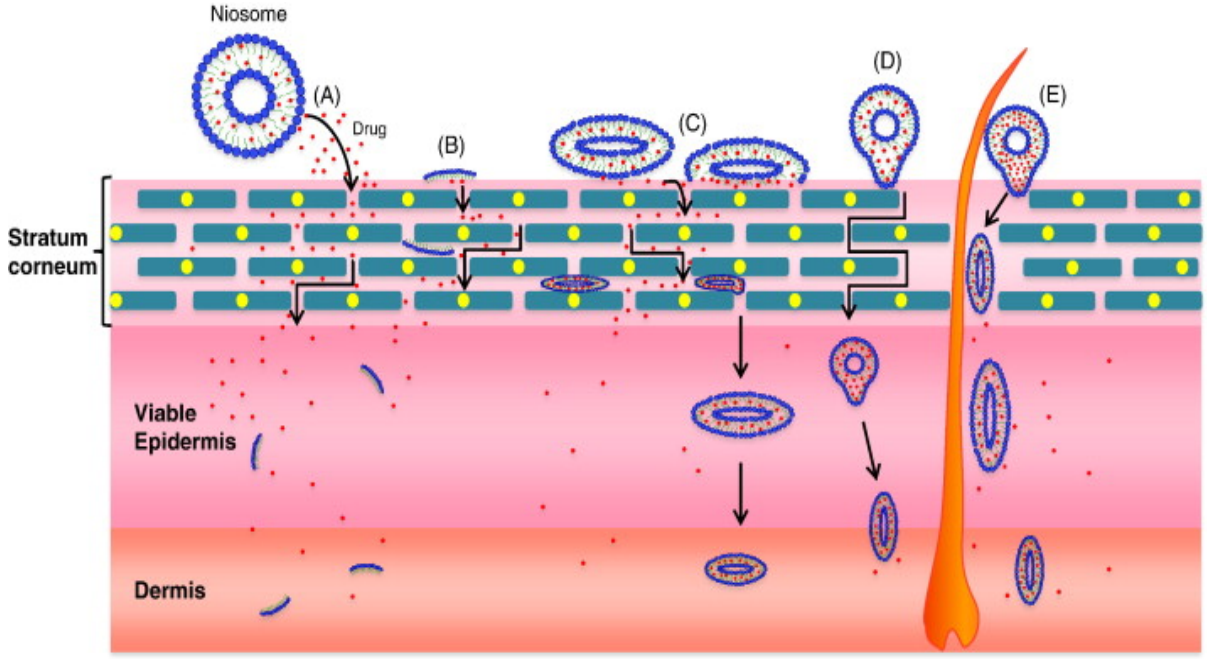

Figure 1-3 Possible permeation pathways for proniosomes drug delivery. (A) drug molecules are released by niosomes; (B) niosome constituents act as penetration enhancer; (C) niosome adsorption and/or fusion with stratum corneum; (D) intact niosome penetration through the intact skin; (E) niosome penetration through hair follicles and/or pilosebaceous units. Reproduced with Permission from (Marianecci et al 2014)

There are three methods to prepare proniosome. These include the coacervation, slurry, and spray coating method as presented in Figure 1.4 (Khatoon et al., 2017). In coacervation, lipids, drug, and surfactants are mixed and heated in a dry wide mouthed glass container in a water bath at 60-70 ºC until surfactant mixture dissolves. The solvent is then added and warmed followed by addition of the aqueous phase. The resultant mixture is allowed to cool overnight to obtain a proniosomal gel. In the slurry method, the drug carrier, surfactant solution, and organic solvent is used to obtain a slurry in the round bottom flask. The slurry is then dried by vacuum to get a free flowing powder. The powder obtained by this method should be stored in 4ºC. In the spray coating method, the proniosome is prepared by dissolving the surfactant in an organic solvent containing drug followed by evaporating the solvent. The surfactant in this case forms a thin film on the surface of the carrier.

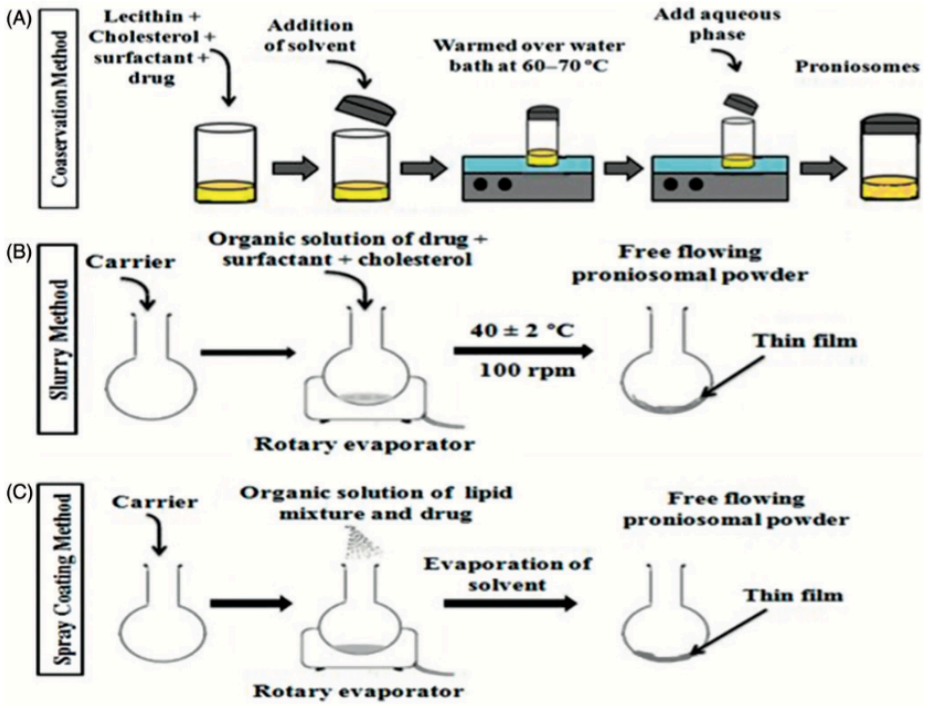

Figure 1-4 Methods of preparing proniosomes (khatoon et al, 2017)

Proniosomal gel has been used for a transdermal and topical delivery system of several drugs for improved penetration across the skin. For example, Vora, Khopade, and Jain (1998) developed a proniosome based transdermal delivery system for levonorgestrel using coacervation and sorbitan monostearate 40 (span 40), lecithin, cholesterol and isopropanol. The proniosomal gel was used to prepare a transdermal patch with surface area of 0.63 cm^2 and 1 mg drug. The patch was designed to achieve a flux of 20 µg/day. An in *vivo* study, in rats, showed that the proniosomal gel patch significantly inhibited the luteinizing hormone (84.4%) more than an ointment-based formulation (56.96 %).

Fang, Yu, Wu, Huang, and Tsai (2001) reported a span 40/span 60 based proniosomal gel for estradiol enhanced permeation across excised rat skin. Proniosomes prepared with span 60 provide a higher estradiol flux across the skin than with span 40 (2 and 1.5 fold the estradiol suspension, respectively).

Thakur et al. (2009) have prepared losartan potassium proniosomes using different surfactants such as Tween 20, 40, and 80; Span 20, 40, 60, and 80 for transdermal drug delivery. The best in vitro skin permeation profile was obtained with a formulation containing span 40. The Proniosome formulation showed a 1.9 fold higher bioavailability of losartan potassium compared to the oral formulation in a rat model.

Solanki, Parikh, and Parikh (2009) developed a proniosomal gel for ketoprofen that had a 1.3 fold higher permeation in comparison to plain ketoprofen gel across rat skin.

Chandra and Sharma (2008) developed piroxicam proniosomes. Proniosomes prepared with span 60 showed smaller particle size and higher encapsulation efficiency than those prepared with span 80. The flux of the proniosome formulation was

significantly higher (7.4 times) in rat skin compared to control (carbopol gel). This formulation showed significantly higher anti-inflammatory activity in vivo compared to carbopol gel in a paw edema rat model.

Alsarra, Bosela, Ahmed, and Mahrous (2005) studied the permeation of ketorolac proniosome gel formulations across rabbit skin. The encapsulation efficiency was about 99% in all the formulations and the drug permeation across rabbit skin of all prepared formulations was 7 (span 60) and 4 (tween 20) fold higher than control (hydroxpropyl methylcellulose gel).

Alam, Baboota, Kohli, Ali, and Ahuja (2010) prepared celecoxib proniosome for enhanced transdermal delivery. This formulation showed significant higher anti-inflammatory activity in the rat paw edema model.

Ammar, Ghorab, El-Nahhas, and Higazy (2011) reported a tenoxicam proniosomal formulation which exhibited higher anti-inflammatory and analgesic effects compared to the market tablet. The formulation showed no rabbit skin irritation from a one week daily application.

Azeem et al. (2008) developed a furosemide proniosomal gel to enhance the permeation of drug across skin. The proniosomal gel formulation of furosemide was able to sustain the drug plasma level in rats within the therapeutic concentration for 12 hours.

1.2.2. Microemulsion for enhanced transdermal delivery

Microemulsions have been used in transdermal delivery because of their ability to penetrate to the deeper layers of the skin. Microemulsions are pseudo-quaternary systems composed of oil, water and surfactant and/or co-surfactant. They are transparent with particle size ranging from 10-100 nm (C.-T. Huang et al., 2013). Microemulsions have

several advantages such as high solubilizing capacity, spontaneous formation, easy to manufacture and scale up, thermodynamic stability, ability to encapsulate both lipophilic and hydrophilic drug, and improve bioavailability (Khodakiya et al., 2012). There are three types of microemulsions which are oil in water (o/w) , water in oil (w/o), and bicontinuous phase system (Talegaonkar et al., 2008). In w/o, the water droplets are surrounded in oil as the continuous phase. In o/w, the oil droplets are surrounded in water as the continuous phase. In bicontinuous phase, a similar amount of both oil and water are the continuous phase separated by surfactant interfaces.

There are different permeation pathways for microemulsion delivery system in skin (Figure 1-5). They include direct diffusion of drug molecules into the stratum corneum due to higher concentration gradient is one. Trans-follicular pathway is the second. The third is the hydration and swelling of the stratum corneum which creates transcutaneous channels for drug to penetrate. Drug diffuse directly into the stratum corneum due to microemulsion droplet collision is the fourth pathway. The fifth pathway is that the microemulsion oil, surfactant or/and co-surfactant create pores or voids in the stratum corneum (Pawar & Babu, 2014).

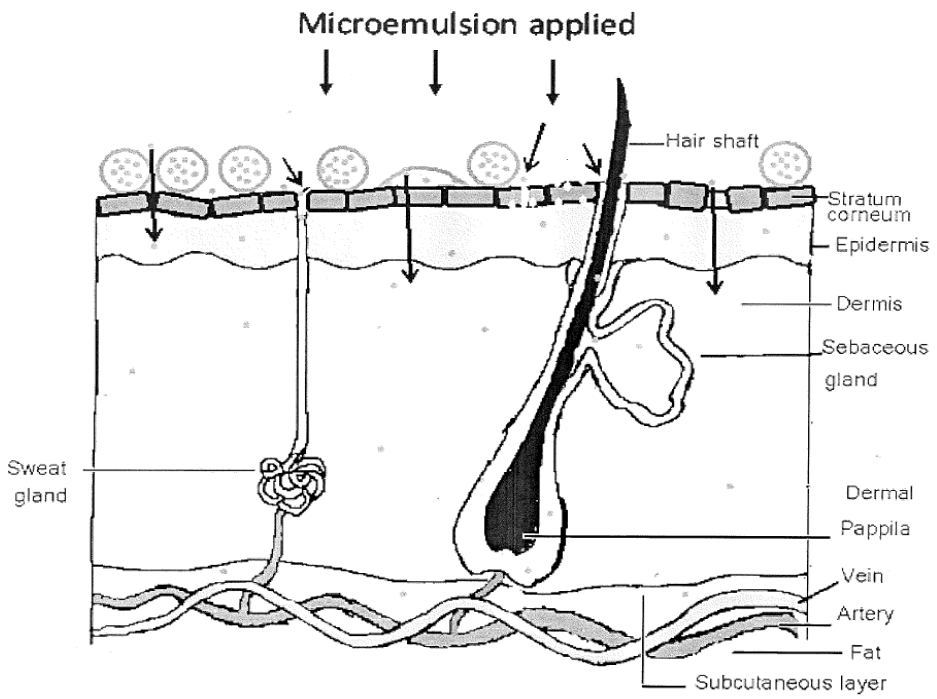

Figure 1-5 Possible permeation pathways for microemulsion drug delivery

For the preparation of microemulsions, the oil and water can be mixed with surfactant. Then co-surfactant is added at a slow rate with constant stirring until the system becomes transparent. The amount of surfactant, co-surfactant, and oil can be determined by a pseudo-ternary phase diagram (Mishra, Panola, & Rana, 2014).

A phase diagram of water, oil, and mixture of surfactant/co-surfactant is constructed at a fixed surfactant/ co-surfactant weight ratio. The oil and surfactant/ co-surfactant in specific weight ratio are weighed and mixed in a glass vial, titrated with water and stirred well at room temperature. The formation of a monophasic or biphasic system is confirmed visually. Monophasic is transparent whereas biphasic is turbid. The samples were noted in the diagram and the area covered by these points is considered the microemulsion region (Saini, Nautiyal, Kumar, Singh, & Anwar, 2014).

Oil phase is an important component in a microemulsion which influences the selection of other components. It is important to choose an oil which can solubilize the drug and facilitate microemulsion formation. In general, oil with a large molecular weight produces a microemulsion with a high solubilizing capacity. However, the microemulsion formulation of the oil will be difficult when the hydrocarbon chain length is increased Thus, it is challenging to find an oil with both high solubilizing capacity and easy microemulsion formation. (Pawar & Babu, 2014). In some cases, two oils are used to achieve those two goals. Fatty acids and their esters, medium chain triglycerides and propylene glycol esters of fatty acids are used as the oil phase to formulate microemulsions (Patel, Li, & Serajuddin, 2016).

Surfactant is another important component of the microemulsion system. The type and amount of surfactant greatly influences drug solubilizing and skin permeation. The surfactants stabilize the system. Surfactants can be classified as synthetic and natural. The synthetic surfactants can be further classified as anionic, cationic, non-ionic and zwitterionic (Lawrence & Rees, 2000; Patel et al., 2016). Natural, like phospholipids, are preferred over synthetic surfactants because they are more biocompatible and tolerable by the body (Schwarz, Klang, Hoppel, Mahrhauser, & Valenta, 2012). The non-ionic class is preferred over both cationic and anionic due to less skin irritation (Effendy & Maibach, 1995). The nonionic surfactants include polysorbates, sorbitan esters, poloxamers, polyoxyethylene alkyl ethers, polyoxyethylene-castor oil derivatives, alkyl polyglucosides, and polyglycolyzed glycerides (Date & Patravale, 2007).

Co-surfactant is used mainly to reduce the interfacial tension and increase the fluidity of the interface. The co-surfactants interact with surfactant molecules at the

interface and affect their packing which keeps the interfacial tension at a minimum, but not equal to zero. The most commonly used co-surfactants are alcohols, such as short chain alcohols like ethanol, short chain glycols like propylene glycol, or medium chain alcohols like amines or acids (Kale & Deore, 2017).

Lecithin microemulsions have been studied extensively to improve the skin permeation of various drugs. Paolino, Ventura, Nistico, Puglisi, and Fresta (2002) studied the effect of lecithin microemulsion on ketoprofen permeation across human skin. The ketoprofen microemulsion showed 6 and 2 fold higher permeation than emulsion and gel, respectively (control formulations). Furthermore, the skin tolerability toward lecithin microemulsions showed a good human skin tolerability.

Kriwet and Müller-Goymann (1995) have compared diclofenac skin permeation from different lecithin formulations (lamellar liquid crystals and liposome) to lecithin microemulsion across human skin. The microemulsions showed 12 fold higher drug permeation compared to lamellar liquid crystals or liposome.

Dreher, Walde, Walther, and Wehrli (1997) studied the effect of lecithin microemulsion gel on the skin permeation of indomethacin and diclofenac across human skin. There was 6 fold higher flux for both drugs by the lecithin microemulsion gels as compared to pure oil solutions.

Brime, Moreno, Frutos, Ballesteros, and Frutos (2002) prepared a novel lecithin based microemulsion containing amphotericin b which consist of isopropyl myristate, Brij, lecithin and water. Acute toxicity study in mice model showed that the lethal dose 50 (LD50) for amphotericin B microemulsion was of 2.9 mg/kg of body weight compared to 4 mg/kg for commercial suspension.

Yuan et al. (2010) showed lidocaine pig ear skin permeation was improved 4 fold when lecithin linker microemulsion was used compared to lidocaine solution. The in vitro cytotoxicity studies on the reconstructed human skin Epiderm^{TM} EPI-200 showed that lecithin linker microemulsions had comparable cytotoxicity to lidocaine solution.

Khanna, Katre, and Drabhu (2010) reported 1.2 fold increased human skin permeation and 4.4 fold increase skin retention when tretinoin loaded into lecithin microemulsion was compared to drug solution.

Hoeller, Klang, and Valenta (2008) evaluated the skin permeability for fluconazole loaded into lecithin microemulsion. The permeation across porcine skin was high when lecithin microemulsion was used and the content of phosphatidylethanolamine in the system play a major role in drug permeation.

Peira, Carlotti, Cavalli, and Trotta (2006) prepared lecithin microemulsion for azelaic acid which is used to treat various skin disorders including acne. The transdermal flux across pig skin for the microemulsion was 115 fold higher than drug solution.

1.3. Introduction to melanoma treatment

Skin cancer is one of the severe diseases that affect skin. There are three types of skin cancers which are basal cell carcinoma, squamous cell carcinoma and melanoma (Koh et al., 2003). Melanoma is the most aggressive skin cancer and leads to more than 79% of skin cancer mortality. Melanoma incidence has increase in the past years more than any other cancer with approximate doubling of rates every 10-20 years. It is estimated that more than 1 in 50 Americans will develop melanoma with about 96,480 new cases and nearly 7,230 deaths in 2019 (American Cancer Society, 2019).

Melanocytes are responsible for producing the melanin pigment that can be found in skin , hair, and eyes (Yamaguchi, Brenner, & Hearing, 2007). Melanoma has a high metastatic rate compared to all types of skin cancer. When a tumor reaches the dermis, it could spread to other parts of the body through the lymphatic system and bloodstream (Naves et al., 2017). Thus, early stage melanoma can be treated with very high recovery by surgery. The advanced metastatic melanoma can be treated with moderate result with dacarbazine, recombinant interferon alpa-2b and high dose interleukin2 (Bhatia, Tykodi, & Thompson, 2009).

Several key molecular pathways have been identified in melanoma progression and proliferation. Mitogen-activated protein kinase (MAPK) and phosphoinositide 3-kinase (PI3K) play a major role in the development and progression of melanoma. Dysregulation of MAPK pathway is common in melanoma due to the mutation in BRAF and RAS genes (Paluncic et al., 2016). The melanoma mutation rate in BRAF gene reaches 50-70% and in NRAS 15-30%. Mutation of BRAF induces hyper activation of MAPK signaling which is involved in melanoma development (Cheng, Lopez-Beltran, Massari, MacLennan, & Montironi, 2018). Some inhibitors target these pathways such as vemurafenib. A significant inhibition in cell proliferation when melanoma cells have been treated with cationic liposomes loaded with siRNA targeting BRAF and Akt pathway (Tran, Gowda, et al., 2008a). Silencing BRAF by using siRNA in combination with PI3K inhibitors enhance the efficacy of the inhibitors on tumor cell cytotoxicity (He et al., 2018).

Melanoma treatment depends on the stage of the disease. Early stage melanoma can be treated with surgery with high survival rate. However, metastatic malignant melanoma is difficult to treat with surgical removal. It can be treated with chemotherapy,

immunotherapy, targeted therapy or their combination (Garbe, Eigentler, Keilholz, Hauschild, & Kirkwood, 2011).

Dacarbazine is commonly used to treat malignant melanoma. Dacarbazine has been used as first line treatment for wild type melanoma from 1970 to the early 2000s. However, this drug failed to show improvement in survival rate. Dacarbazine has been combined with cisplatin and vinblastine for treatment of melanoma, but failed to show a survival benefit compared with dacarbazine alone (Bhatia et al., 2009; Garbe et al., 2011)

Since melanoma is highly immunogenic, immunotherapy has been developed to treat melanoma. The immunotherapy will boost the immune response and it might help eradicate cancer cells. Ipilimumab was approved by FDA in 2011. It is a human IgG1 monoclonal antibody (mAb) against cytotoxic T-lymphocyte-associated antigen-4 (CTLA-4). Severe and fatal autoimmune reaction, however, is associated with the use of this drug (Dany et al., 2016).

The mutation in serine/threonine-protein kinase B-Raf (BRAF) is the genetic mutation which leads to development of malignant melanoma. Nearly 50-70% of metastatic melanomas have mutation in the serine-threonine protein kinase BRAF at V600. By inhibiting the BRAF, tumor cell proliferation can be blocked in patients with active BRAF mutations. BRAF inhibitor such as vemurafenib has shown promising effect initially. However, patients develop resistance after the treatment with vemurafenib in almost all cases (Ascierto et al., 2012).

Several combination therapies have been proposed to treat metastatic melanoma such as dacarbazine co-administered with cisplatin and vinblastine and this combination is known as the CVD regiment (Hofmann et al., 2011). Another combination of dabrafenib

(BRAF inhibitor) and trametinib (MEK inhibitor), vemurafenib (BRAF inhibitor) and cobimetinib (MEK inhibitor) have been used to treat patients with BRAF V600–mutated metastatic melanoma. All combinations did not show improvement in melanoma treatment and they caused serious side effects (Daud & Tsai, 2017).

Most of the melanoma treatments are not adequate and the response rate is low. The median survival duration of patients with metastasized melanoma approaches nearly 6-9 months with traditional cytotoxic chemotherapy (Vosoughi et al., 2018). The main issue with all cancer treatments is the severe adverse effects and multidrug resistance formation. Multidrug resistance is one of the major reasons for low efficiency of current melanoma therapies (La, 2009). The mechanism by which melanoma develops resistance varies. Melanoma can develop resistance by efflux system, amplification of drug targets or changes in drug kinetics (Kurangi & Jalalpure, 2018). Different strategies have been developed to overcome the chemoresistance include using nanocarriers to deliver various anti-cancer drugs with some reported success (Stoelting et al., 2014).

Nanotechnology based delivery have been studied extensively to improve melanoma treatment. It has been used to improve drug targeting to the tumors site and reduce side effects and drug resistance (J. Chen, Shao, Zhang, & Chen, 2013). The vasculature leakiness and poor lymphatic drainage in tumors allow drug-loaded nanoparticles to accumulate at the cancer site to improve drug efficacy and decrease side effects (Bazak, Houri, El Achy, Hussein, & Refaat, 2014). Moreover, drug circulation time and accumulation can be improved by surface modifications of the nanoparticle (e.g., PEGylation). The multidrug resistance can be overcome by co-encapsulating since

nanoparticles can deliver multiple agents (Hu & Zhang, 2012; Tamarov, Näkki, Xu, & Lehto, 2018).

1.3.1. Liposomes

Liposomes are microscopic spherical lipid bilayers which encapsulate one or more drugs in the lipid layer or in the aqueous core of the nanoparticle. Liposomes were invented in 1961 and were the first nanoparticle used in medicine (Bozzuto & Molinari, 2015). The size of the liposome is one of the major factors affecting their tissue distribution. Large particle size liposomes are rapidly cleared from the circulation after intravenous injection by Kupffer cells of the liver and fixed macrophages of the spleen (T. Allen, 1988). The circulation half-lives of the liposomes increase with decreasing size (T. M. Allen, Hansen, & Rutledge, 1989). The clearance of the liposome by the reticuloendothelial system (RES) depends on the non-specific hydrophobic interactions of liposomes with RES cells. Surface modification of liposomes with PEG can help prolong the circulation time (Daraee, Etemadi, Kouhi, Alimirzalu, & Akbarzadeh, 2016). Further, specific ligands can be attached to the liposome surface to improve the cellular uptake and specificity as presented in Figure 1.6. Drug can be loaded into liposomes by passive or active loading. In passive loading, the drug is encapsulated during liposome formulation. Passive encapsulation of hydrophilic drug depends on the ability of the liposome to trap a certain aqueous volume along with dissolved drug in the core of the liposomes during liposome formation. The loading efficiency for hydrophilic drug by passive loading is low. For hydrophobic drugs, passive loading is governed by the drug-lipid interaction. Loading efficiency using passive loading for hydrophobic drug is usually very high, but this depends on the solubility of drug in the liposome membrane. Active

loading means that drug will be loaded after liposome is formed. The hydrophilic drug with protonizable amine functions can be effectively loaded into the aqueous core of liposomes through an ion gradient across the membrane, which allows for high loading efficiency (Akbarzadeh et al., 2013; Bozzuto & Molinari, 2015).

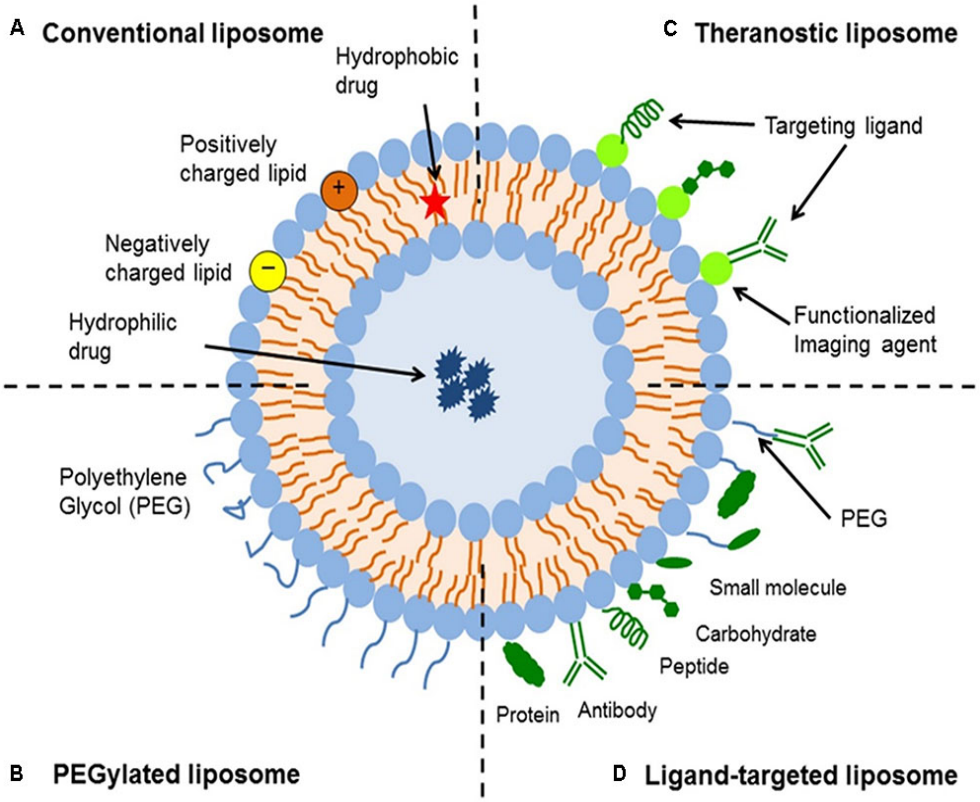

Figure 1-6 Different types of liposomal drug delivery Adapted from (Sercombe et al., 2015)

Liposome as a carrier has been used extensively in melanoma research. Tran et al. (2008b), have reported that the combination of ceramide with sorafenib resulted in synergistic inhibition of melanoma growth in vitro and in vivo. Topical administration of both V600 E BRAF and Akt3 siRNA in a cationic liposome showed a decrease in melanoma development in vivo (Tran, Gowda, et al., 2008a). Y. Chen, Bathula, Yang, and Huang (2010) showed that an antisamide targeted a cationic liposome containing c-

Myc siRNA inhibited tumor growth in B16F10 melanoma cells in vivo. Furthermore, BAX mRNA has been incorporated in a cationic liposome used to treat gingival human malignant melanoma. The tumors were 36.7% smaller than the control group (Okumura et al., 2008).

1.3.2. Niosomes

Niosomes are lamellar vesicle composed of non-ionic surfactant and the lipid cholesterol. It is a promising new drug delivery in comparison with conventional liposomes. They possess greater physicochemical stability, less purity variability, lower cost, and are easy to prepare and scale up. Further, niosome have a high compatibility with biological systems and low toxicity due to their non-ionic nature. Niosomes can encapsulate both hydrophilic and lipophilic drug. Niosome particle size is usually 100 nm to 2 μm. Niosome can be divided into multi lamellar vesicles (MLV), large unilamellar vesicles (LUV), and small unilamellar vesicles (SUV). There are many methods to prepare niosome such as by thin film hydration, by ether injection, reverse phase evaporation, multiple membrane extrusion, sonication, active trapping method, trans membrane pH gradient, and by bubble or coacervation methods. Niosomes have been used for transdermal, ocular, oral, pulmonary, parenteral and gene delivery routes (Sankhyan & Pawar, 2012; Yeo, Lim, Chye, Ling, & Koh, 2018).

A number of studies have used niosomes to deliver cytotoxic drug to treat melanoma. 5-fluorouracil, which is used to treat different types of skin cancers, has been encapsulated in niosome by Cosco et al. (2009) to improve drug efficacy. Results showed an 8-fold improvement of the drug's penetration across human skin and cytotoxicity against a melanoma cell line when compared to drug free aqueous solution. Furthermore,

Dwivedi et al. (2005) encapsulated artemisinin in niosomes and the formulation showed highly selective cytotoxicity against melanoma cells with low toxicity against normal skin cells. Niosomal cisplatin has been prepared by Gude et al. (2002) and the anti-metastatic activity has been studied in a metastatic model of B16F10 melanoma. Cisplatin encapsulated in niosomes showed significant anti-metastatic activity than free drug. Overall, there is great potential for use of niosomes as alternative delivery systems.

1.3.3. Nanoemulsions

Nanoemulsion is a heterogeneous system in which an emulsifying agent is used to stabilize oil phase droplets in an aqueous phase. The nanoemulsion droplet size is usually between 50 to 200 nm based on the components and preparation methods (Khatri, Lohani, & Gandhi, 2013). Emulsifying agents are surfactants or amphiphilic surface active molecules that can reduce interfacial tension between the oil and aqueous phase by adsorbing at their interfaces. The nanoemulsion can exist as oil in water, water in oil or bi-continuous depending on the emulsifying agent used (Jaiswal, Dudhe, & Sharma, 2015).

Nanoemulsions are a promising drug delivery system for anticancer drugs because of their ability to include lipid and water soluble drugs and their reduced particle size which leads to high accumulation of drugs at the tumor site (Ganta, Talekar, Singh, Coleman, & Amiji, 2014). Prete et al. (2006) showed that a etoposide cholesterol-rich lipid nanoemulsion increased drug concentration at the melanoma tumor site four times more than at normal tissue while showing increased half-life and decreased side effects. The maximum tolerated dose was approximately five-fold more than commercial etoposide. The tumor growth was inhibited significantly more when melanoma bearing mice were

treated with etoposide nanoemulsion than commercial etoposide. The combination of etoposide with paclitaxel in cholesterol rich lipid nanoemulsion (LDE-PTX+ETP) has been tested in B16F10 melanoma bearing mice. There was a greater reduction in the number of mice bearing metastases when mice were treated with LDE-PTX+ETP (30%) in comparison to PTX+ETP (82%). After mice were treated with LDE-PTX+ETP, it reduced cellular density and blood vessels and increased collagen fibers in tumor tissues. Further, the toxicity was milder in LDE-PTX+ETP than PTX+ETP group (Kretzer, Maria, & Maranhão, 2012). Dacarbazine, which is approved to treat malignant melanoma, has been prepared as a nanoemulsion. The results showed a significant reduction in tumor size for mice treated with dacarbazine nanoemulsion rather than dacarbazine suspension. Furthermore, dacarbazine nanoemulsion showed a 5-fold higher efficacy (73% versus14%) in preventing tumor growth compared to dacarbazine suspension during a drug cessation period (Tagne, Kakumanu, & Nicolosi, 2008).

Ichikawa et al. (2007), showed that encapsulation of gadolinium (Gd) in a lipid nanoemulsion enhanced its accumulation in tumor after intravenous injection in melanoma bearing hamsters. Furthermore, the maximum level of Gd was higher than the limit required for suppressing tumor growth in neutron capture therapy.

1.3.4. Solid lipid nanoparticles

Solid lipid nanoparticles (SLNs) have been used extensively to encapsulate therapeutic agents because of the unique ability of SLNs to form controlled release and drug targeting by coating/attaching ligands. Furthermore, the lipids used to form SLNs are biodegradable, so it has better biocompatibility than other nanocarriers. Solid nanoparticles provide higher encapsulation and loading efficiency, greater surface area,

and are easy to manufacture and scale up. They bypass the sterilization process that is required during liposome preparation. The lipids in preparing solid lipid nanoparticles are highly purified triglycerides, calixarenes, and sterols. Solid lipid nanoparticles are able to deliver both hydrophilic and lipophilic drugs (Mukherjee, Ray, & Thakur, 2009).

SLNs have been used as a delivery system for several drugs in different cancers including melanoma. Shi et al. (2014) developed cationic SLNs to deliver both microRNA-34a and paclitaxel for synergistic cancer therapy. SLNs prevent both drugs from degradation in serum with an average size less than 200 nm. The combination of microRNA-34a and paclitaxel was a very potent inhibitor of B16F10 bearing tumor growth and can eliminate melanoma metastasized to the lungs compared to monotherapy.

Clemente et al. (2018) developed a delivery system for temozolomide in SLNs for treatment of melanoma. SLNs loaded with temozolomide inhibited growth and vascularization of B16F10 melanoma in mice without any toxicity .

Mosallaei et al. (2013) prepared SLNs loaded with docetaxel for the treatment of melanoma. They inhibited cell growth 2 fold more than cells treated with Taxotere. Furthermore, cellular uptake was significantly higher. SLNs loaded with docetaxel showed better tumor inhibition and survival compared to the group treated with Taxotere.

Athawale et al. (2014) prepared SLNs loaded with etoposide to improve efficacy and therapy of metastasized cancers. The biodistribution of etoposide in liver and lung was high when etoposide was loaded in SLNs. Furthermore, the number of metastasized tumor colonies were significantly reduced when SLNs loaded with etoposide used.

Banerjee et al. (2019) developed a SLN paclitaxel formulation modified with Tyr-3-octerotide (PMS) for the treatment of melanoma. PMS inhibited melanoma cell growth,

migration, and invasion compared to dacarbazine. Furthermore, PMS induced calreticulin exposure, which is one of the biomarkers of immunogenic cell death, on the B16F10 cell surface both in vitro and in vivo. The treatment with PMS generated an immunogenic environment in the tumor which enhanced therapeutic efficacy compared to dacarbazine. PMS exhibited anti melanoma activities without any toxicity.

Shen et al. (2015) developed a paclitaxel SLN coated with haluronan (HA-SLNs) to target CD44 overexpressing B16F10 melanoma cells. HA-SLNs loaded with paclitaxel inhibited sphere formation. Furthermore, coated solid nanoparticle with paclitaxel inhibited cell invasion, migration and adhesion. The HA-SLNs with paclitaxel significantly increased animal survival rate and no tumors were detected in lung.

1.3.5. Nanostructure lipid carriers

Nanostructure lipid carriers (NLCs) is the second generation of lipid nanoparticles. The difference between solid lipid nanoparticles and nanostructure lipid carriers is that the internal structure of the solid lipid nanoparticle is composed of solid lipid whereas the internal structure of nanostructure lipid nanoparticle is composed of a blend of solid and liquid lipids (Naseri, Valizadeh, & Zakeri-Milani, 2015). NLCs have been used to delivery several drugs to treat melanoma. Huang et al. (2008) have developed camptothecin encapsulated into NLCs associated with a quantum dot for integrating imaging and therapy. The camptothecin loaded into NLCs showed significant cytotoxicity against melanoma cells and the cellular uptake was higher compared to other lipid nanoparticles carriers. The real time bioimaging showed that camptothecin loaded nanoparticles were localized at the tumor site for at least 24 hours and camptothecin accumulation was increased. Liu et al. (2011) reported that docetaxel loaded into NLCs showed greater

cytotoxicity against melanoma cells compared to Duopafei® by inducing more apoptosis and more G2/M arrest and inhibited tumor growth more. The NLCs loaded with docetaxel showed lower toxicity than Duopafei® (Free Docetaxel) . In addition, Liu et al. (2011) developed an antibody modified nanostructured lipid loaded with docetaxel (tNLC) to target VEGFR overexpressed tumor cells. The tNLC showed higher cytotoxicity toward melanoma cells and superior antitumor efficacy in murine model bearing B16 compared to Duopafei® and non-targeted NLC.

1.4. Conclusion

Several methods have been proposed to improve drug permeation across skin. The formulations approach, like microemulsions and proniosomes, have enhanced drug permeation. Melanoma treatment is challenging due to the chemotherapeutic agents' toxic effects and the development of chemoresistance. Nanoparticle drug delivery systems, like liposomes, can provide significant advantages in melanoma treatment. They can deliver both lipophilic and hydrophilic drugs. They protect drugs from degradation and increase the circulation time. They improve the therapeutic efficacy and therapeutic index. They decrease toxic effects by passive accumulation or active targeting.

1.5. Study objectives

The objective of this dissertation research was to develop lipid-based nanoparticle delivery systems with various drugs for treatment of melanoma. Six chapters are in this dissertation:

1. Chapter 1 provides a brief review on topical and transdermal drug delivery and various permeation enhancement approaches. Microemulsions and proniosomes application were reviewed. Furthermore, various lipid based nanoparticles and their application in melanoma treatment were discussed.
2. Chapter 2 presents hydroxytyrosol proniosomes data for prevention and treatment of melanoma. Proniosomes were prepared by coacervation. The in vitro release and ex-vivo permeation were explored for a selected formulation. The effect of different components of the formulation on the skin permeation were studied.
3. Chapter 3 presents data on DAB microemulsions formulation to act as transdermal delivery vehicles for prevention and treatment of melanoma. Microemulsions were optimized through pseudo-ternary phase diagrams. The in vitro release and ex vivo permeation were obtained for selected formulations. The cytotoxicity of the formulation was evaluated in B16BL6 melanoma cell line.
4. Chapter 4 shows hispolon effect on melanoma cell lines. Cell proliferation assays were preformed using B16BL6 melanoma cells. The live/dead cell staining assay after hispolon treatment are presented. Several markers associated with cell apoptosis and death were tested after hispolon treatment such as nitrite, lipid peroxidation, caspase 1 and 3 activity, complex I and IV inhibition, reactive oxygen species induction, and bcl-2 and Bax genes expression.

5. Chapter 5 presents the effect of co-administration of PEGylated liposomes of doxorubicin and hispolon. PEGylated liposomes were prepared for both hispolon and doxorubicin. In vitro drug release, cellular uptake, cell cytotoxicity, and cell apoptosis of both formulations and their combination were performed.
6. Chapter 6 gives a summary and conclusion on each project. Also, the author's opinion and future plans are provided

1.6. References

Akbarzadeh, A., Rezaei-Sadabady, R., Davaran, S., Joo, S. W., Zarghami, N., Hanifehpour, Y., . . . Nejati-Koshki, K. (2013). Liposome: classification, preparation, and applications. *Nanoscale Research Letters, 8*(1), 102-111.

Alam, M. I., Baboota, S., Kohli, K., Ali, J., & Ahuja, A. (2010). Pharmacodynamic evaluation of proniosomal transdermal therapeutic gel containing celecoxib. *ScienceAsia, 36*(4), 305-311.

Ali, S., Shabbir, M., & Shahid, N. (2015). The structure of skin and transdermal drug delivery system - A review. *Research Journal of Pharmacy and Technology, 8*(2), 103-109.

Alkilani, A., McCrudden, M. T., & Donnelly, R. (2015). Transdermal drug delivery: innovative pharmaceutical developments based on disruption of the barrier properties of the stratum corneum. *Pharmaceutics, 7*(4), 438-470.

Allen, T. (1988). Toxicity of drug carriers to the mononuclear phagocyte system. *Advanced Drug Delivery Reviews, 2*(1), 55-67.

Allen, T. M., Hansen, C., & Rutledge, J. (1989). Liposomes with prolonged circulation times: Factors affecting uptake by reticuloendothelial and other tissues. *Biochimica et Biophysica Acta (BBA)-Biomembranes, 981*(1), 27-35.

Alsarra, I. A., Bosela, A., Ahmed, S., & Mahrous, G. (2005). Proniosomes as a drug carrier for transdermal delivery of ketorolac. *European Journal of Pharmaceutics and Biopharmaceutics, 59*(3), 485-490.

American Cancer Society. (2019). Cancer Facts & Figures 2019. Atlanta: American Cancer Society; 2019.

Ammar, H., Ghorab, M., El-Nahhas, S., & Higazy, I. (2011). Proniosomes as a carrier system for transdermal delivery of tenoxicam. *International Journal of Pharmaceutics, 405*(1-2), 142-152.

Ascierto, P. A., Kirkwood, J. M., Grob, J.-J., Simeone, E., Grimaldi, A. M., Maio, M., . . . Mozzillo, N. (2012). The role of BRAF V600 mutation in melanoma. *Journal of Translational Medicine, 10*(1), 85-96.

Athawale, R. B., Jain, D. S., Singh, K. K., & Gude, R. P. (2014). Etoposide loaded solid lipid nanoparticles for curtailing B16F10 melanoma colonization in lung. *Biomedicine & Pharmacotherapy, 68*(2), 231-240.

Azeem, A., Jain, N., Iqbal, Z., Ahmad, F. J., Aqil, M., & Talegaonkar, S. (2008). Feasibility of proniosomes-based transdermal delivery of frusemide: Formulation optimization and pharmacotechnical evaluation. *Pharmaceutical Development and Technology, 13*(2), 155-163.

Banerjee, I., De, M., Dey, G., Bharti, R., Chattopadhyay, S., Ali, N., . . . Mandal, M. (2019). A peptide-modified solid lipid nanoparticle formulation of paclitaxel modulates immunity and outperforms dacarbazine in a murine melanoma model. *Biomaterials Science, 7*(3), 1161-1178.

Bazak, R., Houri, M., El Achy, S., Hussein, W., & Refaat, T. (2014). Passive targeting of nanoparticles to cancer: A comprehensive review of the literature. *Molecular and Clinical Oncology, 2*(6), 904-908.

Bhatia, S., Tykodi, S. S., & Thompson, J. A. (2009). Treatment of metastatic melanoma: An overview. *Oncology 23*(6), 488-496.

Bos, J. D., & Meinardi, M. M. (2000). The 500 Dalton rule for the skin penetration of chemical compounds and drugs. *Experimental Dermatology, 9*(3), 165-169.

Bozzuto, G., & Molinari, A. (2015). Liposomes as nanomedical devices. *International Journal of Nanomedicine, 10*, 975-999.

Brime, B., Moreno, M. A., Frutos, G., Ballesteros, M. P., & Frutos, P. (2002). Amphotericin B in oil–water lecithin-based microemulsions: formulation and toxicity evaluation. *Journal of Pharmaceutical Sciences, 91*(4), 1178-1185.

Cevc, G., & Vierl, U. (2010). Nanotechnology and the transdermal route: A state of the art review and critical appraisal. *Journal of Controlled Release, 141*(3), 277-299.

Chandra, A., & Sharma, P. (2008). Proniosome based drug delivery system of piroxicam. *African Journal of Pharmacy and Pharmacology, 2*(9), 184-190.

Chen, J., Shao, R., Zhang, X. D., & Chen, C. (2013). Applications of nanotechnology for melanoma treatment, diagnosis, and theranostics. *International Journal of Nanomedicine, 8*, 2677-2688.

Chen, Y., Bathula, S. R., Yang, Q., & Huang, L. (2010). Targeted nanoparticles deliver siRNA to melanoma. *Journal of Investigative Dermatology, 130*(12), 2790-2798.

Cheng, L., Lopez-Beltran, A., Massari, F., MacLennan, G. T., & Montironi, R. (2018). Molecular testing for BRAF mutations to inform melanoma treatment decisions: A move toward precision medicine. *Modern Pathology, 31*(1), 24-38.

Clemente, N., Ferrara, B., Gigliotti, C., Boggio, E., Capucchio, M., Biasibetti, E., . . . Cangemi, L. (2018). Solid lipid nanoparticles carrying temozolomide for melanoma treatment. Preliminary in vitro and in vivo studies. *International Journal of Molecular Sciences, 19*(2), 255-274.

Dany, M., Nganga, R., Chidiac, A., Hanna, E., Matar, S., & Elston, D. (2016). Advances in immunotherapy for melanoma management. *Human Vaccines & Immunotherapeutics, 12*(10), 2501-2511.

Daraee, H., Etemadi, A., Kouhi, M., Alimirzalu, S., & Akbarzadeh, A. (2016). Application of liposomes in medicine and drug delivery. *Artificial cells, Nanomedicine, and Biotechnology, 44*(1), 381-391.

Date, A. A., & Patravale, V. B. (2007). Microemulsions: applications in transdermal and dermal delivery. *Critical Reviews™ in Therapeutic Drug Carrier Systems, 24*(6), 547-596.

Daud, A., & Tsai, K. (2017). Management of Treatment-Related Adverse Events with Agents Targeting the MAPK Pathway in Patients with Metastatic Melanoma. *The Oncologist, 22*(7), 823-833.

Desai, P., Patlolla, R. R., & Singh, M. (2010). Interaction of nanoparticles and cell-penetrating peptides with skin for transdermal drug delivery. *Molecular Membrane Biology, 27*(7), 247-259.

Dreher, F., Walde, P., Walther, P., & Wehrli, E. (1997). Interaction of a lecithin microemulsion gel with human stratum corneum and its effect on transdermal transport. *Journal of Controlled Release, 45*(2), 131-140.

Dwivedi, A., Mazumder, A., Du Plessis, L., Du Preez, J. L., Haynes, R. K., & Du Plessis, J. (2015). In vitro anti-cancer effects of artemisone nano-vesicular formulations on melanoma cells. *Nanomedicine: Nanotechnology, Biology and Medicine, 11*(8), 2041-2050.

Effendy, I., & Maibach, H. I. (1995). Surfactants and experimental irritant contact dermatitis. *Contact Dermatitis, 33*(4), 217-225.

Fang, J.-Y., Yu, S.-Y., Wu, P.-C., Huang, Y.-B., & Tsai, Y.-H. (2001). In vitro skin permeation of estradiol from various proniosome formulations. *International Journal of Pharmaceutics, 215*(1-2), 91-99.

Ganta, S., Talekar, M., Singh, A., Coleman, T. P., & Amiji, M. M. (2014). Nanoemulsions in translational research—opportunities and challenges in targeted cancer therapy. *American Association of Pharmaceutical Scientists PharmSciTech, 15*(3), 694-708.

Garbe, C., Eigentler, T. K., Keilholz, U., Hauschild, A., & Kirkwood, J. M. (2011). Systematic review of medical treatment in melanoma: current status and future prospects. *The Oncologist, 16*(1), 5-24.

Gude, R., Jadhav, M., Rao, S., & Jagtap, A. (2002). Effects of niosomal cisplatin and combination of the same with theophylline and with activated macrophages in murine B16F10 melanoma model. *Cancer Biotherapy and Radiopharmaceuticals, 17*(2), 183-192.

He, H., Nan, X., Liu, S., Zhang, L., Yang, Z., Wu, Y., & Zhang, L. (2018). Anticancer effects of combinational treatment with BRAFV600E siRNA and PI3K pathway inhibitors in melanoma cell lines harboring BRAFV600E. *Oncology Letters, 16*(1), 632-642.

Heuschkel, S., Goebel, A., & Neubert, R. H. (2008). Microemulsions—modern colloidal carrier for dermal and transdermal drug delivery. *Journal of Pharmaceutical Sciences, 97*(2), 603-631.

Hoeller, S., Klang, V., & Valenta, C. (2008). Skin-compatible lecithin drug delivery systems for fluconazole: effect of phosphatidylethanolamine and oleic acid on skin permeation. *Journal of Pharmacy and Pharmacology, 60*(5), 587-591.

Hofmann, M. A., Hauschild, A., Mohr, P., Garbe, C., Weichenthal, M., Trefzer, U., . . . Kaatz, M. (2011). Prospective evaluation of supportive care with or without CVD chemotherapy as a second-line treatment in advanced melanoma by patient's choice: a multicentre Dermatologic Cooperative Oncology Group trial. *Melanoma Research, 21*(6), 516-523.

Hu, C.-M. J., & Zhang, L. (2012). Nanoparticle-based combination therapy toward overcoming drug resistance in cancer. *Biochemical Pharmacology, 83*(8), 1104-1111.

Huang, C.-T., Tsai, M.-J., Lin, Y.-H., Fu, Y.-S., Huang, Y.-B., Tsai, Y.-H., & Wu, P.-C. (2013). Effect of microemulsions on transdermal delivery of citalopram: optimization studies using mixture design and response surface methodology. *International Journal of Nanomedicine, 8*, 2295-2304.

Huang, Z., Hua, S., Yang, Y., & Fang, J. (2008). Development and evaluation of lipid nanoparticles for camptothecin delivery: a comparison of solid lipid nanoparticles, nanostructured lipid carriers, and lipid emulsion. *Acta Pharmacologica Sinica, 29*(9), 1094-1102.

Ichikawa, H., Watanabe, T., Tokumitsu, H., & Fukumori, Y. (2007). Formulation considerations of gadolinium lipid nanoemulsion for intravenous delivery to tumors in neutron-capture therapy. *Current Drug Delivery, 4*(2), 131-140.

Indira, U., & Shankar, U. (2012). Proniosomes as a drug carrier: a review. *International Journal of Pharmaceutical Sciences and Research, 3*(12), 4617-4625.

Isaac, M., & Holvey, C. (2012). Transdermal patches: the emerging mode of drug delivery system in psychiatry. *Therapeutic Advances in Psychopharmacology, 2*(6), 255-263.

Jaiswal, M., Dudhe, R., & Sharma, P. (2015). Nanoemulsion: an advanced mode of drug delivery system. *3 Biotech, 5*(2), 123-127.

Kale, S. N., & Deore, S. L. (2017). Emulsion micro emulsion and nano emulsion: A review. *Systematic Reviews in Pharmacy, 8*(1), 39-47.

Khanna, S., Katre, O., & Drabhu, S. (2010). Lecithinized microemulsion for topical delivery of tretionoin. *International Journal of Research in Drug Delivery, 2*(4), 711-719.

Khatoon, M., Shah, K. U., Din, F. U., Shah, S. U., Rehman, A. U., Dilawar, N., & Khan, A. N. (2017). Proniosomes derived niosomes: recent advancements in drug delivery and targeting. *Drug Delivery, 24*(2), 56-69.

Khatri, S., Lohani, P., & Gandhi, S. (2013). Nanoemulsions in cancer therapy. *Indo Global Journal of Pharmaceutical Sciences, 3*(2), 124-133.

Khodakiya, A. S., Chavada, J., Jivani, N., Patel, B. N., Khodakiya, M. S., & Ramoliya, A. P. (2012). Microemulsions as enhanced drug delivery carrier: An overview. *American Journal of Pharmtech Research*, 206-226.

Koh, D., Wang, H., Lee, J., Chia, K., Lee, H., & Goh, C. (2003). Basal cell carcinoma, squamous cell carcinoma and melanoma of the skin: analysis of the Singapore Cancer Registry data 1968–97. *British Journal of Dermatology, 148*(6), 1161-1166.

Kretzer, I. F., Maria, D. A., & Maranhão, R. C. (2012). Drug-targeting in combined cancer chemotherapy: tumor growth inhibition in mice by association of paclitaxel and etoposide with a cholesterol-rich nanoemulsion. *Cellular Oncology, 35*(6), 451-460.

Kriwet, K., & Müller-Goymann, C. C. (1995). Diclofenac release from phospholipid drug systems and permeation through excised human stratum corneum. *International Journal of Pharmaceutics, 125*(2), 231-242.

Kurangi, B. K., & Jalalpure, S. S. (2018). Review of selected herbal phytoconstituents for potential melanoma treatment. *Indian Journal of Health Sciences and Biomedical Research, 11*(1), 3-11.

La, C. P. (2009). Mechanism of drug sensitivity and resistance in melanoma. *Current Drug Delivery, 9*(3), 391-397.

Lawrence, M. J., & Rees, G. D. (2000). Microemulsion-based media as novel drug delivery systems. *Advanced Drug Delivery Reviews, 45*(1), 89-121.

Liu, D., Liu, F., Liu, Z., Wang, L., & Zhang, N. (2011). Tumor specific delivery and therapy by double-targeted nanostructured lipid carriers with anti-VEGFR-2 antibody. *Molecular Pharmaceutics, 8*(6), 2291-2301.

Liu, D., Liu, Z., Wang, L., Zhang, C., & Zhang, N. (2011). Nanostructured lipid carriers as novel carrier for parenteral delivery of docetaxel. *Colloids and Surfaces B: Biointerfaces, 85*(2), 262-269.

Lopes, L. B., J Garcia, M. T., & LB Bentley, M. V. (2015). Chemical penetration enhancers. *Therapeutic Delivery, 6*(9), 1053-1061.

Marianecci, C., Di Marzio, L., Rinaldi, F., Celia, C., Paolino, D., Alhaique, F., ... & Carafa, M. (2014). Niosomes from 80s to present: the state of the art. *Advances in colloid and interface science*, *205*, 187-206.

Mishra, A., Panola, R., & Rana, A. (2014). Microemulsions: As drug delivery system. *Journal of Scientific and Innovative Research, 3*(4), 467-474.

Moghimi, H. R., Williams, A. C., & Barry, B. W. (1996). A lamellar matrix model for stratum corneum intercellular lipids. II. Effect of geometry of the stratum corneum on permeation of model drugs 5-fluorouracil and oestradiol. *International Journal of Pharmaceutics, 131*(2), 117-129.

Morrow, D., McCarron, P., Woolfson, A., & Donnelly, R. (2007). Innovative strategies for enhancing topical and transdermal drug delivery. *The Open Drug Delivery Journal, 1*, 36-59.

Mosallaei, N., Jaafari, M. R., Hanafi-Bojd, M. Y., Golmohammadzadeh, S., & Malaekeh-Nikouei, B. (2013). Docetaxel-loaded solid lipid nanoparticles: preparation, characterization, in vitro, and in vivo evaluations. *Journal of Pharmaceutical Sciences, 102*(6), 1994-2004.

Mukherjee, S., Ray, S., & Thakur, R. (2009). Solid lipid nanoparticles: a modern formulation approach in drug delivery system. *Indian Journal of Pharmaceutical Sciences, 71*(4), 349-358.

Naseri, N., Valizadeh, H., & Zakeri-Milani, P. (2015). Solid lipid nanoparticles and nanostructured lipid carriers: structure, preparation and application. *Advanced Pharmaceutical Bulletin, 5*(3), 305-313.

Naves, L. B., Dhand, C., Venugopal, J. R., Rajamani, L., Ramakrishna, S., & Almeida, L. (2017). Nanotechnology for the treatment of melanoma skin cancer. *Progress in Biomaterials, 6*(1-2), 13-26.

Okumura, K., Nakase, M., Inui, M., Nakamura, S., Watanabe, Y., & Tagawa, T. (2008). Bax mRNA therapy using cationic liposomes for human malignant melanoma. *The Journal of Gene Medicine: A cross-Disciplinary journal for Research on the Science of Gene Transfer and its Clinical Applications, 10*(8), 910-917.

Paluncic, J., Kovacevic, Z., Jansson, P. J., Kalinowski, D., Merlot, A. M., Huang, M. L.-H., . . . Richardson, D. R. (2016). Roads to melanoma: Key pathways and emerging players in melanoma progression and oncogenic signaling. *Biochimica et Biophysica Acta (BBA)-Molecular Cell Research, 1863*(4), 770-784.

Paolino, D., Ventura, C. A., Nistico, S., Puglisi, G., & Fresta, M. (2002). Lecithin microemulsions for the topical administration of ketoprofen: percutaneous adsorption through human skin and in vivo human skin tolerability. *International Journal of Pharmaceutics, 244*(1-2), 21-31.

Patel, D. P., Li, P., & Serajuddin, A. T. (2016). Enhanced microemulsion formation in lipid-based drug delivery systems by combining mono-esters of mediumchain fatty acids with di-or tri-esters. *Journal of Excipients and Food Chemicals, 3*(2), 29-44.

Pawar, K. R., & Babu, R. J. (2014). Lipid materials for topical and transdermal delivery of nanoemulsions. *Critical Reviews™ in Therapeutic Drug Carrier Systems, 31*(5).

Peira, E., Carlotti, M. E., Cavalli, R., & Trotta, M. (2006). Azelaic acid sodium salt in the formulation of microemulsions for topical applications. *Journal of Drug Delivery Science and Technology, 16*(5), 375-379.

Prausnitz, M. R., & Langer, R. (2008). Transdermal drug delivery. *Nature Biotechnology, 26*(11), 1261-1268.

Prete, A. C. L., Maria, D. A., Rodrigues, D. b. G., Valduga, C. J., Ibañez, O. C., & Maranhão, R. C. (2006). Evaluation in melanoma-bearing mice of an etoposide derivative associated to a cholesterol-rich nanoemulsion. *Journal of Pharmacy and Pharmacology, 58*(6), 801-808.

Radha, G., Rani, T. S., & Sarvani, B. (2013). A review on proniosomal drug delivery system for targeted drug action. *Journal of Basic and Clinical Pharmacy, 4*(2), 42-48.

Raut, S., Chougule, V., Dongare, S., Nemade, L., & Devmore, P. (2014). Novel approaches to increase transdermal absorption. *International Journal of Biopharmaceutics, 5*(2), 129-136.

Saini, J. K., Nautiyal, U., Kumar, M., Singh, D., & Anwar, F. (2014). Microemulsions: A potential novel drug delivery system. *International Journal of Pharmaceutical and Medicinal Research, 2*(1), 15-20.

Sankhyan, A., & Pawar, P. (2012). Recent trends in niosome as vesicular drug delivery system. *Journal of Applied Pharmaceutical Science, 2*(6), 20-32.

Schwarz, J. C., Klang, V., Hoppel, M., Mahrhauser, D., & Valenta, C. (2012). Natural microemulsions: formulation design and skin interaction. *European Journal of Pharmaceutics and Biopharmaceutics, 81*(3), 557-562.

Sercombe, L., Veerati, T., Moheimani, F., Wu, S. Y., Sood, A. K., & Hua, S. (2015). Advances and challenges of liposome assisted drug delivery. *Frontiers in Pharmacology, 6*, 286-299.

Shen, H., Shi, S., Zhang, Z., Gong, T., & Sun, X. (2015). Coating solid lipid nanoparticles with hyaluronic acid enhances antitumor activity against melanoma stem-like cells. *Theranostics, 5*(7), 755-771.

Shi, S., Han, L., Deng, L., Zhang, Y., Shen, H., Gong, T., . . . Sun, X. (2014). Dual drugs (microRNA-34a and paclitaxel)-loaded functional solid lipid nanoparticles for synergistic cancer cell suppression. *Journal of Controlled Release, 194*, 228-237.

Singh, S., Chaudhari, Y., Singh, R., & Kunwarpuriya, A. (2015). Proniosomes: a recent advancement in vesicular drug delivery system. *World Journal of Pharmaceutical Research,4(4),* 1671-1689.

Singla, S., Hari Kumar, S., & Aggarwal, G. (2012). Proniosomes for penetration enhancement in transdermal system. *International Journal of Drug Development & Research, 4*, 1-13.

Solanki, A. B., Parikh, J. R., & Parikh, R. H. (2009). Preparation, optimization and characterization of ketoprofen proniosomes for transdermal delivery. *International Journal of Pharmaceutical Sciences and Nanotechnology, 2*, 413-420.

Stoelting, D. P., Borrmann, M., Koch, M., Wiese, M., Royer, H.-D., & Bendas, G. (2014). How liposomal cisplatin overcomes chemoresistance in ovarian tumour cells. *Anticancer Research, 34*(1), 525-530.

Tagne, J.-B., Kakumanu, S., & Nicolosi, R. J. (2008). Nanoemulsion preparations of the anticancer drug dacarbazine significantly increase its efficacy in a xenograft mouse melanoma model. *Molecular Pharmaceutics, 5*(6), 1055-1063.

Talegaonkar, S., Azeem, A., Ahmad, F. J., Khar, R. K., Pathan, S. A., & Khan, Z. I. (2008). Microemulsions: a novel approach to enhanced drug delivery. *Recent Patents on Drug Delivery & Formulation, 2*(3), 238-257.

Tamarov, K., Näkki, S., Xu, W., & Lehto, V.-P. (2018). Approaches to improve the biocompatibility and systemic circulation of inorganic porous nanoparticles. *Journal of Materials Chemistry B, 6*(22), 3632-3649.

Thakur, R., Anwer, M. K., Shams, M. S., Ali, A., Khar, R. K., Shakeel, F., & Taha, E. I. (2009). Proniosomal transdermal therapeutic system of losartan potassium: development and pharmacokinetic evaluation. *Journal of Drug Targeting, 17*(6), 442-449.

Tran, M. A., Gowda, R., Sharma, A., Park, E.-J., Adair, J., Kester, M., . . . Robertson, G. P. (2008a). Targeting V600EB-Raf and Akt3 using nanoliposomal-small interfering RNA inhibits cutaneous melanocytic lesion development. *Cancer Research, 68*(18), 7638-7649.

Tran, M. A., Smith, C. D., Kester, M., & Robertson, G. P. (2008b). Combining nanoliposomal ceramide with sorafenib synergistically inhibits melanoma and breast cancer cell survival to decrease tumor development. *Clinical Cancer Research, 14*(11), 3571-3581.

Van Der Maaden, K., Jiskoot, W., & Bouwstra, J. (2012). Microneedle technologies for (trans) dermal drug and vaccine delivery. *Journal of Controlled Release, 161*(2), 645-655.

Vora, B., Khopade, A. J., & Jain, N. (1998). Proniosome based transdermal delivery of levonorgestrel for effective contraception. *Journal of Controlled Release, 54*(2), 149-165.

Vosoughi, E., Lee, J. M., Miller, J. R., Nosrati, M., Minor, D. R., Abendroth, R., . . . Wu, M. (2018). Survival and clinical outcomes of patients with melanoma brain metastasis in the era of checkpoint inhibitors and targeted therapies. *Biomed Central Cancer, 18*(1), 490-497.

Xie, F., Chai, J.-k., Hu, Q., Yu, Y.-h., Ma, L., Liu, L.-y., . . . Zhang, D.-h. (2016). Transdermal permeation of drugs with differing lipophilicity: Effect of penetration enhancer camphor. *International Journal of Pharmaceutics, 507*(1-2), 90-101.

Yamaguchi, Y., Brenner, M., & Hearing, V. J. (2007). The regulation of skin pigmentation. *Journal of Biological Chemistry, 282*(38), 27557-27561.

Yasam, V. R., Jakki, S. L., Natarajan, J., & Kuppusamy, G. (2014). A review on novel vesicular drug delivery: Proniosomes. *Drug Delivery, 21*(4), 243-249.

Yeo, P. L., Lim, C. L., Chye, S. M., Ling, A. P. K., & Koh, R. Y. (2018). Niosomes: a review of their structure, properties, methods of preparation, and medical applications. *Asian Biomedicine, 11*(4), 301-314.

Yuan, J. S., Yip, A., Nguyen, N., Chu, J., Wen, X.-Y., & Acosta, E. J. (2010). Effect of surfactant concentration on transdermal lidocaine delivery with linker microemulsions. *International Journal of Pharmaceutics, 392*(1-2), 274-284.

Chapter 2 : Hydroxytyrosol Proniosomal Formulation for Enhancing Drug Delivery Across Human Cadaver Skin

2.1. Introduction

Oxidative stress (OS) has been proposed to play a major role in developing many diseases such as atherosclerosis, cancer, diabetes, rheumatoid arthritis, and neurological disorders. Thus, the involvement of OS in these diseases highlights the necessity of using antioxidant and anti-inflammatory agents to counteract the effect of overproduction of reactive oxygen species (ROS) related to chronic diseases (Uttara, Singh, Zamboni, & Mahajan, 2009). The OS occurs when there is overproduction of ROS in living cells. ROS are produced by living cells as result of oxidation which are counterbalanced by biological repairing systems. ROS are highly reactive molecules and can damage biomolecules including lipids proteins and nucleic acids and alter their functions (Birben, Sahiner, Sackesen, Erzurum, & Kalayci, 2012). Antioxidants have been proposed to counter OS. Therefore, antioxidants have been used as preventive and therapeutic tools to reduce the oxidative damage that occurs during OS or chronic inflammation (Rahal et al., 2014).

Polyphenol compounds, commonly found in natural products such as fruits, vegetables, wine, olive oil, etc., are known to have anti-oxidant effects (Khurana, Venkataraman, Hollingsworth, Piche, & Tai, 2013). Hydroxytyrosol (2-[3,4-dihydroxyphenyl] ethanol, HT), in olives, is one of the most potent antioxidant agents in nature. It has many biological activities such as antioxidant, anticancer, cardio-protective, neuroprotective and anti-inflammatory activities (Cicerale, Lucas, & Keast, 2012). The presence of an o-dihydroxyphenyl moiety is the main reason for its high antioxidant activity (Fernández-Bolaños, López, López-García, & Marset, 2012). Further, HT has

antioxidant ability by inhibiting the oxidative stress after lipopolysaccharide (LPS) induced effects (Fuccelli, Fabiani, & Rosignoli, 2018). HT shows a protective effect against UVB induced DNA damage through its antioxidant effect (Guo, An, Jiang, Geng, & Zhong, 2010). HT lowers the lipid profile by inhibiting the oxidation of low density lipoproteins (LDLs) and low density lipoproteins carrying cholesterol (LDL-C). Inhibiting the oxidation of LDLs and LDL-C, HT helps prevent the development of atherosclerosis and other cardiovascular diseases (Bulotta et al., 2014). HT also has been reported to inhibit platelet aggregation in rats (Peyrol, Riva, & Amiot, 2017) and has antitumor effect in breast cancer (Sirianni et al., 2010), colon cancer, (Terzuoli et al., 2017), melanoma (D'angelo et al., 2005), and prostate cancer cell lines (Zubair et al., 2017). HT has anti-inflammatory effects by inhibiting lipoxygenases like lipoxgenase-5, and lipoxgenase-12 and inflammatory markers cyclooxygenase 2 (COX2) and Tumor Necrosis Factor alfa (TNF-alpha) (Kohyama, Nagata, Fujimoto, & Sekiya, 1997). (Fuccelli et al., 2018).

Although HT is well absorbed, it has very low oral bioavailability due to extensive first pass metabolism in (De La Torre, 2008). Topical delivery of HT would be beneficial especially when high local skin concentrations are desired for chemopreventive and skin anti-aging effects.

Nanocarrier systems have been widely studied for improving the efficacy of drugs by the transdermal route. Liposome and niosome are non-polymeric nanoparticle or vesicular systems which show promise to cross the skin barrier. Those carriers interact with, and improve the permeability of drug across stratum corneum (Schreier & Bouwstra, 1994). The main problem with nanocarriers is physical instability such as sedimentation, aggregation and leakage (Yasam, Jakki, Natarajan, & Kuppusamy, 2014). Proniosomes,

the dry form of niosomes, overcome the physical instability problem of the niosomal preparations and provide additional suitability in transportation, distribution, storage and dosing. Proniosome gel is a semisolid liquid crystal product of nonionic surfactants which can be prepared by dissolving the surfactant and phospholipid in small amount of alcohol and the least amount of water (Radha, Rani, & Sarvani, 2013).

The main objective of this study is developing and optimizing a topical and transdermal formulation for HT.

2.2. Materials

Hydroxytyrosol was obtained from Allicon pharmaceuticals (Changzhou,Jiangsu,China). Phosphatidylcholine was purchased from Spectrum Chemical Corporation (Gardena, CA). Ethanol was purchased from Letco Medical (Decatur, AL). Trifluoroacetic acid and acetonitrile were purchased from EMD Chemical Inc. (Gibbstown, NJ). Cholesterol was purchased from JT Baker (Phillipsburg, NJ) and other reagents were purchased from VWR International (West Chester, PA).

2.3. Methods

2.3.1. Preparation of proniosomes

The composition of formulations is shown in Table 1. Proniosomes were prepared by coacervation in which the surfactant, lecithin and cholesterol were taken in a dry wide mouth glass vial and mixed with ethanol. After mixing, the vial was covered to prevent solvent loss and heated in a water bath at 40^{o}C until all ingredients dissolved. After that, HT as an aqueous solution was added and mixed well, and the mixture was further heated in a water bath (40^{o}C) for ~5 min until a clear solution was obtained. Then, the solution

was left in dark at room temperature until the dispersion was converted to a proniosomal gel (Vora, Khopade, & Jain, 1998).

2.3.2. HT encapsulation efficiency

The drug entrapment efficiency was determined by hydrating the proniosomes to the corresponding niosome. For this, 1 g of proniosomal gel was weighed in a glass tube and 10 ml of distilled water was added and mixed well. The aqueous suspension thus obtained was sonicated for 30 min. After that, the resulting niosomes were incubated in a dialysis sac (cellulose tubing, molecular weight cut off 12,000 Daltons) and dialyzed against 100 ml of distilled water for 6 hours at 4 ºC. The amount of drug in the dialysate was taken as a measure of the free drug. To calculate the encapsulation efficiency:

$$\text{Entrapment efficiency (\%)} = [(C_t - C_f)/C_t]100$$

where C_t the total concentration of the drug and C_f is the concentration of free drug (El Maghraby, Ahmed, & Osman, 2015).

2.3.3. Viscosity measurements

The flow behavior and viscosity of the gel were tested using a Bohlin CVO plate and cone rheometer. The viscosity of each formulation was measured at 37 ºC with increasing shear rate from 0 to 100 s^{-1}.

2.3.4. pH and particle size measurement

The pH of the niosome formulations was measured using an Accumet Excel XL15 pH Meter (Fisher Scientific, Suwannee GA). Particle size distribution of the niosome formulations was determined by dynamic light scattering method using a Nicomp 380 ZLS

particle size analyzer (Particle Sizing Systems, Santa Barbara, CA). Each formulation was tested in three replicates. Mean particle size and polydispersity index of the formulations after approprate dilutions were calculated. The particle size was measured in the intensity-weighted mode.

2.3.5. In vitro drug release and skin permeation studies on HT formulations

HT release from the proniosome formulation was preformed using Franz diffusion cells. The dialysis membrane (Regenerated cellulose, molecular weight cut off 12,000 Da, Fisher Scientific Suwanne, GA) was soaked in phosphate buffer solution (PBS) for 30 min before the experiment. The membrane was mounted between the receptor and donor chambers of the vertical Franz diffusion cell apparatus (PermeGear, Bethlehem, PA). The receptor surface area of the membrane was 0.64 cm^2. The receptor chamber was filled with 5 mL of PBS (pH 7.4). The receptor cell was stirred with a magnetic bead at 600 rpm. The temperature of the jacket was maintained at 37±0.5 C°. The donor chamber was filled with 0.5 mL of the formulation. One mL was withdrawn from the receptor cell at 2, 4, 6, 8, 12 and 24 hours, replenished with fresh buffer solution, and a correction factor was applied for drug removed due to sampling. The samples were assayed by HPLC. Each formulation was tested in three replicates.

2.3.6. Drug release analysis

The release data were subjected to analysis to find the best fit by a particular kinetic model. The Korsmeyer and Peppas model (Alsaqr, Rasoully, & Musteata, 2015) was used to describe drug release:

$$M_t/M_\infty = k \cdot t^n$$

where M_t/M_∞ was the fraction of drug released at time t, k is the kinetic constant of the system, and n is the release exponent. The n value was used to differentiate between different release mechanisms as follows: Fickian diffusion (Higuchi release) for n=0.5, non-Fickian release for 0.5 < n < 1, zero-order release (case II transport) for n=1, and super case II transport for n >1.

Other models were analyzed to determine the best fit like zero order, first order (Wagner, 1969), and Higuchi model (Higuchi, 1961). Microsoft Excel 2010 and Graphpade prism (Graphpad software, La Jolla, CA) were used to perform the curve fitting. The model with highest the R^2 was consider the best fitting model.

For skin permeation studies, the dialysis membrane was replaced by human cadaver skin. The dermatomed human skin (thickness: 0.5 mm) was obtained from Sciencecare (Phoenix AZ). It was collected from a single donor within 8 h of death and frozen at 80 ^{o} C until use. The frozen skin was thawed at room temperature for about 45 minutes prior to skin permeation experiments. To remove any traces of glycerol, the skin was washed and thoroughly rinsed with pH 7.4 PBS.

The cumulative amount of DAB that diffused through the membrane or skin was calculated as:

$$\mathrm{Cum_n} = \mathrm{V_R} \cdot \mathrm{C_n} + \mathrm{V_{col.}} \sum_{i=1}^{n-1} \mathrm{C_i}$$

Where Cum_n was the cumulative amount of HT in the receptor medium, V_R was the receptor volume; C_n was the concentration of the n^{th} sample, $V_{col.}$ was the collected sample volume, and C_i was the concentration of the i^{th} sample. In this study, the receptor solution volume was 5 mL and the collected volume was 1 mL.

Diffusion parameters were calculated by plotting the cumulative amount permeated for 24 hours versus time. The slope of the curve was the flux (J) and the enhancement factor (EF) of each penetration enhancer was calculated using:

$$EF = J_p / J$$

where J_p is the flux for the formulation and J_c is the flux for the drug solution.

2.3.7. Skin retention

Following the 24 hour permeation study, the residual formulation on the surface of the skin was removed using a dropper pipette, and the skin was cleaned with PBS buffer using cotton swabs. The active diffusion area of the skin was cutout, weighed, minced and placed in individual vials with 1 mL of receptor media and refrigerated overnight. The samples were then warmed to room temperature, sonicated for 15 minutes and the supernatant was filtered using 0.22 µm syringe filters into HPLC vials for assay. The amount of drug (µg) retained in the skin was normalized to 1 gram of skin.

2.3.8. High performance liquid chromatography analysis

A Waters high performance liquid chromatography (HPLC) system equipped with PDA-UV detector (Alliance 2695 Separation module and 2998 PDA detector) (Waters Corporation, Milford, MA) was used in this study. The chromatographic separation was performed on a reversed phase Phenomenex, Luna® C18 Column (5 µm, 250 × 4.6 mm). The mobile phase consisted of acetonitrile: water (0.05 Trifluoroacetic acid) 90:10. Samples were eluted isocratically at a flow rate of 1mL/min at ambient temperature. The absorbance wavelength was 210 nm and the run time was 20 minutes.

2.3.9. Statistical analysis

All results were presented as mean ± standard error of mean (SEM). Statistical analysis was preformed using graph Pad Prism software. All data was subjected to one-way analysis of variance (ANOVA) followed by Turkey-Kramer multiple comparisons test to determine the statistical levels of significance. P values less than 0.05 were considered statistically significant.

2.4. Results and discussion

Although HT is well absorbed after oral dosing, the bioavailability is poor (6%) due to extensive first pass metabolism. HT is absorbed quickly with a C_{max} of 13 min, rapidly metabolized and eliminated. One hour from the administration no HT is detectable. The estimated half-life for HT was approximately 8 min (González-Santiago, Fonollá, & Lopez-Huertas, 2010). This short systemic time proves that HT is extensively metabolized or degraded. Therefore, in this study, proniosomes of HT were formulated, optimized and evaluated for transdermal drug delivery. However, transport across the epidermis is governed by physicochemical properties of the drug and skin barrier. The drug released from the formulation diffuses through the stratum corneum to the dermal layer and then into the blood vessels. The diffusion rate of the drug depends upon its molecular weight, partition coefficient, and solubility. HT is water soluble compound with molecular weight of 154.16 g/mol. The Log P of HT is 0.1 (Khalil, Abdelbary, Basha, Awad, & El-Hashemy, 2017). Drugs with Log P values of 1-3 show optimal permeability across the stratum corneum. The hydrophilicity of HT might limit systemic delivery. Proniosome is a promising delivery system which improves the skin permeation of water soluble

compounds such as tolterondine tartrate (Rajabalaya, Leen, Chellian, Chakravarthi, & David, 2016), and non-polar drugs such as bromocriptine (Lather, Sharma, & Pandita, 2016) risperidone (Sambhakar, Paliwal, Sharma, & Singh, 2017), and celecoxib (Alam, Baboota, Kohli, Ali, & Ahuja, 2010).

2.4.1. Preparation of proniosomes

The proniosome gel was prepared by coacervation (Lather et al., 2016; Madan, Ghuge, & Dua, 2016). The main components of the proniosomal gel used in this study are span 60, lecithin, cholesterol, ethanol, and water. Span 60 was selected for the study because of its high transition temperature (53-57 ºC) and chemical structure (long alkyl chain), which provides high drug encapsulation efficiency and low drug leaking (Ramkanth et al., 2018). Lecithin acts as a co-surfactant and penetration enhancer. Cholesterol is important for vesicle formation and acts as a stabilizer for the noisome structure. Using span 60 with cholesterol to prepare proniosomal gel increases the encapsulation efficiency and stability (Thomas & Viswanad, 2012).

The amount of span 60, lecithin, cholesterol, ethanol, and water used in the formulation influenced proniosomal gel formation. The effect of increasing the amount of span 60 on drug encapsulation efficiency and permeation was studied. Further, the effect of lecithin on the encapsulation efficiency and permeation was investigated. The effect of water content on the proniosomal gel permeation was also studied.

Initially, several trials were made to optimize the amount of span 60 that is sufficient to form proniosomal gel. After selecting the amount of span 60 required to form a proniosomal gel, another screening selected the amount of lecithin that will not affect the proniosomal gel formation. From these initial studies six formulations were selected

(Table 2-1). These formulations were then characterized for particle size, drug encapsulation efficiency, viscosity, and pH.

2.4.2. Characterization of formulations

The size of the vesicle is an important factor that affects the biopharmaceutical properties of the carrier. As shown in Table 2-2, the formulations with only span 60 as a surfactant have similar particle sizes and an acceptable polydispersity index value. The formulations with lecithin had a smaller particle size. Furthermore, the formulations exhibit a high encapsulation efficiency and a dermatological pH range (6.2-7.4). Span 60 provided a high encapsulation efficiency but with a larger particle size for atenolol. This appears to be due to the hydrophobicity of the alkyl chain of the sorbitan esters (Ramkanth et al., 2018). Similarly diclofenac ethosomes made with span 80 had a high encapsulation efficiency, but with a larger particle size as compared with liposomes (Ghanbarzadeh & Arami, 2013).

The rheological behavior is an important factor for a transdermal formulation because it affects uniformity and ease of application on the skin. As shown in Figure 2-1, the viscosity decreased with an increase in the rate of shear and the formulations demonstrated a good flow behavior. For topical and transdermal application, the formulation needs an appropriate viscosity to provide longer contact time with skin to achieve better drug accumulation and absorption. In the present study, all the formulations showed similar rheological behavior because they have similar lipid/surfactant composition of 45 to 50%. Different surfactants at similar concentration could demonstrate different rheological behavior based on their ionic nature (Ardelean, Ionescu, & Năstase). However, in the current study, we have fixed the surfactant

composition to achieve similar viscosity so that drug release and skin permeation data of the formulations can be compared.

2.4.3. In vitro drug release

The in vitro release of HT from different proniosome formulations is represented in Figure 2-2. The release profile of HT from proniosomal formulations was significantly slower than the drug solution where 95% was released within 2 hours. This is due to the high transition temperature of span 60 which provides high encapsulation with low drug leakage. Increasing the lecithin content from 13.3% to 15% led to an increase in HT release as seen in P3, P4, and P6. P6, which had a high amount of water and lecithin, and low amount of span 60, showed the maximum HT amount. This might be because of low amounts of span 60 which might make the preparation leakier. Similar results were reported for span 60 used in low amount (Khalil et al., 2017).

P1, P2, and P4 followed zero order release as indicated by the highest correlation coefficient (R^2), where as P3, P5, and P6, followed Higuchi model as indicated by the highest correlation coefficient (R^2) (Table 2-3). There is no direct explanation for the difference in the release profile for the prepared formulations. The difference in the amount of span 60 and water in the formulations might cause different release profiles. Also, the bilayer composition could influence drug release from vesicles. Formulations P2 and P4 with a low water content followed zero order release. Formulation P1 with a low amount of span 60 also followed zero order release. All the other formulations (P2, P5, P6) with a high content of span 60 and water followed Higuchi release kinetics. Since span 60 is the major component responsible for bilayer formation, an increase in surfactant concentration resulted in an increase in drug entrapment and increase in

number of niosomes formed. This can be explained by the fact that all the formulations with a high amount of span 60 showed Higuchi drug release, which is controlled by diffusion. Khalili et al. (2017) showed that different release kinetic profiles (Zero order and Higuchi model) were obtained when span 60 blended with another surfactant changed the bilayer flexibility or drug affinity.

2.4.4. Ex-vivo skin permeation study

The ex-vivo permeation study was conducted across human skin to determine formulation variables on drug permeation and deposition in the skin. The cumulative amount of drug permeated from different formulations is presented in Figure 2-3. All the formulations improved flux dramatically compared to the drug solution as shown in Figure 2-4. This demonstrates the potential of using proniosomes as a carrier for transdermal and topical delivery of a relatively hydrophilic molecule such as HT. As mentioned, the outer layer of skin is the rate limiting step for drugs to pass through the skin. There are several mechanisms that could explain the ability of the niosomes to help drug penetrate across skin including (i) penetration or adsorption of niosomes onto the surface of the skin, (ii) the component of the vesicles act as penetration enhancers and (iii) the niosomes lipid bilayers act as a rate limiting membrane barrier for drugs (Singla, Hari Kumar, & Aggarwal, 2012).

Flux and enhancement ratio were calculated (Table 2-4). The maximum flux obtained was 9.36 $\mu g/cm^2/hr$ from a formulation with a high amount (45%) of span 60. The main reason for this improvement in the permeation of HT is that the span 60 acts as a penetration enhancer by modifying the structure of the stratum corneum. Fang et al (2001) reported that proniosome with span 60 increases skin permeation of estradiol and

improves permeation and flux of ketorolac through the skin (Alsarra, Bosela, Ahmed, & Mahrous, 2005).

Lower flux was observed with formulations that contained lecithin (P3, P4, P6, P7) as compared to those without lecithin (P1, P2, P5). This might due to the reduction in span 60 when adding lecithin to the formulation which might lead to leakage of the drug from the vesicle before it crosses into the skin. Furthermore, span 60 is known as a skin penetration enhancer and lowering the amount of span 60 might affect the drug permeability.

Water is an important factor in the transdermal drug delivery. HT permeation through human skin from different water content proniosomal formulations was tested. Increasing water content led to improved skin permeation and retention of HT (Figure 2-3). The formulation with 0% water (P7) showed very low permeation compared to those with 5% (P2) and 10%(P5). The maximum permeation of HT was with 10% water. This is expected since proniosome should be hydrated to form niosome in order to release and permeate the skin (Ibrahim, Sammour, Hammad, & Megrab, 2008).

2.4.5. Drug retention in human skin

The amount of drug deposited in the skin after treatment with the formulations and drug solution is shown in Figure 2-5. All formulations have a higher deposition of HT in skin compared to the control. This indicates the potential effect of these formulations in crossing the stratum corneum and enhancing drug permeability through the skin. The formulation containing lecithin showed a higher amount of drug retained in skin. This might be due to the high affinity of the lecithin formulation to the skin layer.

2.5. Conclusion

Proniosome is a potential carrier for transdermal delivery of HT. Both skin permeation and retention were improved by the noisome formulations compared to the drug solution. The composition and amount of the proniosome plays a major role in skin absorption. The formulation with higher amounts of span 60 showed the highest permeation. The formulation with lecithin was retained in skin more. The higher the amount of water in the formulation the better the permeation.

Table 2-1 Composition of various HT proniosomal formulations (% w/w)

Code formulation	Span 60	Lecithin	Cholesterol	Ethanol	PBS	Drug	Total
P1	40	-	5	45	9	1	100
P2	45	-	5	45	4	1	100
P3	26.7	13.3	5	45	9	1	100
P4	30	15	5	45	4	1	100
P5	45	-	5	40	9	1	100
P6	30	15	5	40	9	1	100
P7	45	0	5	49	0	1	100

Table 2-2 Entrapment efficiency, particle size and pH of HT proniosomal gel.

Formulation	Entrapment efficiency %	Particle size (μm)	pH
P1	92.8 ± 0.5	1.34	5.12
P2	94.1 ± 0.2	1.43	5.59
P3	92.1 ± 0.2	1.04	5.72
P4	93.1 ± 0.5	1.57	5.80
P5	94.1 ± 1.1	3.52	5.78
P6	92.6 ± 0.4	1.23	6.45

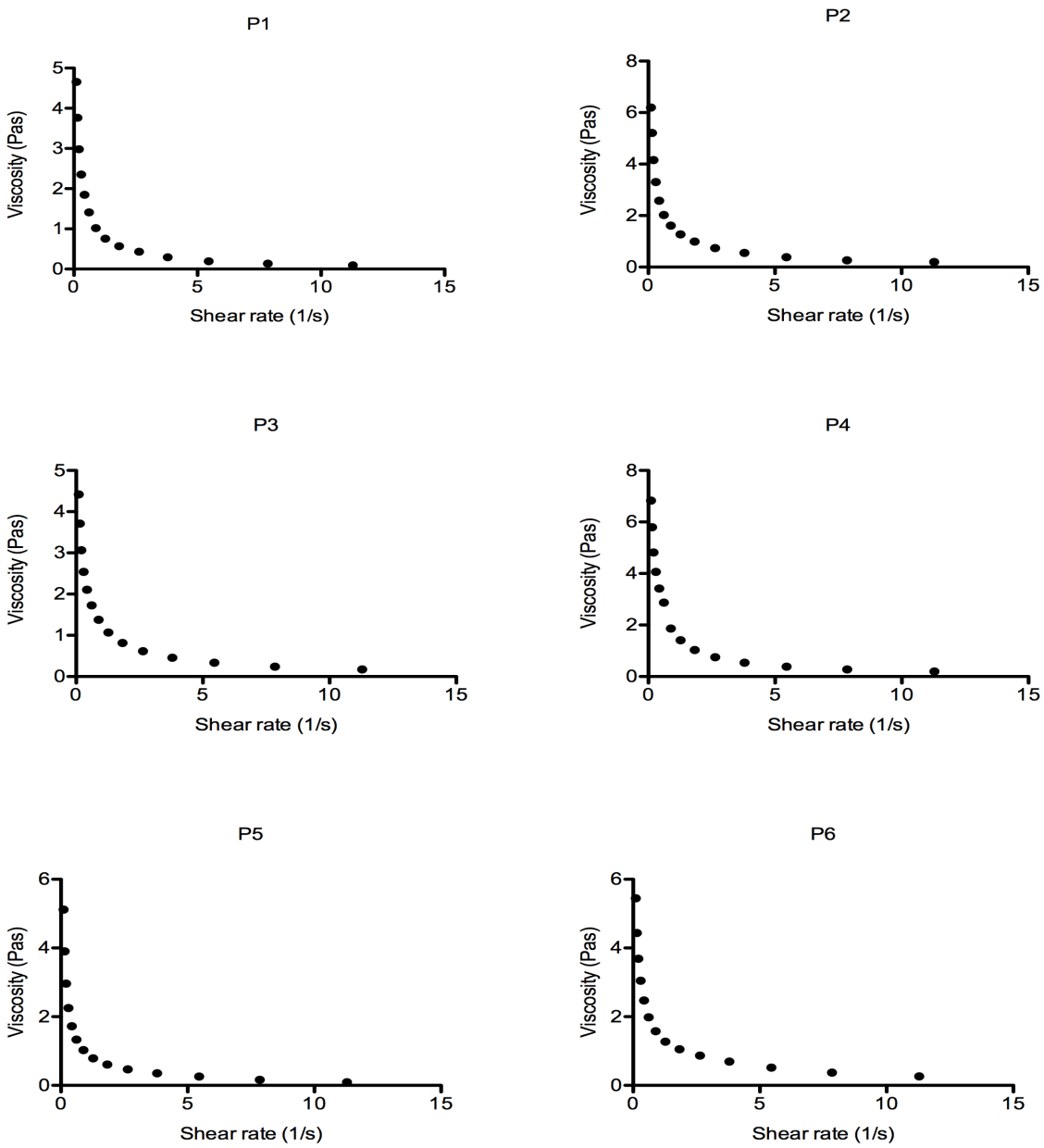

Figure 2-1 Rheological behavior of various proniosomal formulations. Inset of viscosity at specific shear rate ($0.192s^{-1}$). P1, P2, and P3 are proniosomes without lecithin. P3, P4, and P6 are proniosomes with lecithin.

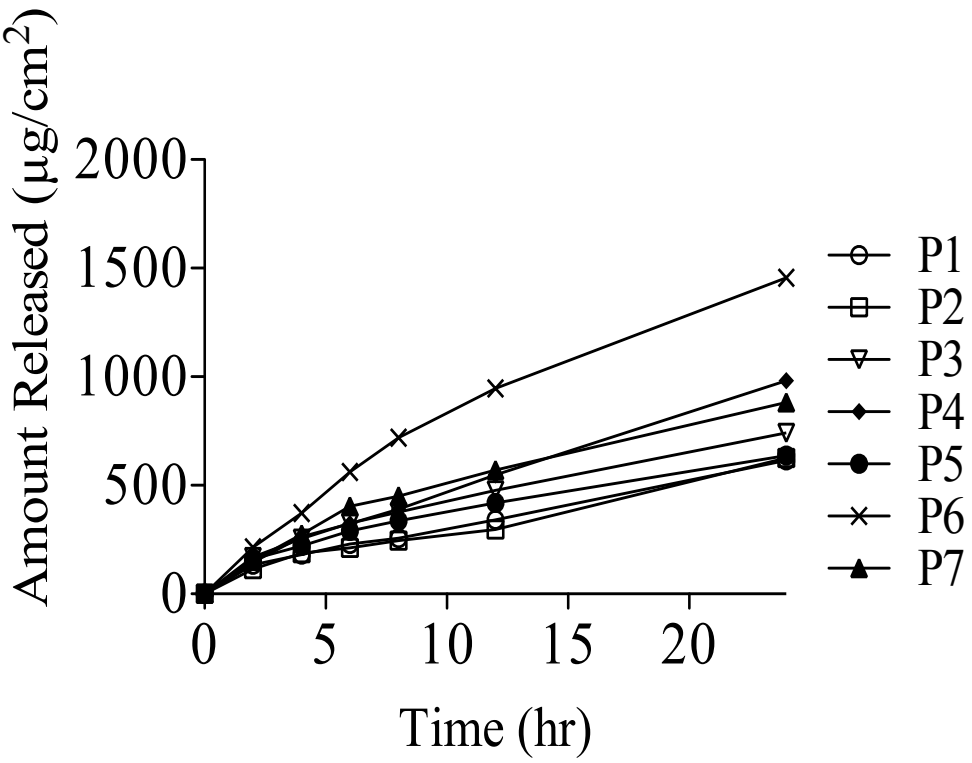

Figure 2-2 In vitro release across dialysis membrane. P1, P2, and P3 are proniosomes without lecithin. P3, P4, and P6 are proniosomes with lecithin.

Table 2-3 Drug release kinetics of HT proniosomes

Formulation code	Zero order	Higuchi order	Krosmeyer and peppas release
	R^2	R^2	R^2
P1	0.998	0.963	0.974
P2	0.980	0.929	0.950
P3	0.986	0.997	0.995
P4	0.998	0.978	0.988
P5	0.984	0.999	0.997
P6	0.970	0.998	0.992

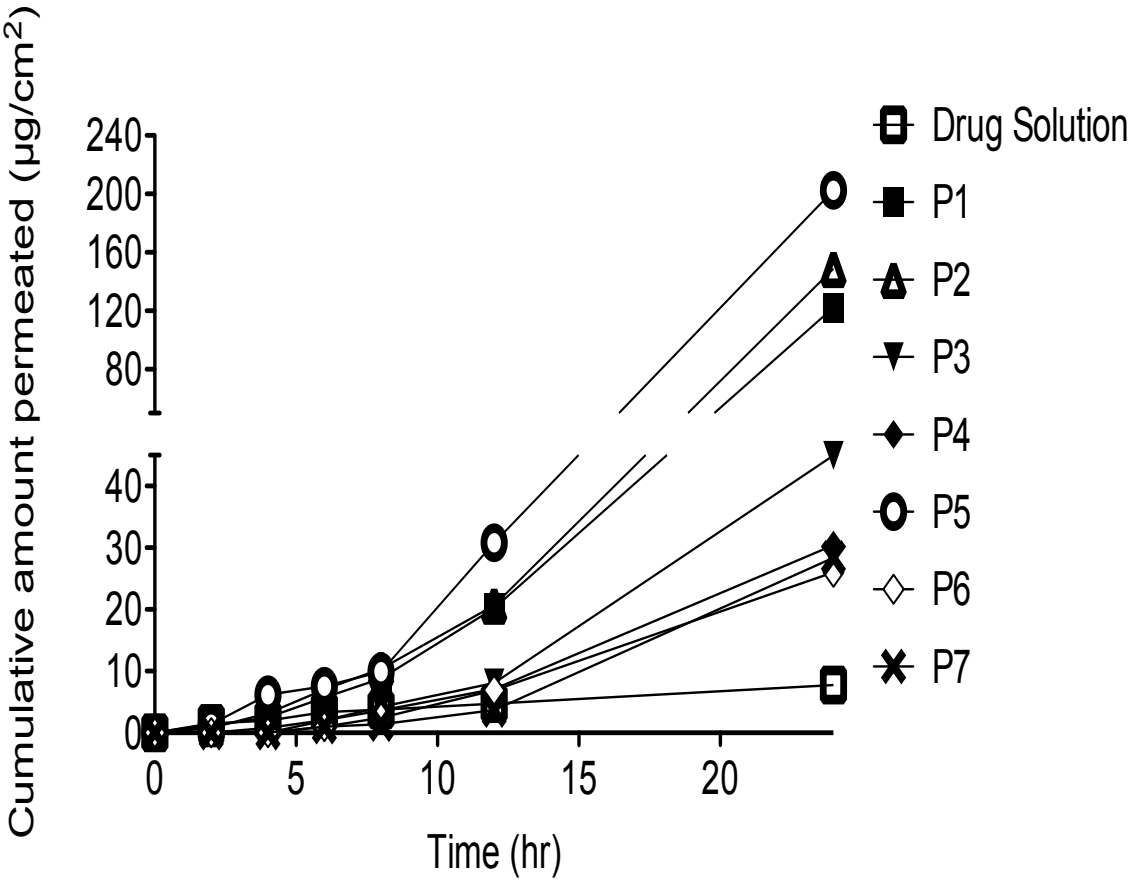

Figure 2-3 HT permeation from proniosomal gel formulation through human skin. P1, P2, and P3 are proniosomes without lecithin. P3, P4, and P6 are proniosomes with lecithin.

Table 3-4 Permeation parameters of HT formulations

Formulation	Flux ($\mu g/cm^2/hr$)	Skin content ($\mu g/gm$)	Enhancement ratio
Drug solution	0.28 ± 0.05	59.9 ± 27	1
P1	6.73 ± 1.42	224 ± 61	24
P2	2.74 ± 1.88	175 ± 64	10
P3	2.11 ± 0.98	619 ± 36	7.5
P4	1.42 ± 0.82	324 ± 102	7.5
P5	7.95 ± 2.30	170 ± 19	28.4
P6	1.24 ± 0.37	483 ± 90	4.4

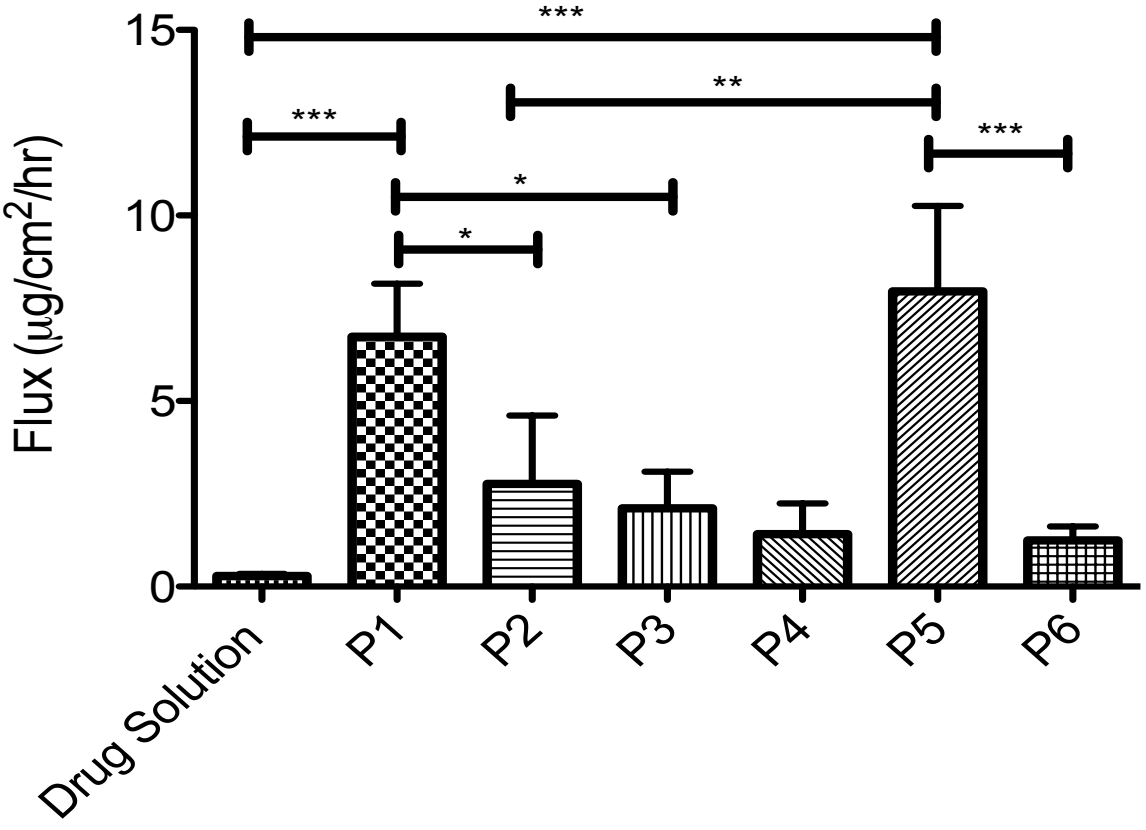

Figure 2-4 Flux of HT permeation across human skin. P1, P2, and P3 are proniosomes without lecithin. P3, P4, and P6 are proniosomes with lecithin. *p<0.05, **p<0.01, ***p<0.001

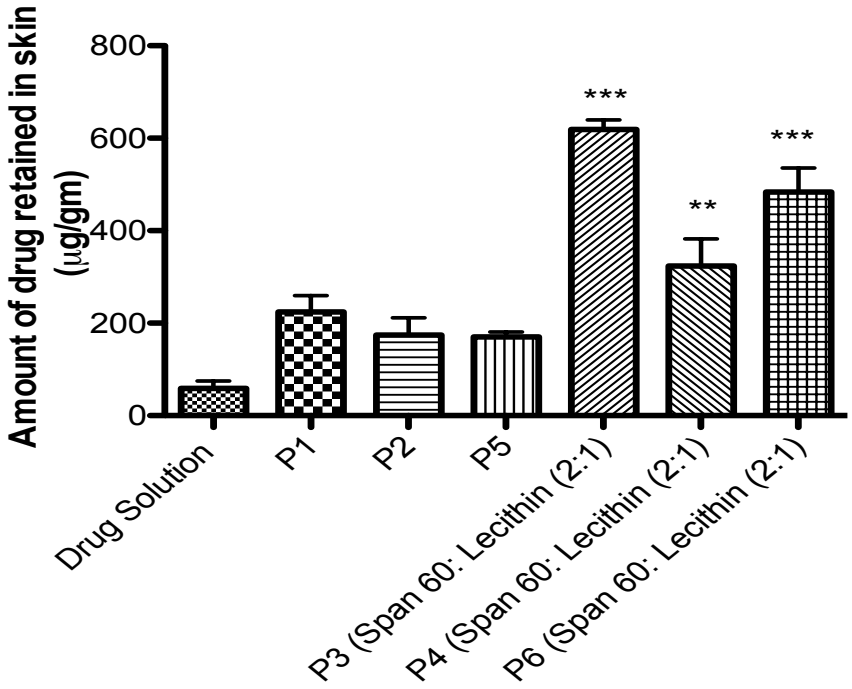

Figure 2-5 HT retention within skin after 24 hour permeation studies. P1, P2, and P3 are proniosomes without lecithin. P3, P4, and P6 are proniosomes with lecithin. *p< 0.05, p<0.01, ***p<0.001

2.6. Reference

Alam, M. I., Baboota, S., Kohli, K., Ali, J., & Ahuja, A. (2010). Pharmacodynamic evaluation of proniosomal transdermal therapeutic gel containing celecoxib. *ScienceAsia, 36*(4), 305-311.

Alsaqr, A., Rasoully, M., & Musteata, F. M. (2015). Investigating transdermal delivery of vitamin D 3. *American Association of Pharmceutical Scientists PharmSciTech, 16*(4), 963-972.

Alsarra, I. A., Bosela, A., Ahmed, S., & Mahrous, G. (2005). Proniosomes as a drug carrier for transdermal delivery of ketorolac. *European Journal of Pharmaceutics and Biopharmaceutics, 59*(3), 485-490.

Ardelean, S., Ionescu, D., & Năstase, V. Rheological and noxious analysis of some semisolid formulations with different types of surfactants. *Journal of Agroalimentary Processes and Technologies, 17(1)*,85-92.

Birben, E., Sahiner, U. M., Sackesen, C., Erzurum, S., & Kalayci, O. (2012). Oxidative stress and antioxidant defense. *World Allergy Organization Journal, 5*(1), 9-19.

Bulotta, S., Celano, M., Lepore, S. M., Montalcini, T., Pujia, A., & Russo, D. (2014). Beneficial effects of the olive oil phenolic components oleuropein and hydroxytyrosol: Focus on protection against cardiovascular and metabolic diseases. *Journal of Translational Medicine, 12*(1), 219-228.

Cicerale, S., Lucas, L., & Keast, R. (2012). Antimicrobial, antioxidant and anti-inflammatory phenolic activities in extra virgin olive oil. *Current Opinion in Biotechnology, 23*(2), 129-135.

D'angelo, S., Ingrosso, D., Migliardi, V., Sorrentino, A., Donnarumma, G., Baroni, A., . . . Galletti, P. (2005). Hydroxytyrosol, a natural antioxidant from olive oil, prevents protein damage induced by long-wave ultraviolet radiation in melanoma cells. *Free Radical Biology and Medicine, 38*(7), 908-919.

de la Torre, R. (2008). Bioavailability of olive oil phenolic compounds in humans. *Inflammopharmacology, 16*(5), 245-247.

El Maghraby, G. M., Ahmed, A. A., & Osman, M. A. (2015). Penetration enhancers in proniosomes as a new strategy for enhanced transdermal drug delivery. *Saudi Pharmaceutical Journal, 23*(1), 67-74.

Fang, J.-Y., Yu, S.-Y., Wu, P.-C., Huang, Y.-B., & Tsai, Y.-H. (2001). In vitro skin permeation of estradiol from various proniosome formulations. *International Journal of Pharmaceutics, 215*(1-2), 91-99.

Fernández-Bolaños, J. G., López, Ó., López-García, M. Á., & Marset, A. (2012). Biological properties of hydroxytyrosol and its derivatives. *In Olive Oil-Constituents, Quality, Health Properties and Bioconversions*: InTechOpen.376-396

Fuccelli, R., Fabiani, R., & Rosignoli, P. (2018). Hydroxytyrosol exerts anti-inflammatory and anti-oxidant activities in a mouse model of systemic inflammation. *Molecules, 23*(12), 3212-3226.

Ghanbarzadeh, S., & Arami, S. (2013). Enhanced transdermal delivery of diclofenac sodium via conventional liposomes, ethosomes, and transfersomes. *BioMed Research International, 2013*.1-7

González-Santiago, M., Fonollá, J., & Lopez-Huertas, E. (2010). Human absorption of a supplement containing purified hydroxytyrosol, a natural antioxidant from olive oil, and evidence for its transient association with low-density lipoproteins. *Pharmacological Research, 61*(4), 364-370.

Guo, W., An, Y., Jiang, L., Geng, C., & Zhong, L. (2010). The protective effects of hydroxytyrosol against UVB-induced DNA damage in HaCaT cells. *Phytotherapy Research: An International Journal Devoted to Pharmacological and Toxicological Evaluation of Natural Product Derivatives, 24*(3), 352-359.

Higuchi, T. (1961). Rate of release of medicaments from ointment bases containing drugs in suspension. *Journal of Pharmaceutical Sciences, 50*(10), 874-875.

Ibrahim, M. M. A., Sammour, O. A., Hammad, M. A., & Megrab, N. A. (2008). In vitro evaluation of proniosomes as a drug carrier for flurbiprofen. *American Association of Pharmceutical Scientists PharmSciTech, 9*(3), 782-790.

Khalil, R. M., Abdelbary, G. A., Basha, M., Awad, G. E., & El-Hashemy, H. A. (2017). Design and evaluation of proniosomes as a carrier for ocular delivery of lomefloxacin HCl. *Journal of Liposome Research, 27*(2), 118-129.

Khurana, S., Venkataraman, K., Hollingsworth, A., Piche, M., & Tai, T. (2013). Polyphenols: Benefits to the cardiovascular system in health and in aging. *Nutrients, 5*(10), 3779-3827.

Kohyama, N., Nagata, T., Fujimoto, S.-i., & Sekiya, K. (1997). Inhibition of arachidonate lipoxygenase activities by 2-(3, 4-dihydroxyphenyl) ethanol, a phenolic compound from olives. *Bioscience, Biotechnology, and Biochemistry, 61*(2), 347-350.

Lather, V., Sharma, D., & Pandita, D. (2016). Proniosomal gel-mediated transdermal delivery of bromocriptine: in vitro and ex vivo evaluation. *Journal of Experimental Nanoscience, 11*(13), 1044-1057.

Madan, J. R., Ghuge, N. P., & Dua, K. (2016). Formulation and evaluation of proniosomes containing lornoxicam. *Drug Delivery and Translational Research, 6*(5), 511-518.

Peyrol, J., Riva, C., & Amiot, M. J. (2017). Hydroxytyrosol in the prevention of the metabolic syndrome and related disorders. *Nutrients, 9*(3), 306-224.

Radha, G., Rani, T. S., & Sarvani, B. (2013). A review on proniosomal drug delivery system for targeted drug action. *Journal of Basic and Clinical Pharmacy, 4*(2), 42-48.

Rahal, A., Kumar, A., Singh, V., Yadav, B., Tiwari, R., Chakraborty, S., & Dhama, K. (2014). Oxidative stress, prooxidants, and antioxidants: the interplay. *BioMed Research International, 2014*.1-19

Rajabalaya, R., Leen, G., Chellian, J., Chakravarthi, S., & David, S. (2016). Tolterodine tartrate proniosomal gel transdermal delivery for overactive bladder. *Pharmaceutics, 8*(3), 27-42.

Ramkanth, S., Chetty, C. M., Sudhakar, Y., Thiruvengadarajan, V., Anitha, P., & Gopinath, C. (2018). Development, characterization & invivo evaluation of proniosomal based transdermal delivery system of Atenolol. *Future Journal of Pharmaceutical Sciences, 4*(1), 80-87.

Sambhakar, S., Paliwal, S., Sharma, S., & Singh, B. (2017). Formulation of risperidone loaded proniosomes for effective transdermal delivery: An in-vitro and in-vivo study. *Bulletin of Faculty of Pharmacy, Cairo University, 55*(2), 239-247.

Schreier, H., & Bouwstra, J. (1994). Liposomes and niosomes as topical drug carriers: Dermal and transdermal drug delivery. *Journal of Controlled Release, 30*(1), 1-15.

Singla, S., Hari Kumar, S., & Aggarwal, G. (2012). Proniosomes for penetration enhancement in transdermal system. *Inernational Journal of Drug Development & Research, 4*, 1-13.

Sirianni, R., Chimento, A., De Luca, A., Casaburi, I., Rizza, P., Onofrio, A., . . . Maggiolini, M. (2010). Oleuropein and hydroxytyrosol inhibit MCF-7 breast cancer cell proliferation interfering with ERK1/2 activation. *Molecular Nutrition & Food Research, 54*(6), 833-840.

Terzuoli, E., Nannelli, G., Frosini, M., Giachetti, A., Ziche, M., & Donnini, S. (2017). Inhibition of cell cycle progression by the hydroxytyrosol–cetuximab combination yields enhanced chemotherapeutic efficacy in colon cancer cells. *Oncotarget, 8*(47), 83207-83224.

Thomas, L., & Viswanad, V. (2012). Formulation and optimization of clotrimazole-loaded proniosomal gel using 32 factorial design. *Scientia Pharmaceutica, 80*(3), 731-748.

Uttara, B., Singh, A. V., Zamboni, P., & Mahajan, R. (2009). Oxidative stress and neurodegenerative diseases: A review of upstream and downstream antioxidant therapeutic options. *Current Neuropharmacology, 7*(1), 65-74.

Vora, B., Khopade, A. J., & Jain, N. (1998). Proniosome based transdermal delivery of levonorgestrel for effective contraception. *Journal of Controlled Release, 54*(2), 149-165.

Wagner, J. G. (1969). Interpretation of percent dissolved-time plots derived from in vitro testing of conventional tablets and capsules. *Journal of Pharmaceutical Sciences, 58*(10), 1253-1257.

Zubair, H., Bhardwaj, A., Ahmad, A., Srivastava, S. K., Khan, M. A., Patel, G. K., . . . Singh, A. P. (2017). Hydroxytyrosol induces apoptosis and cell cycle arrest and suppresses multiple oncogenic signaling pathways in prostate cancer cells. *Nutrition and Cancer, 69*(6), 932-942.

Chapter 3 : Evaluation of DAB compound (a Phyto-Quinoline) Loaded Microemulsion Formulations for Topical Drug Delivery: Preparation, Characterization, In Vitro Release and Cytotoxicity Studies

3.1. Introduction

Natural products from medicinal plants have been used to treat and prevent several diseases. Those medicinal plants are composed of biological active compounds such as flavonoids and alkaloids which are responsible for their effect in treating and preventing some diseases (Atanasov et al., 2015). The anti-cancer effect of those natural products has received much attention. Approximately 60% of commercially available anticancer drugs are from natural plants (Sithranga Boopathy & Kathiresan, 2010).

Boldo is one plant that is extensively studied. Boldine is the major active compound extracted from the leaves and bark of boldo. Studies show a boldine anticancer effect against breast, bladder carcinoma, and glioma cancer cells (Gerhardt et al., 2013). In addition to its anticancer and antioxidant effects, it is also effective in preventing UV induced skin damage and melanoma (Russo et al., 2011). Further, DAB which is a tyrosinase inhibitor, it has been reported that is more effective than kojic acid which is a well known natural product to treat hyperpigmentation. Furthermore, a clinical study conducted in a small group of Caucasians and Asians confirm the strong inhibition of melanogenesis after treatment with topical 4% DAB (Mas-Chamberlin et al., 2004). However, it exhibits a short half-life (30min) and low oral bioavailability as result of extensive first pass metabolism (Joseph, 2016). Therefore, topical administration is an attractive route for delivering DAB as a chemoprevention or lightening agent.

The major advantages of transdermal and topical drug delivery systems are the avoidance of hepatic metabolism, the ability to increase the bioavailability of the drug and reduction of inter-patient difference in gastrointestinal tract absorption.

Microemulsion is a promising drug delivery system for both lipophilic and hydrophilic drugs. The topical or/and transdermal drug delivery of many naturally derived phytochemicals has been improved by microemulsion formulation (Lv et al., 2017; Panapisal, Charoensri, & Tantituvanont, 2012; Rangsimawong et al., 2018; Tabosa et al., 2018). This is a spontaneously formed dispersion composed of oil, water, surfactant and co-surfactant. They are clear and optically isotropic. The droplet size is usually 10-100 nm (Rhee, Choi, Park, & Chi, 2001). Microemulsions have attracted much attention as a topical/transdermal delivery system for several reasons: (1) they are thermodynamically stable, (2) easy to prepare, (3) may enhance the penetration of drug throw skin, and (4) have the capacity to solubilize poorly water-soluble drugs. There are several proposed mechanisms that explain the penetration effect of microemulsions. Increasing skin hydration is suggested as well as small droplet size and large surface. Further, oils or surfactants of the microemulsion could be disrupting the lipid structure of the stratum corneum or increase drug solubility in the stratum cornuem. Microemulsions also have a high drug loading capacity which could improve penetration by providing a high concentration gradient to increase the driving force across the skin (Dreher, Walde, Walther, & Wehrli, 1997; Kogan & Garti, 2006; Kreilgaard, 2002; Salerno, Carlucci, & Bregni, 2010).

To date, there are no published studies on the topical delivery of DAB as a chemopreventive agent against melanoma and skin cancer. Therefore, the object of this

study is to prepare novel microemulsion formulations, study the permeation and retention of DAB in dermatomed human skin, and evaluate its in vitro cytotoxicity against a melanoma cell line (B16 BL6).

3.2. Materials

DAB was obtained from South American Pharmaceutical (Santiago,Chile). Phosphatidylcholine was purchased from Spectrum Chemical Corporation (Gardena, CA). Solutol HS 15 was purchased from BASF (Ludwigshafen, Germany). Ethanol was purchased from Letco Medical (Decatur, AL). Formic acid and acetonitrile were purchased from EMD Chemical Inc. (Gibbstown, NJ). All other reagents were purchased from VWR International (West Chester, PA). Fetal bovine serum, Dulbecco's Modified Eagle's Medium, and other reagents for cell culture were purchased from Mediatech (Manassa, VA). A mouse melanoma cell line (B16BL6) was obtained from the National Cancer Institute (Frederick, MD). Dermatomed human skin (thickness: 0.5 mm) was obtained from Sciencecare (Phoenix AZ). It was collected from a single donor within 8 h of death and frozen at -80 ºC until use.

3.3. Methods

3.3.1. Construction of pseudo ternary phase diagram and preparation of microemulsions

Aqueous titration method was used to construct the phase diagram of the ternary system (oil phase, surfactant, aqueous phase). A mixture of surfactants was dissolved in the oil phase in ratios of 0.5:9.5, 1:9, 1.5:8.5, 2:8, 2.5:7.5, 3:7, 4:6, 5:5, 6:4,7:3, 7.5:2.5, 8:2, 8.5:1.5, 9:1 and 9.5:0.5 in glass vials. Each ratio of surfactant and oil phase was then

titrated drop wise with water using a micropipette with continuous stirring at 25^{o}C until it turned turbid. The percentage composition of each component was determined and plotted on triangular co-ordinates to construct the phase diagrams. The microemulsion compositions are shown in Table 3-1. DAB was dissolved in medium chain triglyceride (MCT) oil under magnetic stirring at room temperature. Then lecithin, solutol and propylene glycol were dissolved in the oil. Finally, water was added and mixed well under stirring for 30 min to obtain clear microemulsion formulations.

3.3.2. In vitro release of DAB from microemulsions

DAB release from the microemulsion formulation was preformed using Franz diffusion cells (PermeGear, Bethlehem, PA). The dialysis membrane (Regenerated cellulose, molecular weight cut off 14,000 Da, Fisher Scientific Suwanne, GA) was soaked in water for 2 hours and mounted between the receptor and donor chambers of the diffusion cell apparatus. The cells had a diffusion surface area of 0.64 cm^2. The receptor chamber was filled with 5 mL of phosphate buffered saline (pH 7.4). The donor chamber was filled with 0.5 mL of the microemulsion. The diffusion cells were maintained at 37±0.5 ^{o}C and stirred with a magnetic beads at 600 rpm. One millimeter samples were withdrawn from the receptor cell at 1, 2, 4, 6, 8, 12 and 24 hours and replenished with fresh buffer solution. A correction factor was applied to account for drug removed due to sampling. The samples were assayed by HPLC. Each formulation was tested in three replicates. There are possible different release mechanisms such as zero order, first order, and Higuchi release, as described in chapter 2. Microsoft Excel 2010 and SigmaPlot 10 were used to perform the curve fitting and statistical analysis were used to find the best fit.

3.3.3. Skin Permeation

The frozen skin was thawed at room temperature for about 20 minutes prior to skin permeation experiments. To remove any traces of glycerol, the skin was washed and thoroughly rinsed with phosphate buffered saline pH 7.4. The skin permeation studies were conducted by the same procedure as the “in vitro release” studies replacing the dialysis membrane with skin.

3.3.4. Data analysis

The cumulative amount of DAB that diffused through the membrane and skin was calculated as:

$$\mathrm{Cum_n} = \mathrm{V_R} \cdot \mathrm{C_n} + \mathrm{V_{col.}} \sum_{\mathrm{i=1}}^{\mathrm{n-1}} \mathrm{C_i}$$

where Cum_n is the cumulative amount of DAB in the receptor medium, V_R is the receptor volume; C_n is the concentration of the n^{th} sample, $V_{col.}$ is the collected sample volume, and C_i is the concentration of the i^{th} sample.

Diffusion parameters were calculated by plotting the cumulative amount permeated in 24 hours versus time. The slope of the curve was the flux (J) and the x-intercept of the straight line was the lag time (Alsaqr, Rasoully, & Musteata, 2015).

3.3.5. Skin retention

Following the 24 hour permeation study, the residual formulation on the surface of the skin was removed using a dropper pipette and the skin was cleaned with phosphate buffered saline using cotton swabs. The active diffusion area of the skin was cut, weighed,

minced and placed in individual vials with 1 mL of receptor media and refrigerated overnight. The samples were then warmed to room temperature, sonicated for 15 minutes, and the supernatant was filtered using 0.22 μm syringe filters into HPLC vials for the assay. The amount of drug (μg) retained in the skin was normalized to 1 gram of skin.

3.3.6. Measurement of cytotoxicity by MTT assay

For cytotoxicity assessment, B16BL6 cells were cultured in flat bottom 96-well plates for 24 hours. The cell density in the wells was 5000 cells/well. The cells received treatments for 24 hours. After 24 hours, 10 μL of 3-[4, 5-dimethylthiazol-2-yl]-2, 5-diphenyl tetrazolium bromide (MTT) was added to each well and the cells were incubated at 37 ºC for an additional 2 hours. Finally, the medium was aspirated and 100 μL dimethylsulfoxide (DMSO) was added to each well to solubilize the dye remaining in the plates. The absorbance was measured using a microplate reader (spectramax M5, molecular devices, Sunnyvale, CA, USA) at 544 nm. All experiments were run in triplicate and mean data were presented.

3.3.7. Live/dead cell staining

Fluorescein diacetate (FDA) and propidium iodide (PI) dyes were used to assess cell cytotoxicity after DAB incubation at a concentration of 50 μg/ml. Cells were incubated with 5 mg/mL FDA and 2 mg/mL propidium iodide (PI) for 4 to 5 mins at 37 ºC to stain live and dead cells, respectively. FDA is a cell-permeable compound and emits a green fluorescence when it is cleaved by esterases. FDA is used to measure both enzymatic

activity and cell membrane integrity. PI is a nucleus staining dye which cannot pass through a viable cell membrane. PI binds to DNA in the nucleus and emits a red fluorescence by passing through the disordered area of dead cell membranes.

3.3.8. High performance liquid chromatography analysis

A Waters high performance liquid chromatography (HPLC) system equipped with PDA-UV detector (Alliance 2695 Separation module and 996 PDA detector) (Waters Corporation, Milford, MA) was used in this study. The chromatographic separation was performed on a reversed phase Phenomenex, Luna® C18 Column (5 µm, 250 × 4.6 mm). The mobile phase consisted of 0.3% formic acid in water (A) and acetonitrile (B) in 80:20 ratio. Samples were eluted at a flow rate of 1mL/min at ambient temperature. The absorbance wavelength was 254 nm and the run time was 30 minutes.

3.3.9. Statistical analysis

All results are presented as mean ± standard error of the mean (SEM). Statistical analysis was preformed using Graph Pad Prism software. All data were subjected to one-way analysis of variance (ANOVA) followed by Turkey-Kramer multiple comparisons test to determine the statistical levels of significance. P value less than 0.05 was considered statistically significant.

3.4. Results and Discussion

3.4.1. Pseudo-ternary phase diagram

Figure 3-1 shows the pseudo-ternary phase diagram of the microemulsion system. The microemulsion system which contains MCT as an oil phase, and lecithin and solutol as a surfactant mixture (S), and propylene glycol as co-surfactant (co-S) demonstrated a very large microemulsion region in the phase diagram. Formulations F1 and F2 were designed based on the location of the stable microemulsion region of the phase diagram.

3.4.2. Characterization of microemulsions

The physical characteristics of the microemulsions are showed in Table 3-2. The particle sizes were below 50 nm and the pH values were around 6. There was no change in the droplet size or transparency when DAB was loaded to the microemulsion formulation. The PDI values were smaller than 0.2, which shows a narrow distribution of particle size. The viscosity of select formulations was 129.2 cP for F1 and 620.6 cP for F2. An increasing the percentage of oil in F2 resulted in a significant increase in the viscosity. The lower viscosity of the formulations enable easy spreadability on skin.

3.4.3. In vitro release and skin permeation studies

The in vitro release study was conducted to show that the drug is not strongly encapsulated by the microemulsion components and readily available for skin permeation. Figure 3-2 shows F1 and F2 had a similar drug release pattern. A steady increase in DAB as a function of time was observed. The in vitro release profiles follow zero-order release kinetics based on the R^2 value. This result is in accordance with other

reports of zero-order release kinetics. Mortazavi SA et al. (2013) have prepared a tretinoin microemulsion formulation which followed zero-order kinetics. Furthermore, the release profile of metronidazole microemulsion followed zero order kinetics (Singh, Anis, Al-Zahrani, & Pal, 2015).

The skin permeation studies on the microemulsion formulations showed no detectable levels of DAB in the receptor phase. However, the drug was significantly retained in the skin after a 24-hour treatment (Figure 3-3). F2 showed significantly higher DAB levels in the skin compared to both F1 and MCT oil. Thus, microemulsion formulation greatly facilitates the accumulation of the drug in the skin as compared to control. F2 penetrated skin up to 13 fold higher than the control (DAB-MCT oil). Microemulsions have been used to improve skin permeation for many drugs. Paolino, et al. (2002) reported that ketoprofen microemulsion showed higher permeation than conventional formulations (emulsion and gel). Furthermore, a microemulsion improved the diclofenac skin permeation compared to liposome formulation (Kriwet & Müller-Goymann, 1995). The transdermal flux for a azelaic acid microemulsion was significantly higher than drug solution (Peira, Carlotti, Cavalli, & Trotta, 2006).

In order to understand the mechanism of skin permeation enhancement by microemulsion formulations, we conducted permeation studies across tape stripped skin (Figure 3-4). As expected, the permeation across the skin after the tape stripping was high. The tape stripping technique removes the stratum corneum enabling the drug to cross the skin. Maximum cumulative amount permeated in 24 hours was seen with microemulsion formulations F1 (437 ± 22 μg/cm^2) and F2 (351 ± 24 μg/cm^2) whereas the permeation for the control was 43.6 ± 28.8 μg/cm^2. This study proves that the stratum

corneum is a significant barrier for skin permeation of DAB. The steady state flux of DAB by the microemulsions (F1 and F2) were 8.61 and 6.54 fold higher as compared to control (MCT oil) (Figure 3-5). The skin content of DAB was highest for F1 (628 ± 43 μg/gm) followed by F2 (546 ± 57 μg/gm) when compared with control (150 ± 62 μg/gm) (Figure 3-6).

Stratum corneum is the rate limiting step for transdermal delivery for many drugs. By removing the stratum corneum DAB permeation and skin retention was enhanced in all formulations. Similar results were obtained for different drugs. Arima et al. (1998) have reported that the flux of 4-biphenylyl acetate, which is a prodrug of the non-steroidal anti-inflammatory drug, across tape stripped skin was greater than that through full thickness skin. Furthermore, the tetramethylpyrazine microemulsion showed a two-fold increase in drug permeation across skin when skin treated with microneedles compared with formulation alone (Zu, Yu, Bi, Zhang, & Di, 2017). A combination of microneedle with microemulsion to deliver celecoxib increased skin permeation more than microemulsion alone (Mojeiko, de Brito, Salata, & Lopes, 2019). All these studies suggest that drug permeation is much higher, especially for hydrophilic drugs, for barrier compromised skin

3.4.4. Cell cytotoxicity assays

Cell cytotoxicity assays were performed using the MTT assay. The effect of microemulsions in the absence and presence of DAB was determined in comparison to DAB dissolved in MCT oil. The percentage of cell cytotoxicity 24 h after treatment is shown in Figures 7 and 8 (DMEM was used as control). Blank microemulsion at the highest concentration did not inhibit cell proliferation. Microemulsion loaded with DAB significantly inhibited cell proliferation compared to the control (DAB dissolved in MCT

oil). The F1 and F2 formulations showed 160-180% higher cytotoxicity toward B16BL6 cell lines compared to control. The half-maximal inhibitory concentrations (IC50) of F1, F2, and MCT formulations against B16BL6 cells were calculated to be 1 μg/mL, 10 μg/mL, and 50 μg/mL, respectively. The live/dead cell staining demonstrated that the microemulsion treated cells showed lower live signal, while DAB-Free showed more live signal and less dead signal (Figure 3-9). In addition, the morphology of cells with DAB-MEs was more spherical, which inhibited the cells were probably damaged.

Microemulsion showed more cytotoxicity and live/dead signal compare to oil solution due to high homogeneity and nanoscale which lead to endocytosis and increased drug uptake. Cells membrane is impermeable to large particles. Particles 10-30 nm can easily cross cell membrane (Kettler, Veltman, van de Meent, van Wezel, & Hendriks, 2014). The amphiphilic properties of surfactant and the small droplet size of the microemulsion have facilitated drug diffusion into the cells and cell endocytosis for several drugs such as etoposide and coix seed oil (Ding Qu et al., 2015), caffeic acid phenethyl ester (Chen, Guan, Baek, & Zhong, 2019), and tamoxifen (Monteagudo, Gándola, González, Bregni, & Carlucci, 2012). Because the droplet size in our microemulsion were less than 40 nm, similar mechanisms likely have contributed to enhanced cellular uptake of DAB and enhanced drug anti-proliferation activities. Many studies have shown improved anti-proliferative activity of drugs after nanoencapsulation. For example, myricetin microemulsion exhibited a significant increase of anti-proliferative activity against liver cancer cells compared to free myricetin (Guo, Fu, Chen, Zhou, & Chen, 2016). A significant better anti-proliferation effect on colon cancer cells for tangeretin prepared in emulsion with lecithin and medium chain triacylglycerol compared to

tangeretin solution (Ting, Chiou, Pan, Ho, & Huang, 2015). Curcumin loaded in nanostructured lipid carriers inhibit the growth of ovarian cancer more than curcumin solution (Bondì et al., 2017).

3.5. Conclusion

An HPLC method for DAB was established by optimizing isocratic flow parameters of the mobile phase. Based on the pseudo-ternary phase diagram, two microemulsion formulations were selected for further studies. The pH of F1 and F2 were 5.26 and 6.5, respectively. The formulations showed a particle size of <50 nm and polydispersity index of <0.2. The ex vivo skin retention study demonstrated that the microemulsions exhibited skin permeation 8-13 fold higher compared with DAB oil in the MCT oil (Control, DAB-MCT). Furthermore, there is a significant increase ($p<0.05$) in cancer cell death for all DAB microemulsions compared to control. The optimized formulations showed 160-180% higher cytotoxicity toward B16BL6 cell lines compared to control. Results of the present study suggest that a microemulsion could be a promising formulation for topical administration of DAB.

Table 3-1 Composition of microemulsion formulations (% w/w)

Formulation	DAB	MCT Oil	Lecithin	Solutol	PG	Water	Total
F1	1%	20%	13%	13%	25%	29%	100%
F2	1%	30%	13%	13%	25%	19%	100%

Table 3-2 Physical properties of microemulsion formulations

Formulation	pH	Particle size (nm)	PI	Viscosity (cP)
F1	5.63	35.7 ± 0.2	0.088	129
F2	6.55	37.6 ± 0.3	0.106	621

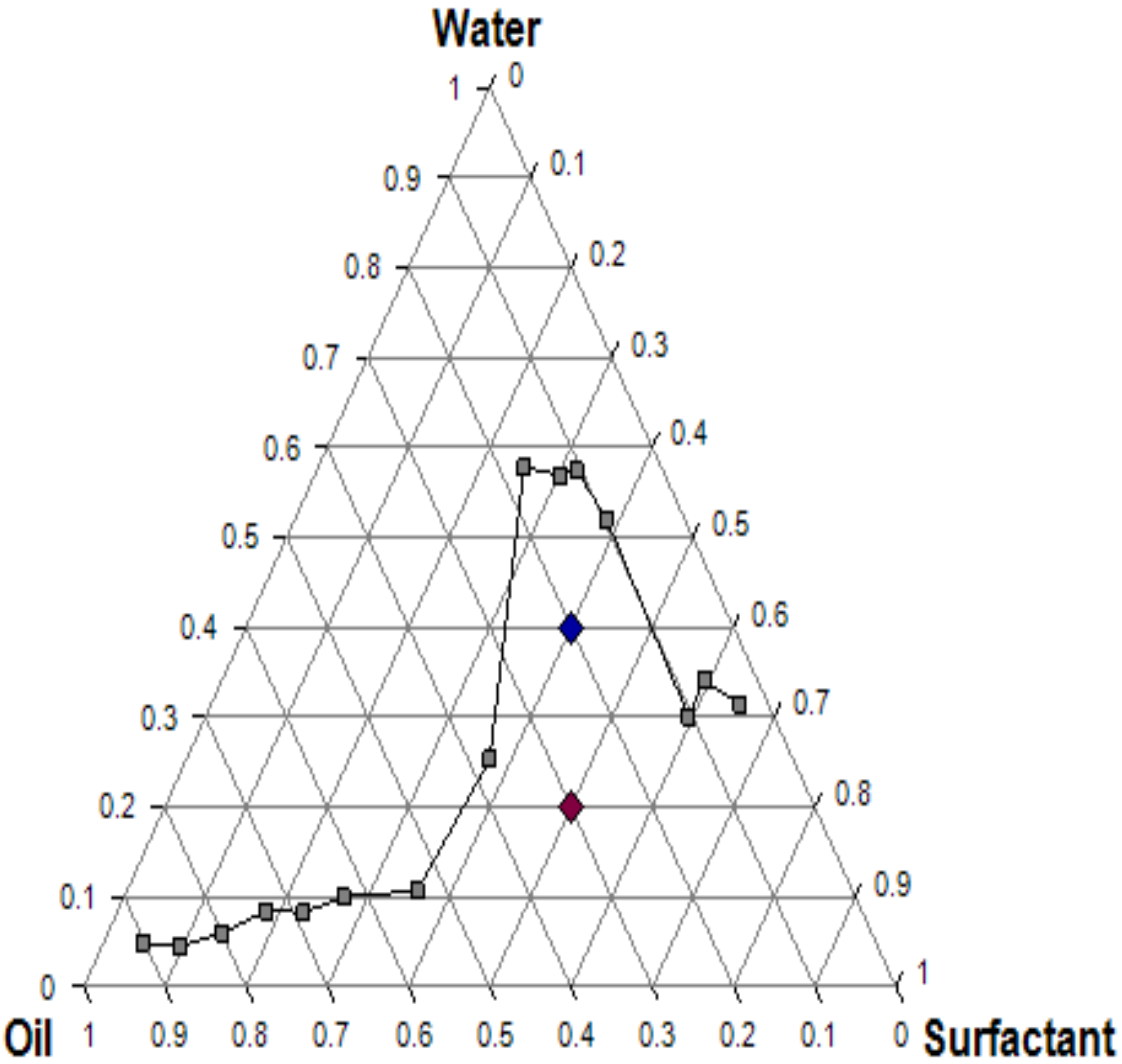

Figure 3-1 Pseudo-ternary phase diagram of MCT Oil, Lecithin, Solutol, Propylene glycol, Water system.

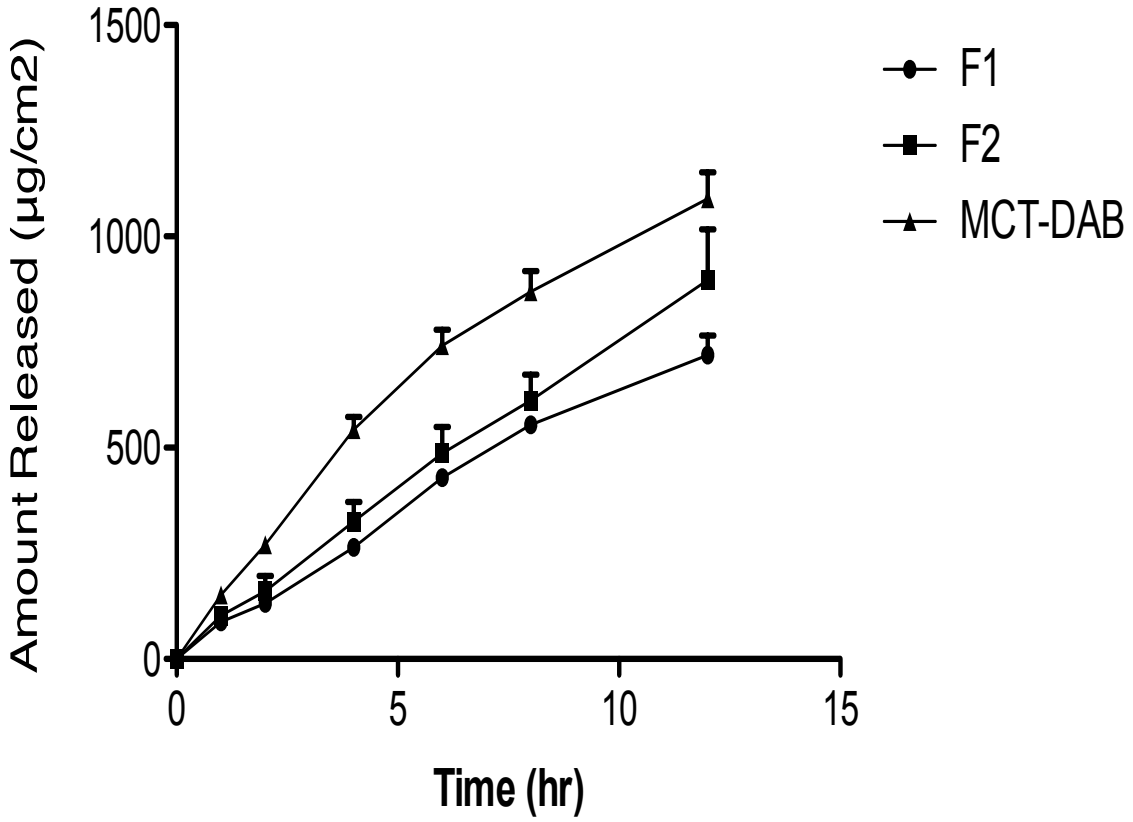

Figure 3-2 In vitro release of F1/F2 formulations across dialysis membrane.

All data are expressed as mean ± S.E.M of n = 3

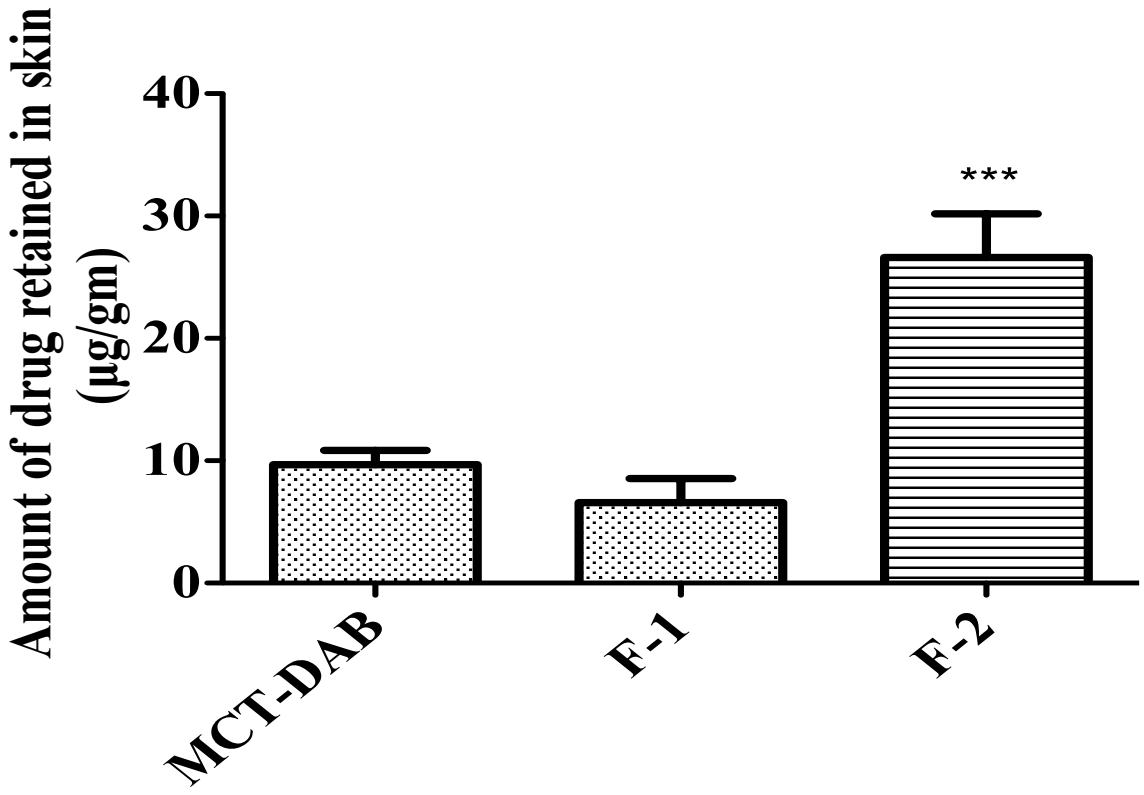

Figure 3-3 DAB retention within skin. All data are expressed as mean ± S.E.M of n = 3.

***p< 0.001 as compared to MCT-DAB and F1.

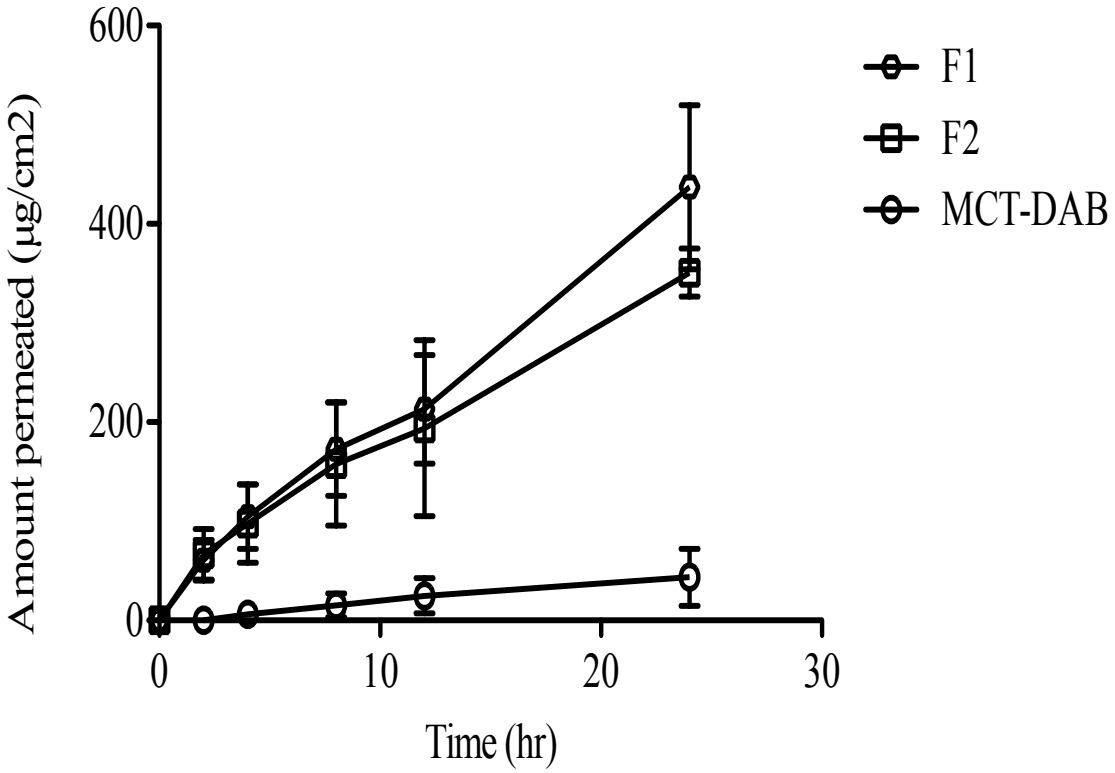

Figure 3-4 Effect of stratum corneum removal on the permeation of DAB across human skin. All data are expressed as mean ± S.E.M of n = 3

.

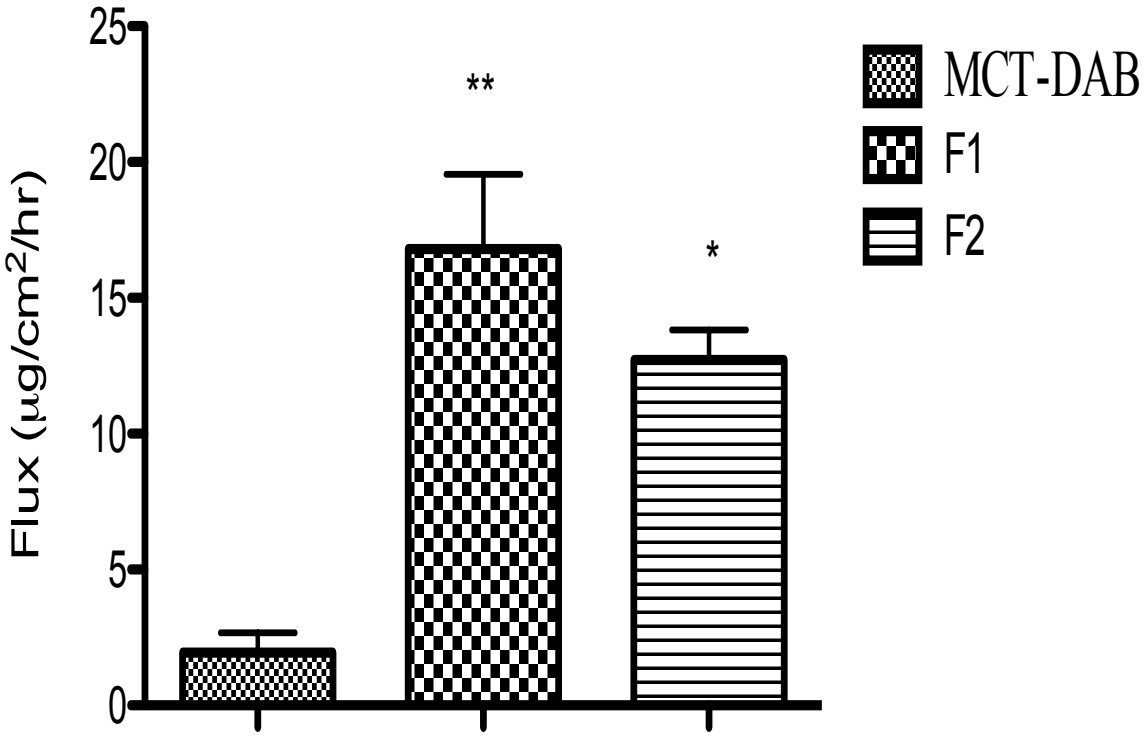

Figure 3-5 Flux of DAB across tape stripped skin. All data are expressed as mean ± S.E.M of n = 3. ** P< 0.01 as compare to MCT-DAB, *p<0.05 as compared to MCT-DAB.

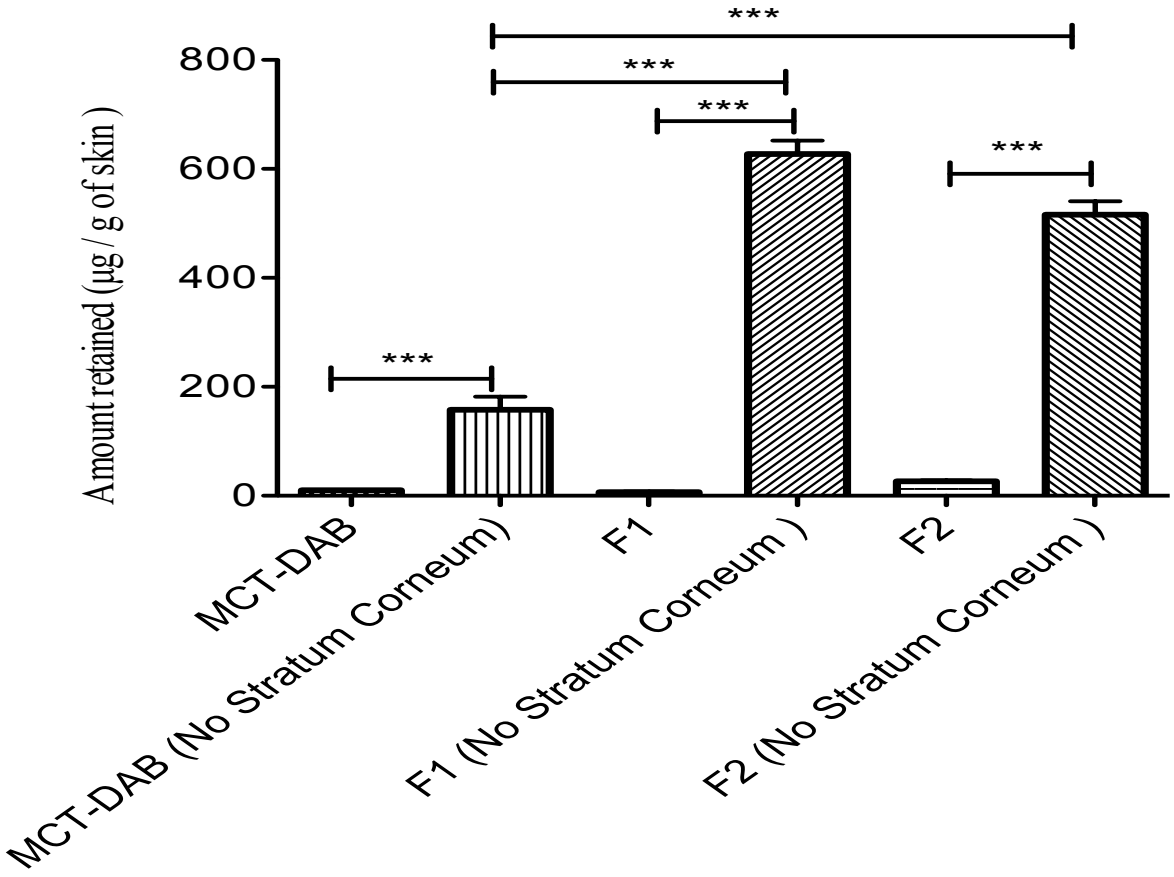

Figure 3-6 Effect of stratum corneum on DAB retained in human skin. All data are expressed as mean ± S.E.M of n = 3. ***p<0.001 as compared with MCT-DAB.

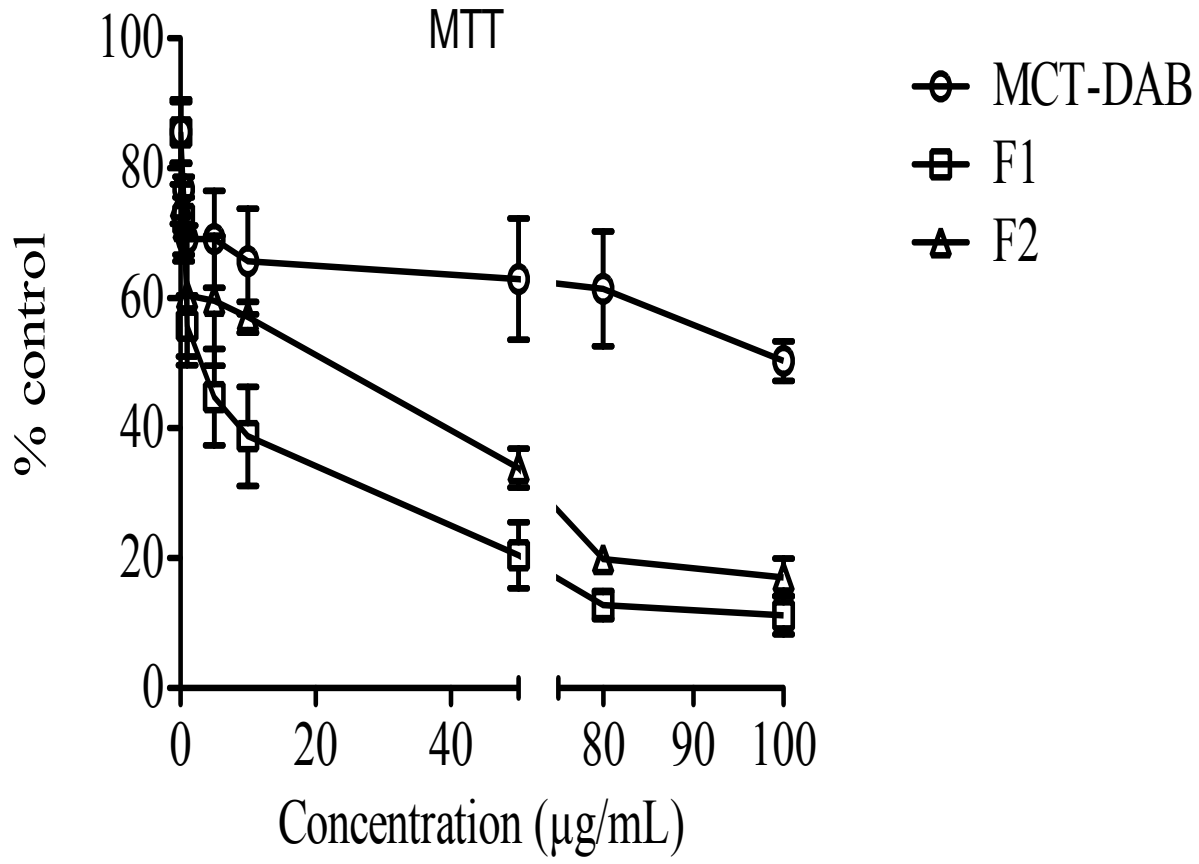

Figure 3-7 Cytotoxic effect of DAB on the B16BL6 cell line. Cells were incubated with various concentrations (0.1,0.5,1,5,10,50,80,100 µg/ml) of different formulations for 24 hours. All data expressed as mean percentages to untreated control cells (n=3).

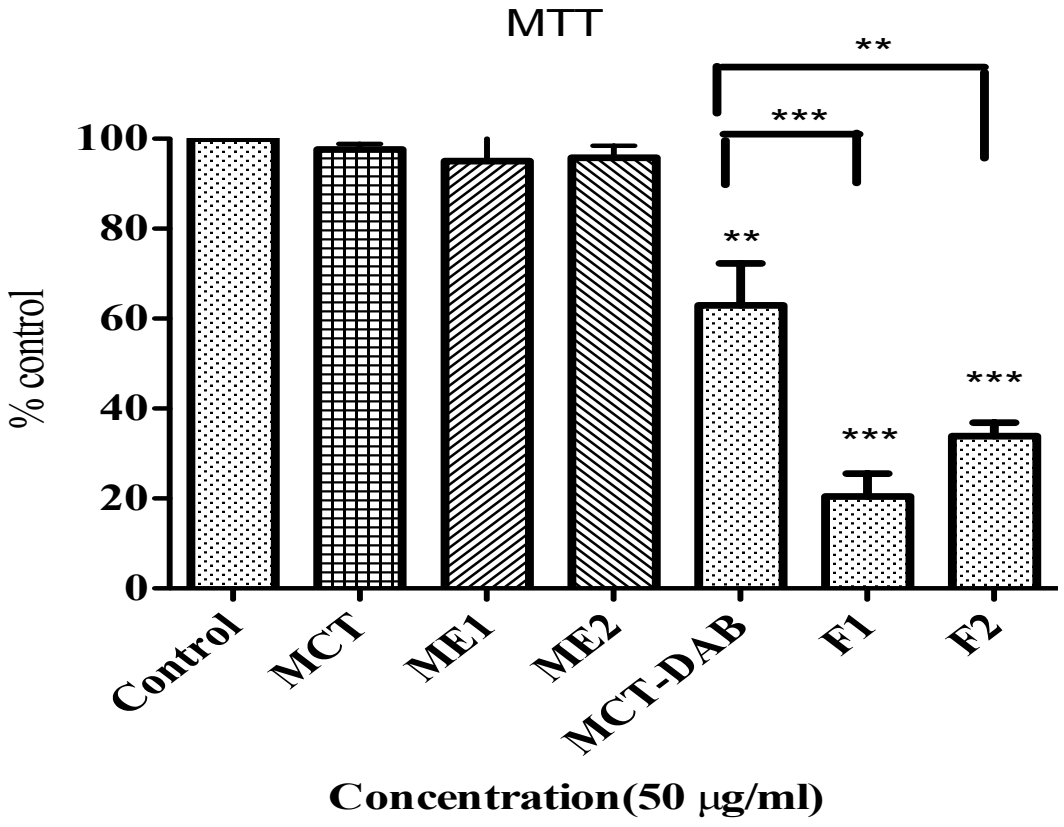

Figure 3-8 In vitro cytotoxicity of formulations with or without DAB in B16BL6 melanoma cell line. All data are expressed as mean ± S.E.M of n = 3. ***p <0.001 when F1and F2 compared to control. **p <0.01 when MCT-DAB compared to control. *** p < 0.001 when F1 compared MCT-DAB. **p <0.01 when F2 compared to MCT-DAB.

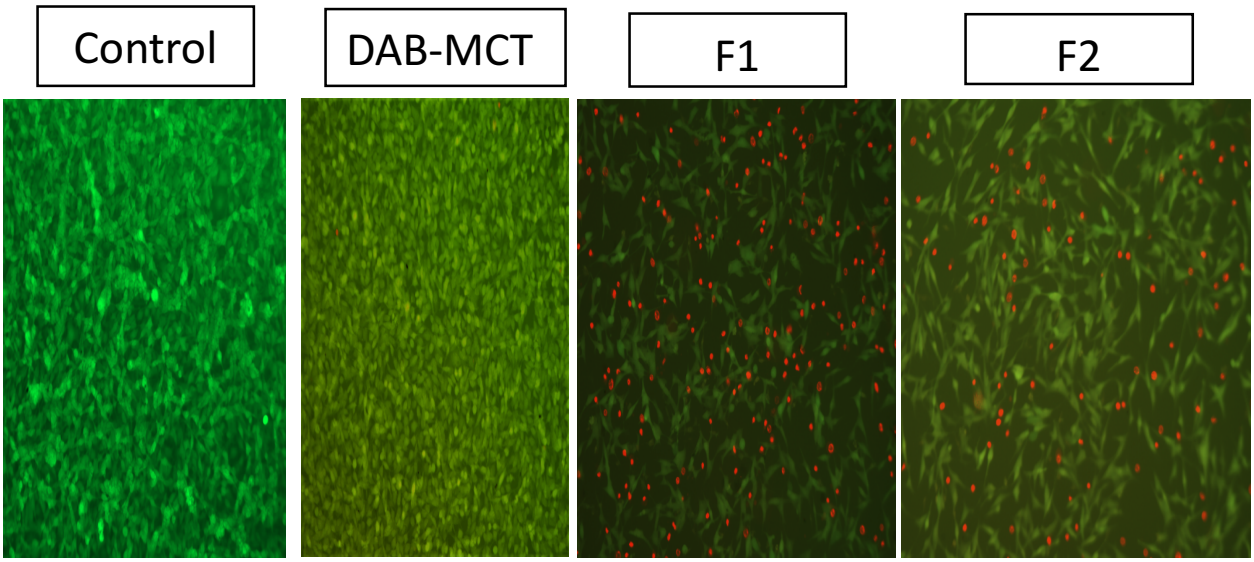

Figure 3-9 Live/dead cell staining of melanoma cell line. Cells were treated with 50 µg/ml for 24 hours. Live cells appear green, while dead cells appear red.

3.6. References

Alsaqr, A., Rasoully, M., & Musteata, F. M. (2015). Investigating Transdermal Delivery of Vitamin D 3. *American Association of Pharmceutical Scientists PharmSciTech, 16*(4), 963-972.

Arima, H., Miyaji, T., Irie, T., Hirayama, F., & Uekama, K. (1998). Enhancing effect of hydroxypropyl-β-cyclodextrin on cutaneous penetration and activation of ethyl 4-biphenylyl acetate in hairless mouse skin. *European Journal of Pharmaceutical Sciences, 6*(1), 53-59.

Atanasov, A. G., Waltenberger, B., Pferschy-Wenzig, E.-M., Linder, T., Wawrosch, C., Uhrin, P., . . . Heiss, E. H. (2015). Discovery and resupply of pharmacologically active plant-derived natural products: A review. *Biotechnology Advances, 33*(8), 1582-1614.

Bondì, M. L., Emma, M. R., Botto, C., Augello, G., Azzolina, A., Di Gaudio, F., . . . Cervello, M. (2017). Biocompatible lipid nanoparticles as carriers to improve curcumin efficacy in ovarian cancer treatment. *Journal of Agricultural and Food Chemistry, 65*(7), 1342-1352.

Chen, H., Guan, Y., Baek, S. J., & Zhong, Q. (2019). Caffeic Acid Phenethyl Ester Loaded in Microemulsions: Enhanced In Vitro Activity against Colon and Breast Cancer Cells and Possible Cellular Mechanisms. *Food Biophysics, 14*(1), 80-89.

Ding Qu, Y. M., Sun, W., Chen, Y., Zhou, J., Liu, C., & Huang, M. (2015). Microemulsion-based synergistic dual-drug codelivery system for enhanced apoptosis of tumor cells. *International Journal of Nanomedicine, 10*, 1173-1187.

Dreher, F., Walde, P., Walther, P., & Wehrli, E. (1997). Interaction of a lecithin microemulsion gel with human stratum corneum and its effect on transdermal transport. *Journal of Controlled Release, 45*(2), 131-140.

Gerhardt, D., Bertola, G., Bernardi, A., Pires, E., Frozza, R., Edelweiss, M., . . . Salbego, C. (2013). Boldine Attenuates Cancer Cell Growth in an Experimental Model of Glioma. *vivo. Journal of Cancer Science & Therapy, 5*, 194-199.

Guo, R. X., Fu, X., Chen, J., Zhou, L., & Chen, G. (2016). Preparation and characterization of microemulsions of myricetin for improving its antiproliferative and antioxidative activities and oral bioavailability. *Journal of Agricultural and Food Chemistry, 64*(32), 6286-6294.

Joseph, S. (2016). *Synthetic and Biological Exploration of (+)-Boldine-Identification of potential CNS receptor ligands*. A thesis in Biochemistery (master's thesis). Hunter College of the City Univeristy of New York.

Kettler, K., Veltman, K., van de Meent, D., van Wezel, A., & Hendriks, A. J. (2014). Cellular uptake of nanoparticles as determined by particle properties, experimental conditions, and cell type. *Environmental Toxicology and Chemistry, 33*(3), 481-492.

Kogan, A., & Garti, N. (2006). Microemulsions as transdermal drug delivery vehicles. *Advances in Colloid and Interface Science, 123*, 369-385.

Kreilgaard, M. (2002). Influence of microemulsions on cutaneous drug delivery. *Advanced Drug Delivery Reviews, 54*, S77-S98.

Kriwet, K., & Müller-Goymann, C. C. (1995). Diclofenac release from phospholipid drug systems and permeation through excised human stratum corneum. *International Journal of Pharmaceutics, 125*(2), 231-242.

Lv, X., Liu, T., Ma, H., Tian, Y., Li, L., Li, Z., . . . Tang, Z. (2017). Preparation of essential oil-based microemulsions for improving the solubility, pH stability, photostability, and skin permeation of quercetin. *American Association of Pharmceutical Scientists PharmSciTech, 18*(8), 3097-3104.

Mas-Chamberlin, C., Peschard, O., Leroux, R., Mondon, P., Lamy, F., & Lintner, K. Di-acetyl-nor-aporphines: Novel Molecules and Novel Mechanism, *Cosmetics, 130(3),* 2004-2012.

Mojeiko, G., de Brito, M., Salata, G. C., & Lopes, L. B. (2019). Combination of microneedles and microemulsions to increase celecoxib topical delivery for potential application in chemoprevention of breast cancer. *International Journal of Pharmaceutics 560,*365-376.

Monteagudo, E., Gándola, Y., González, L., Bregni, C., & Carlucci, A. (2012). Development, characterization, and in vitro evaluation of tamoxifen microemulsions. *Journal of Drug Delivery, 2012,* 1-11.

Mortazavi, S. A., & Pishrochi, S. (2013). Formulation and in-vitro evaluation of tretinoin microemulsion as a potential carrier for dermal drug delivery. *Iranian Journal of Pharmaceutical Research, 12*(4), 599-609.

Panapisal, V., Charoensri, S., & Tantituvanont, A. (2012). Formulation of microemulsion systems for dermal delivery of silymarin. *American Association of Pharmceutical Scientists PharmSciTech, 13*(2), 389-399.

Paolino, D., Ventura, C. A., Nistico, S., Puglisi, G., & Fresta, M. (2002). Lecithin microemulsions for the topical administration of ketoprofen: Percutaneous adsorption through human skin and in vivo human skin tolerability. *International Journal of Pharmaceutics, 244*(1-2), 21-31.

Peira, E., Carlotti, M. E., Cavalli, R., & Trotta, M. (2006). Azelaic acid sodium salt in the formulation of microemulsions for topical applications. *Journal of Drug Delivery Science and Technology, 16*(5), 375-379.

Rangsimawong, W., Wattanasri, P., Tonglairoum, P., Akkaramongkolporn, P., Rojanarata, T., Ngawhirunpat, T., & Opanasopit, P. (2018). Development of microemulsions and microemulgels for enhancing transdermal delivery of kaempferia parviflora extract. *American Association of Pharmceutical Scientists PharmSciTech,19*, 2058-2067.

Rhee, Y.-S., Choi, J.-G., Park, E.-S., & Chi, S.-C. (2001). Transdermal delivery of ketoprofen using microemulsions. *International Journal of Pharmaceutics, 228*(1-2), 161-170.

Russo, A., Cardile, V., Caggia, S., Gunther, G., Troncoso, N., & Garbarino, J. (2011). Boldo prevents UV light and nitric oxide-mediated plasmid DNA damage and reduces the expression of Hsp70 protein in melanoma cancer cells. *Journal of Pharmacy and Pharmacology, 63*(9), 1219-1229.

Salerno, C., Carlucci, A. M., & Bregni, C. (2010). Study of in vitro drug release and percutaneous absorption of fluconazole from topical dosage forms. *American Association of Pharmceutical Scientists PharmSciTech, 11*(2), 986-993.

Singh, V. K., Anis, A., Al-Zahrani, S., & Pal, K. (2015). Microemulsions of Sorbitans and its Derivatives for Iontophoretic Drug Delivery. *International Journal of Electrochemical Science, 10*, 2239-2252.

Sithranga Boopathy, N., & Kathiresan, K. (2010). Anticancer drugs from marine flora: An overview. *Journal of Oncology, 2010,* 1-18.

Tabosa, M. A. M., De Andrade, A. R. B., Lira, A. A. M., Sarmento, V. H. V., De Santana, D. P., & Leal, L. B. (2018). Microemulsion formulations for the transdermal delivery of lapachol. *American Association of Pharmceutical Scientists PharmSciTech, 19*(4), 1837-1846.

Ting, Y., Chiou, Y.-S., Pan, M.-H., Ho, C.-T., & Huang, Q. (2015). In vitro and in vivo anti-cancer activity of tangeretin against colorectal cancer was enhanced by emulsion-based delivery system. *Journal of Functional Foods, 15*, 264-273.

Zu, Q., Yu, Y., Bi, X., Zhang, R., & Di, L. (2017). Microneedle-Assisted percutaneous delivery of a tetramethylpyrazine-loaded microemulsion. *Molecules, 22*(11), 2022-2031.

Chapter 4 : Cytotoxicity of Hispolon in Melanoma (B16BL6) Cell Lines

4.1. Introduction

Skin cancer is one of the leading skin diseases which significantly affects human health. Basel cell carcinoma, squamous cell carcinoma and melanoma are different types of skin cancer, the latter being the most aggressive. (De Gruijl, 1999). According to the American Cancer Society, one person dies due to melanoma every hour. Furthermore, approximately 9,320 people will die of melanoma in the United Stated in 2019 (Society, 2019). Malignant melanoma is a major global threat to public health and is responsible for more than 75% of deaths associated with skin cancer. Metastatic malignant melanoma is highly aggressive and difficult to treat with surgical procedures. The overall survival rate for metastatic melanoma ranges from 4.7 to 11 months, which indicates a lack of effective treatment for melanoma. As in many other cancer types, chemo-resistance to a cytotoxic agent is the main problem in melanoma. Furthermore, the severe side effects of these chemotherapies are another major issue. Hence, it is highly desirable to find novel, effective, and less toxic drugs for the treatment of melanoma. (Looi et al., 2013).

Phellinus linteus (PL) is a medicinal mushroom used widely as a traditional medicine for many years in China, Korea, and Japan to treat gastric disorder, inflammation, peptic ulcer, lymphatic disease, and various cancers (W. Chen, Feng, Huang, & Su, 2012). Polysaccharides, proteoglycans, furan derivatives, hispidin, and hispolon are bioactive components that have been identified from PL (Hsieh et al., 2014). The most important is Hispolon, a polyphenol compound which possesses potent antioxidant, anti-inflammatory, and anticancer properties (Huang, Deng, Huang, & Hu, 2011). Several studies reported hispolon's effects in various types of tumor cells. Hispolon

induced apoptosis to human epidermoid KB cells (W. Chen, He, & Li, 2006). Furthermore, hispolon showed inhibition of cell proliferation, cell cycle arrest at G2/M, and induction of apoptosis in breast and bladder cancer (Lu et al., 2009). Hispolon showed its cytotoxic effect on lung cancer cells lines via induction of G0/G1 cell cycle arrest and apoptosis (Wu et al., 2014). Furthermore, hispolon suppressed the migration of breast cancer by inhibiting the ROS/ERK/Slug/E-cadherin pathway (Z. Zhao, Sun, Chen, Lv, & Li, 2016). Hispolon also induced ROS-mediated apoptosis in gastric cancer cells (W. Chen et al., 2008). Moreover, hispolon suppressed migration and invasion by inhibiting the urokinaseplasmainogen activator (uPA) as well as the phosphorylation of Akt on nasopharyngeal carcinoma cells (Hsieh et al., 2014). Hsiao et al. (2013), reported that hispolon induces apoptosis through JNK—mediated caspase activation in acute myeloid leukemia (AML) cells and inhibits AML xenograft tumor growth in vivo (Hsiao et al., 2013). Hsin et al (2017) showed that hispolon suppressed tumor cell metastasis in both in vitro and in vivo models by autophagic degradation of lysosomal protease cathepsin S (CTSS) on cervical cancer (Hsin et al., 2017). Although the effect of hispolon has been reported in several tumor cell lines, the effect on melanoma cells is poorly understood. Therefore, we studied the mechanism of hispolon induced cytotoxicity in melanoma (B16Bl6) cell line.

4.2. Materials

Hispolon was obtained from Natsol Laboratories (Visakhapatnam, India). Fetal bovine serum, Dulbecco's Modified Eagle's Medium, and other reagents for cell culture were purchased from Mediatech (Manassa, VA), PBS was purchased from Sigma-Aldrich (St. Louis, MO). A mouse melanoma cell line (B16BL6) was obtained from the National

Cancer Institute (Frederick, MD). Bicinchoninic acid protein kit was purchased from Thermo Scientific (IL, USA). Tetrazolium bromide (MTT) was purchased from Calbiochem (Darmstadt, Germany). All other reagents were purchased from VWR International (West Chester, PA)

4.3. Methods

4.3.1. Cell culture

The B16BL6 cells were grown in Dulbecco's Modified Eagle's Medium (DMEM) supplemented with 10% fetal bovine serum (FBS), 100 U/mL penicillin, and 100 µg/mL streptomycin at 37°C in a humidified atmosphere containing 5% CO_2.

4.3.2. Cell cytotoxicity

MTT (3-[4, 5-dimethylthiazol-2-yl]-2, 5-diphenyl tetrazolium bromide) was used to determine in vitro cell cytotoxicity. Cells were seeded into a 96 well plate at $5*10^3$ cells/ml, and 24 hours later they were treated with various concentrations of hispolon (0.0, 0.5,1, 5 ,10, 30, 50,100 µM). The cells were then incubated for an additional 24 h at 37ºC. MTT stock solution (10 µL; 5mg/ml in PBS) was added to each well to provide a total reaction volume of 210 µL. Culture were then incubated for 2 hours, and the supernatants were aspirated. The formazan crystals in each well were dissolved in 200 µL DMSO and the absorbance was measured in a microplate reader at 540 nm. Cells that were not treated with hispolon served as the control. The cell cytotoxicity was expressed as a percentage relative to the untreated control cells. Curcumin has been used in this assay as a positive control.

4.3.3. Live/dead cell staining assay

Fluorescein diacetate (FDA) and propidium iodide (PI) dyes were used to assess cell viability after hispolon incubation. Cells were incubated with 5 mg/mL FDA and 2 mg/mL propidium iodide (PI) for 4 to 5 mins at 37ºC to stain live and dead cells, respectively after cells where treated with different concentrations of hispolon (0, 5, 10, 30 μM). FDA is a cell-permeable compound and emits a green fluorescence when it is cleaved by esterases. FDA is used to measure both enzymatic activity and cell membrane integrity. PI is a nucleus staining dye which cannot pass through a viable cell membrane. PI binds to DNA in the nucleus and emits a red fluorescence by passing through the disordered areas of dead cell membranes.

4.3.4. Quantification of reactive oxygen species (ROS)

The determination of intracellular reactive oxidant species generated by hispolon was based on the oxidation of 2',7'-dichlorodihydrofluorescein diacetate to the fluorescent product, 2',7'-dichlorofluorescein. B16BL6 cells were cultured in flat bottom 24-well plates for 24 hours. At confluence, cells were exposed to various concentration of hispolon for 24 hours. Following treatment, medium was aspirated and the cells were washed three times with PBS before being placed into 1 ml of cell culture medium without FBS. 2',7'-dichlorodihydrofluorescein diacetate was added to a final concentration of 10 μM, and cells were incubated for 20 min. The cells were again washed twice with PBS and maintained in 1 ml of culture medium. Intracellular fluorescence was measured at wavelengths of 480nm (excitation) and 535 nm (emission) using a microplate reader (spectramax M5, molecular devices, Sunnyvale, CA USA). Each study was repeated

three times and the mean fluorescence was determined.

4.3.5. Effect of hispolon on lipid peroxidation

Lipid peroxidation occurs due to the oxidative breakdown of lipids when ROS attack the polyunsaturated fatty acids in the progression reaction process. Various doses of hispolon were used to treat B16BL6 cells, and a colorimetric method at 532 nm was used to quantify the lipid peroxidation. A method was used to measure the lipid peroxidation by the formation of thiobarbituric acid-reactive substances (TBARS). TBARS was normalized to total protein content as TBARS formed/mg protein (Majrashi et al., 2018).The results are expressed as % change compared to control.

4.3.6. Effect of hispolon on nitrite content

The final products of nitric oxide oxidation pathways are nitrite and nitrate, which are used as an expression of nitric oxide production. Various doses of hispolon were treated used to treat B16BL6 cells and a colorimetric method was used to assess the nitrite content. An azo product formed due to treatment with Griess reagent was measured spectrophotometrically at 545 nm. Nitrite content was normalized to total protein content as nitrite/mg protein (Majrashi et al., 2018). The results are expressed as % change compared to control.

4.3.7. Effect of hispolon on caspase-1 and caspase-3 activities

Caspase (caspase-1 and caspase-3) activities in the control and hispolon treated cells were measured using a fluorimetric method. AC-DEVD-AMC and AC-YVAD-AMC were used as specific substrates to measure the caspase-1 and caspase-3 activities. The

product formed by the caspase activation was measured spectrofluorometrically. The results are expressed as % change compared to control.

4.3.8. Effect of hispolon on mitochondrial complex-I and complex-IV activities

Mitochondrial Complex-I and Complex-IV activities in the control and hispolon treated cells were measured using a spectrophotometric method. NADH and Cytochrome C were used as specific substrates to measure the Complex-I and Complex-IV activities. The results are expressed as % change compared to control.

4.3.9. Western blot analysis

Cells were cultured in Dulbecco's modified essential medium growth containing 10% fetal bovine serum (FBS) at 37°C in a 6- well plate. Cells were incubated with hispolon at different concentrations (0, 5, 10, 30 μM) for 24 hours. After incubation, the cells were lysed for both the control and hispolon treated cells with a lysis buffer. The samples were collected and stored at -80°C until used. Cell extracts were mixed with 4x Laemmli buffer and loaded into 10% sodium dodecyl sulfate-polyacrylamide gel electrophoresis (SDS-PAGE). The cell extracts were separated on the gel and transferred to PVDF membranes (Immobilon-p Millipore, Germany) by an electrophoresis chamber obtained from Bio-Rad. After the transfer, the membrane was blocked with 5% non-fat dry milk in Tris-Buffered Saline (TBS) containing 0.01 % Tween 20 for 3 hours. The membrane was then washed with TBS for 5 minutes and incubated with Bax, Bcl-2 or βactin overnight at 4°C. All primary antibodies were used at 1:1000 dilution. Then the membrane was immersed into the secondary anti rabbit antibody (1:10,000) for 1 hour. FluorChem Q System imager ((Proteinsimple, San Jose, California,

USA) was used to visualize the membrane. The excitation and emission were at λ_{535} and $\lambda_{606,}$ respectively. Automatic image capture AlphaView software was used to analyze the band density of both control and treated cells.

4.3.10. Statistical analysis

All data were subjected to one-way analysis of variance (ANOVA) to determine the statistical levels of significance. P value < 0.05 was considered to be statistically significant.

4.4. Results and discussion

4.4.1. Hispolon induced dose-dependent reduction of melanoma (B16BL6) cell viability

Cell cytotoxicity studies on melanoma cell line (B16BL6) showed that hispolon was significantly cytotoxic to these cells (Figure 4-1). The half-maximal inhibitory concentration (IC_{50}) was 10 μM, which was lower than the IC_{50} reported in other cancer cells. The IC_{50} values obtained for gastric cells treated with hispolon was 30 μM and was between 36-88 μM for liver cancer (W. Chen et al., 2008; Huang et al., 2011). This showed that this melanoma cell line (B16BL6) was sensitive to hispolon treatment.

Curcumin was used as a positive control due to the structural similarity between hispolon and curcumin. Hispolon lacks an aryl moiety. As shown in Figure 4-2, both hispolon and curcumin significantly enhanced cell cytotoxicity, but hispolon was more potent than curcumin by IC_{50}. The IC_{50} value of curcumin was 2 times higher than hispolon. A similar result was reported by Ravindran et al. (2010). Hispolon was a more

potent anti-proliferative agent than curcumin against prostate, breast, and colorectal cancer and against human myeloid leukemia and multiple myeloma cells.

4.4.2. Live/dead cell staining

As presented in Figure 4-3, hispolon was cytotoxic in a concentration-dependent manner. The number of dead cells increased and the number of live cells decreased significantly with increasing concentration from 5-30 μM. This result correlate well with MTT assay data that hispolon showed that has a cytotoxicity effect against B16BL6. Kim et al (2016) reported live dead staining data to prove the cell death effect of hispolon against human colon cancer cells.

4.4.3. Hispolon generates ROS

ROS are highly reactive molecules and can damage biomolecules, including lipids, proteins, and nucleic acid, and alter their functions (Birben, Sahiner, Sackesen, Erzurum, & Kalayci, 2012). The oxidative stress forms when there is an overproduction of ROS which has been proposed to play a major role in developing many diseases such as atherosclerosis, cancer, diabetes, rheumatoid arthritis, and neurological disorders (Uttara, Singh, Zamboni, & Mahajan, 2009). As shown in Figure 4-4, hispolon increased the production of ROS in a dose-dependent manner. Hispolon increased the generation of ROS by 5, 10, 23, and 35 at 5, 10, 30, and 50 μM concentration, respectively when compared to controls. Hispolon generates ROS in gastric cancer as well (W. Chen et al., 2008). This suggest that hispolon induces apoptosis by ROS accumulation in the cells.

4.4.4. Hispolon induces lipid peroxidation

Lipid peroxidation occurs due to degradation of lipids and is increased by the effect of free radicals (ROS). To assess the oxidation of lipids, we performed a lipid peroxidation assay. The level of lipid peroxide was enhanced by increasing the hispolon concentration (Figure 4-5). Hispolon significantly increased the level of lipid peroxide up to six times compared to the control up to a concentration of 50 μM.

4.4.5. Hispolon increases nitrite production

The level of nitrite was enhanced by increasing the concentration of hispolon (Figure 4-6). The level of nitrite significantly increased up to three times compared to the control when cells treated with 50 μM. This also suggested that hispolon significantly induce oxidative stress by increase nitrite content.

4.4.6. Mitochondrial complex-I and IV activity

The mitochondrial respiratory chain (complexes I-V) is the major site of ATP production and plays a major role in cell death (Kwong, Henning, Starkov, & Manfredi, 2007). As presented in Figure 4-6 A-B, hispolon significantly inhibited complex-I and complex IV activity in a dose dependent manner. The inhibition of lead to mitochondrial dysfunction, accumulation of ROS and apoptosis.

4.4.7. Caspase 3 and Caspase 1 assay

Caspases are the executioners of apoptosis and play key roles in apoptotic cell death. Enhanced caspases activities can result in accelerated programmed cell death

(McIlwain, Berger, & Mak, 2013). To confirm the apoptosis-induction effect of hispolon on B16BL6 cells, we analyzed the activity of apoptotic enzymes, caspase-1 and -3, in hispolon-treated B16-BL6 cells. Caspase-1 and -3 activity of the cells treated with varied concentrations of hispolon are shown in Figure 4-7 A-B. The activity of caspase-1 and caspase-3 were increase by hispolon in a dose-dependent manner compared to non-treated cells. These results indicated that hispolon induced apoptosis was through the mitochondrial pathway. Several studies showed that hispolon induce apoptosis through the activation of caspase in various cancers such acute myeloid leukemia (Hsiao et al., 2013), colon cancer (Kim, Kim, & Park, 2016), and nasopharyngeal carcinomas (Hsieh et al., 2014)

4.4.8. Western blot analysis

Apoptosis is a process of cell death that occurs in multicellular organisms. Apoptosis is generally characterized by distinct morphological characteristics including a rounding of the cell, a reduction of cellular volume, chromatin condensation, nuclear fragmentation, and plasma membrane blebbing (He, Lu, & Zhou, 2009). There are two main pathways leading to apoptosis: a mitochondrion-mediated intrinsic pathway and a death-receptor-induced extrinsic pathway. The mitochondria dependent apoptosis is controlled by the Bcl-2 family. The Bcl-2 family consists of anti-apoptotic and pro-apoptotic members (Sprick & Walczak, 2004). The balance and location between those two groups of proteins controls the fate of the cell. This family regulates cell death by controlling the mitochondrial membranes' permeability during apoptosis (Shamas-Din, Kale, Leber, & Andrews, 2013). We studied the effect of hispolon treatment in Bcl-2 protein expression, which is an anti-apoptotic protein and Bax protein expression, which

is a pro-apoptotic protein. As can be seen in Figure 4-8, hispolon remarkably increased the expression of Bax in a dose dependent manner. Likewise, the expression of Bcl-2 decreased with hispolon (Figure 4-9). After treatment with 30 μM hispolon, the level of Bax expression was increased by 150% in comparison to the control. Likewise, hispolon treatment at 30 μM significantly decreased Bcl-2 expression by 75% in comparison with control. Altogether, these findings suggested that hispolon induced apoptosis in B16BL6 cells is controlled by the mitochondrial pathway. Huang, G (2011), showed that hispolon decreased the expression of Bcl-2 protein and increased the expression of Bax protein in hepatocellular carcinoma (Huang et al., 2011). Another study conducted on NB4 human leukemia cells showed that the hispolon treatment increased the expression of Bax protein and decreased expression of Bcl-2 protein (Y.-C. Chen et al., 2013).

4.5. Conclusion

We have established that hispolon is a potent inducer of reactive oxygen species. It inhibits the expression of bcl-2 gene, promotes the expression of Bax gene, promotes expression of caspase enzymes. It also inhibits complex I and IV, stimulates nitrite content and lipid peroxidation levels. All these effects are associated with cell death or apoptosis. Further investigating on mechanism of the chemotherapeutic potential of hispolon is warranted.

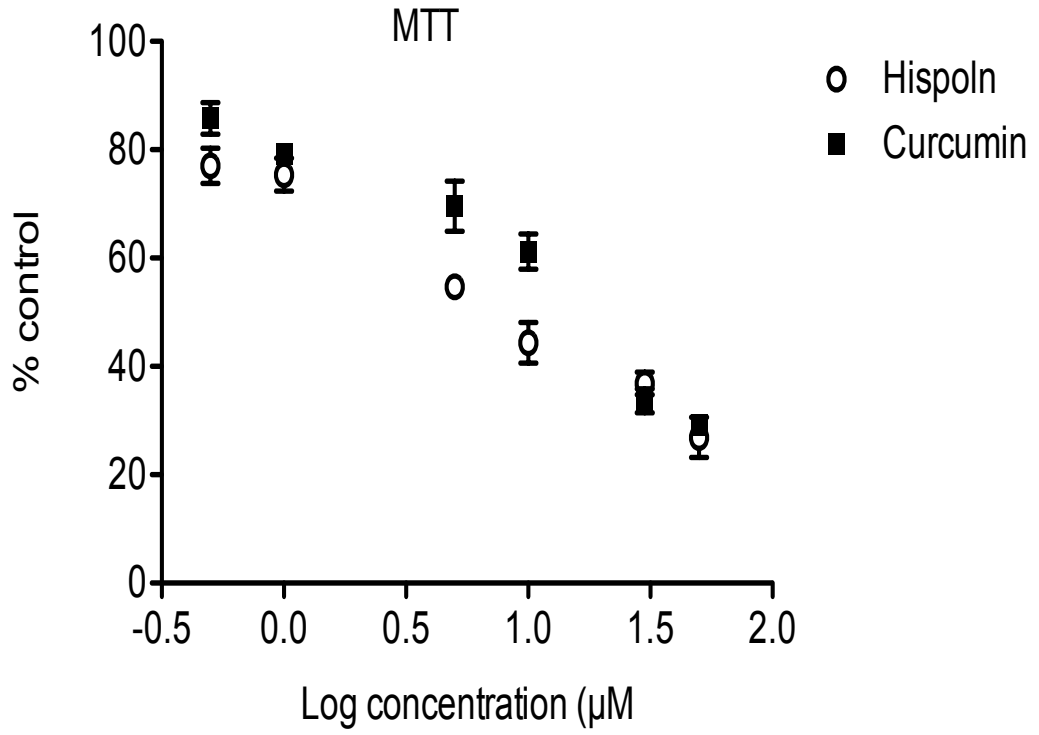

Figure 4-1 The cytotoxic effect of hispolon against B16 BL6 cell line. Cells were incubated with various concentrations of hispolon (0.5,1, 5 ,10,30,50, and 100 µM) for 24 hours. Data are mean ±S.E to untreated control cells (n=3).

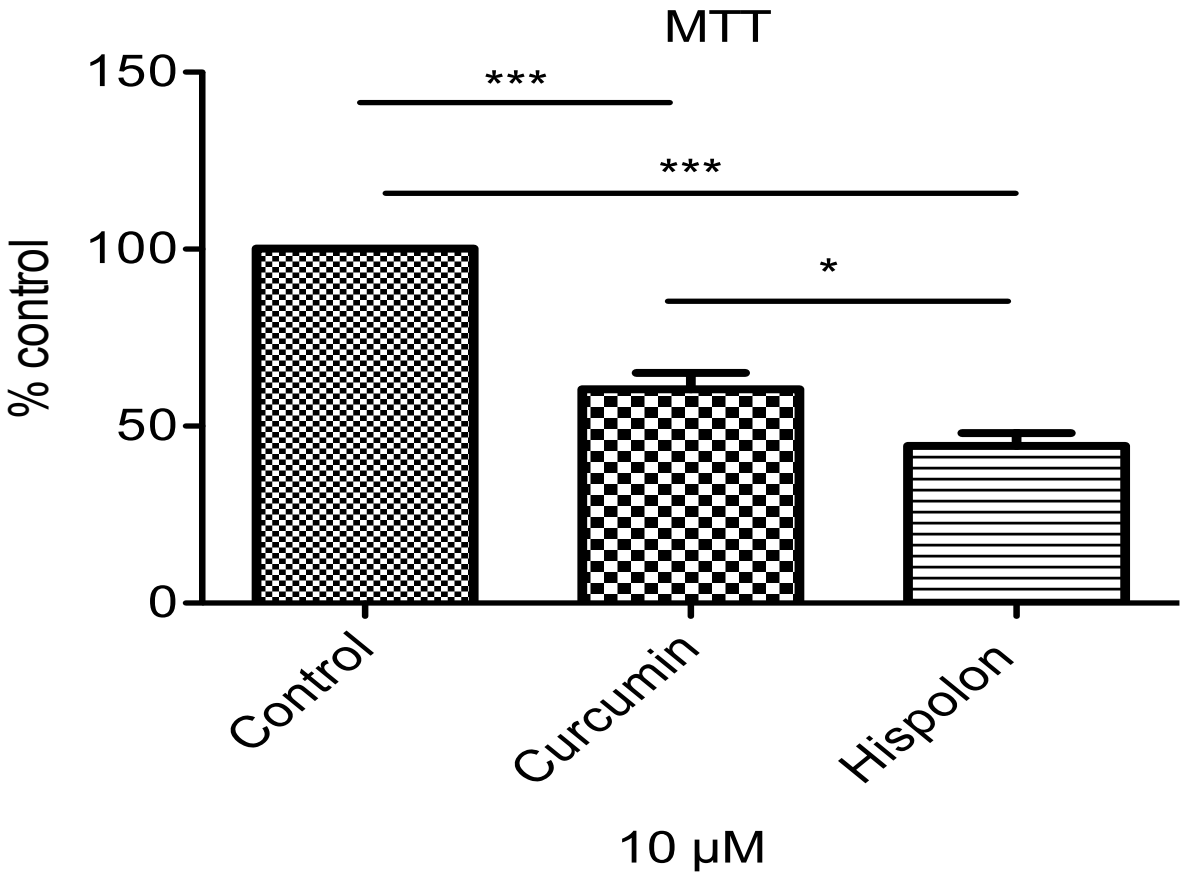

Figure 4-2 In vitro cytotoxicity of hispolon and curcumin in B16BL6 cell line. Data are mean ± S.E.M. of n = 3. *p <0.05, ***p <0.001 when hispolon is compared to curcumin

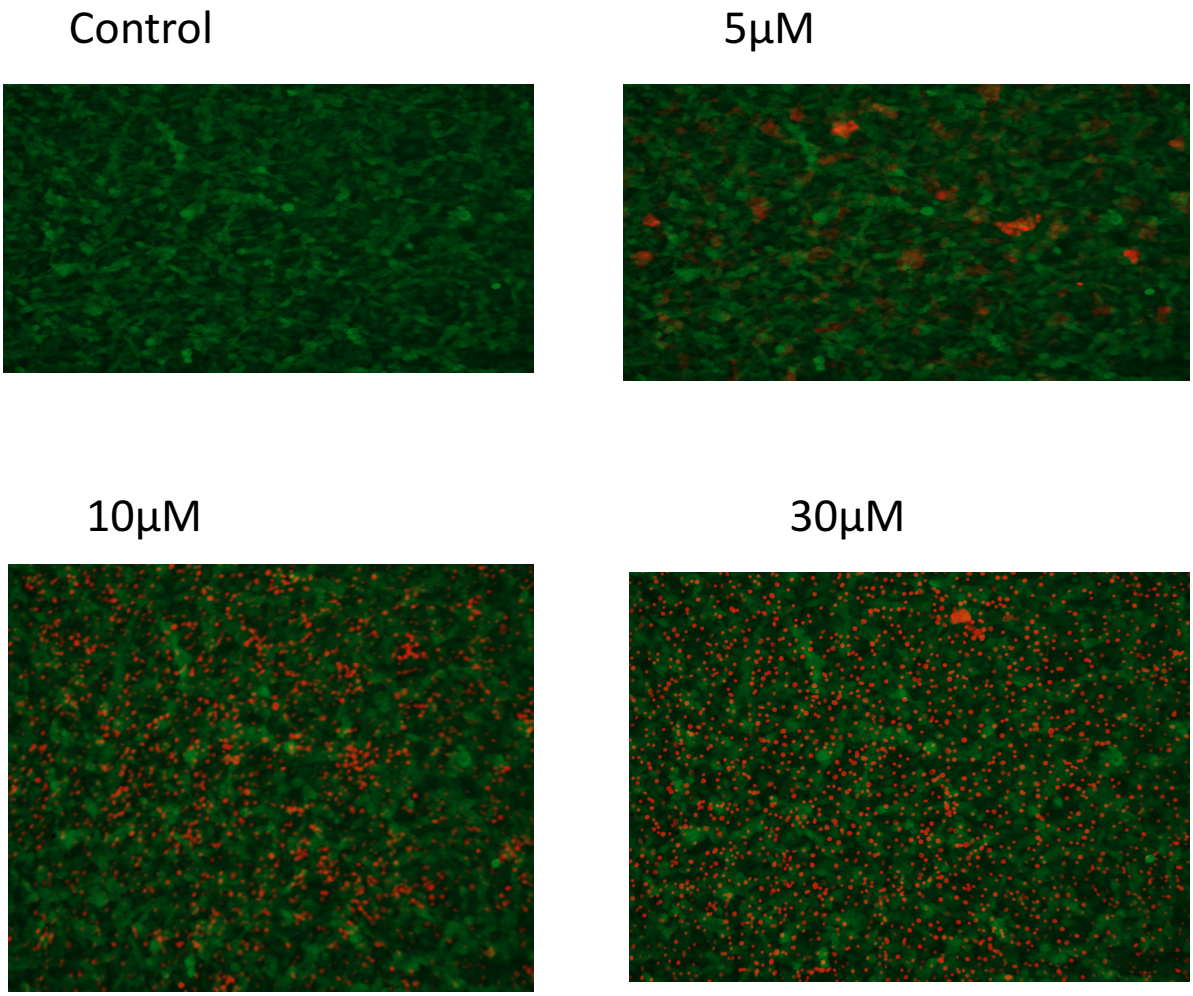

Figure 4-3 Live/dead cell staining of melanoma. Cells were treated for 24 h with different concentrations of hispolon (0-30 µM). Live cells appear green, while dead cells appear red.

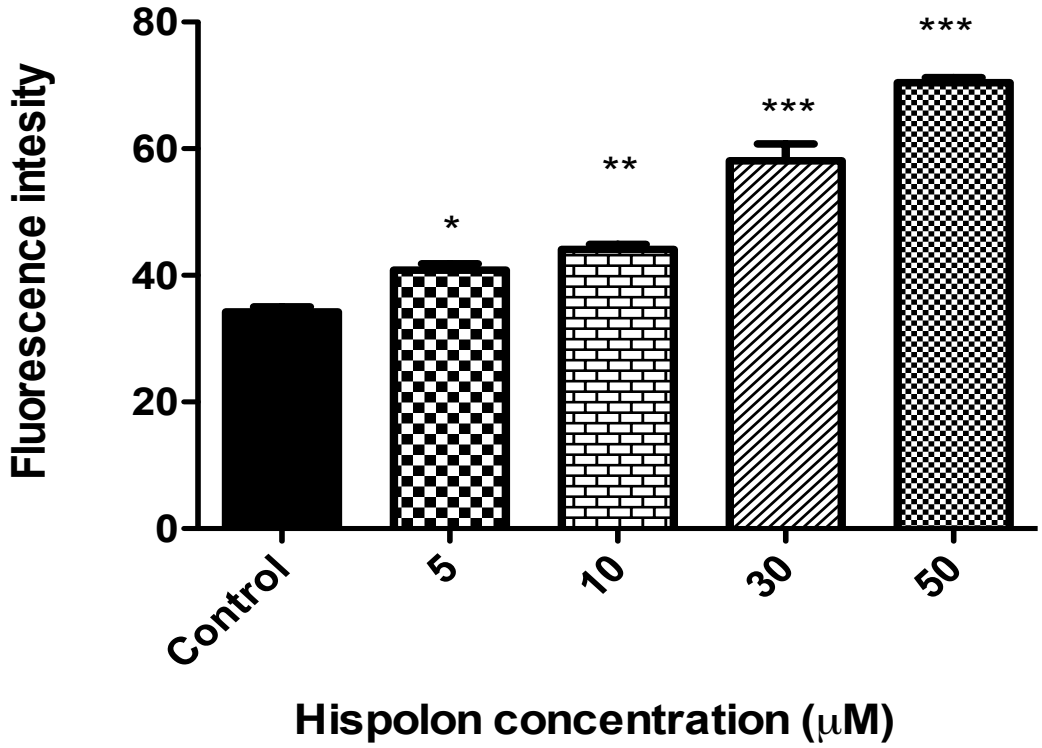

Figure 4-4 Hispolon-induced ROS generation in B16BL6 cell line. Data are means ± S.E.M. of n=3.*p<0.05, **p<0.01, ***p<0.001.

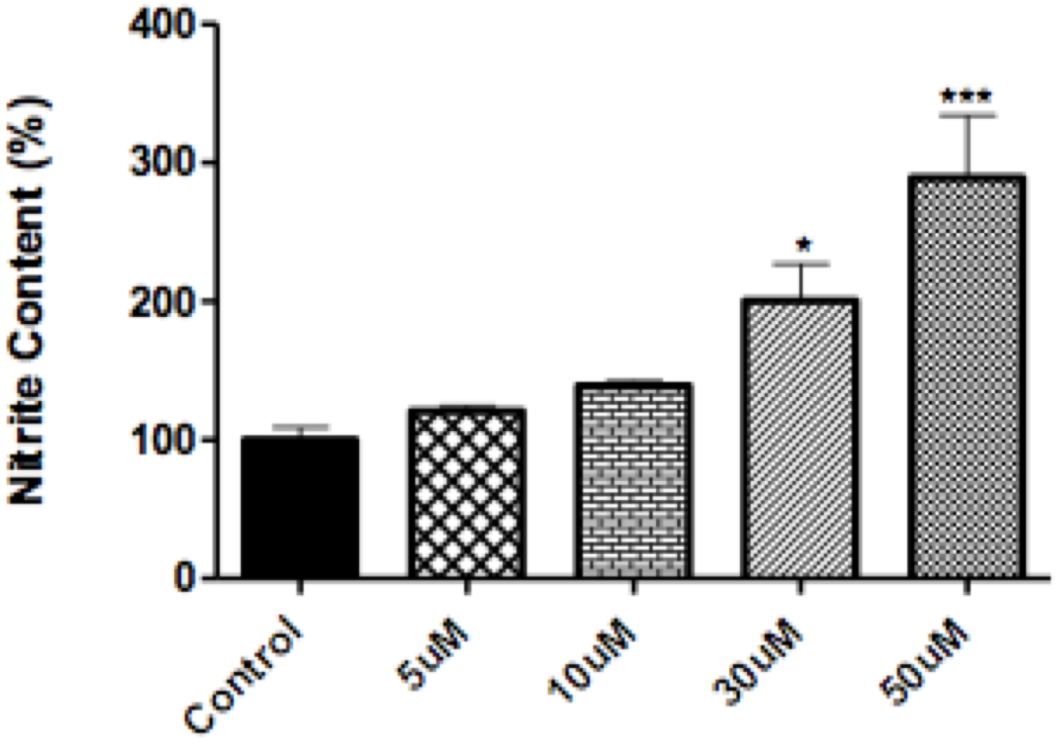

Figure 4-5 Dose-dependent effect of hispolon on nitrite production in B16BL6 cells. Cells were treated for 24 h with different concentrations of hispolon (0-50 μM). Data are means ± S.E.M. of n=3.*p<0.05, ***p<0.001.

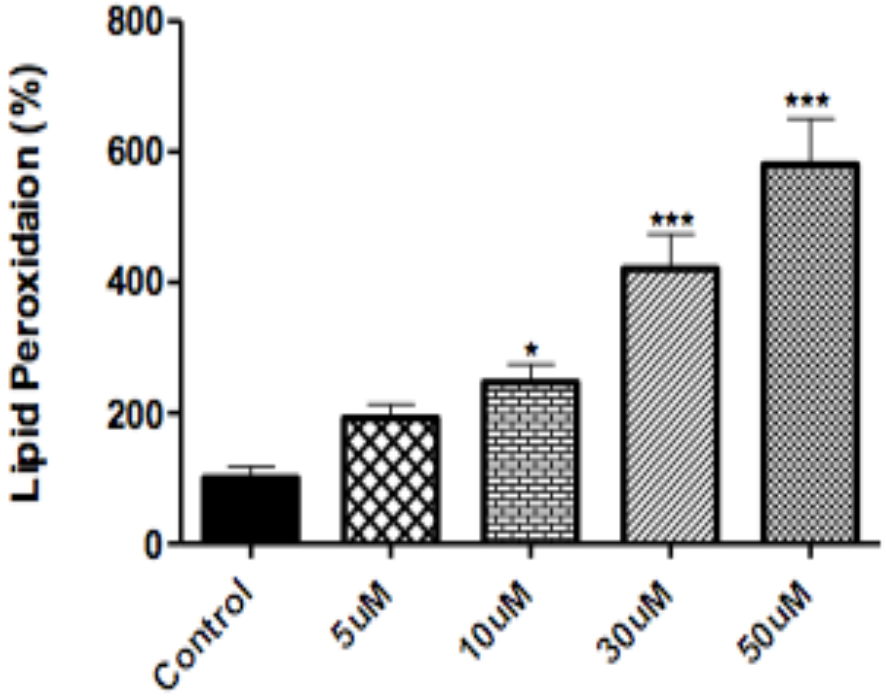

Figure 4-6 Dose-dependent effect of Hispolon on lipid peroxidation production in B16BL6 cells. Cells were treated for 24 h with different concentrations of hispolon (0-50 μM). Data are means ± S.E.M. of n=3.*p<0.05, ***p<0.01, ***p<0.001.

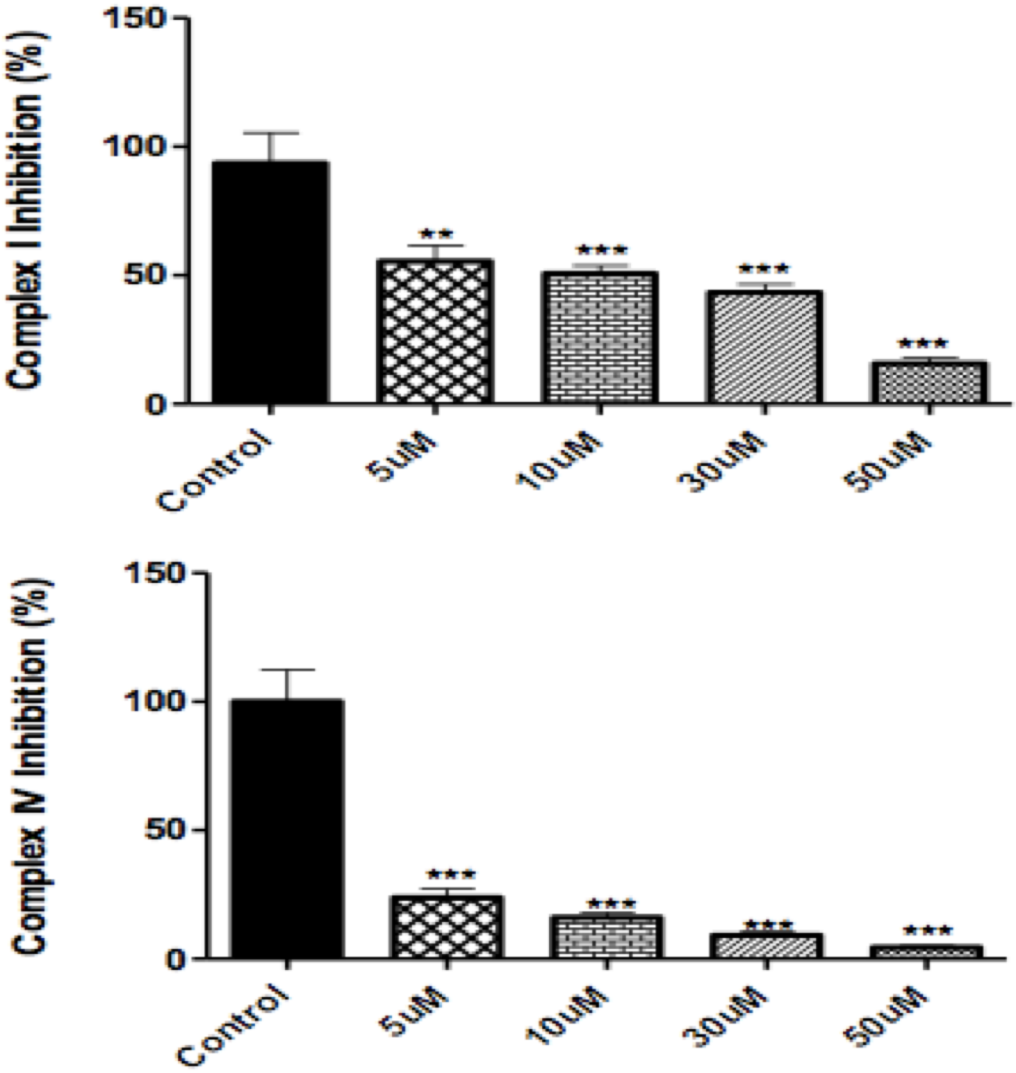

Figure 4-7 Dose-dependent effect of hispolon on complex I and IV activities in B16BL6 cells. Cells were treated for 24 h with different concentrations of hispolon (0-50 μM). Data are means ± S.E.M. of n=3.*p<0.05,**p<0.01 ***p<0.001.

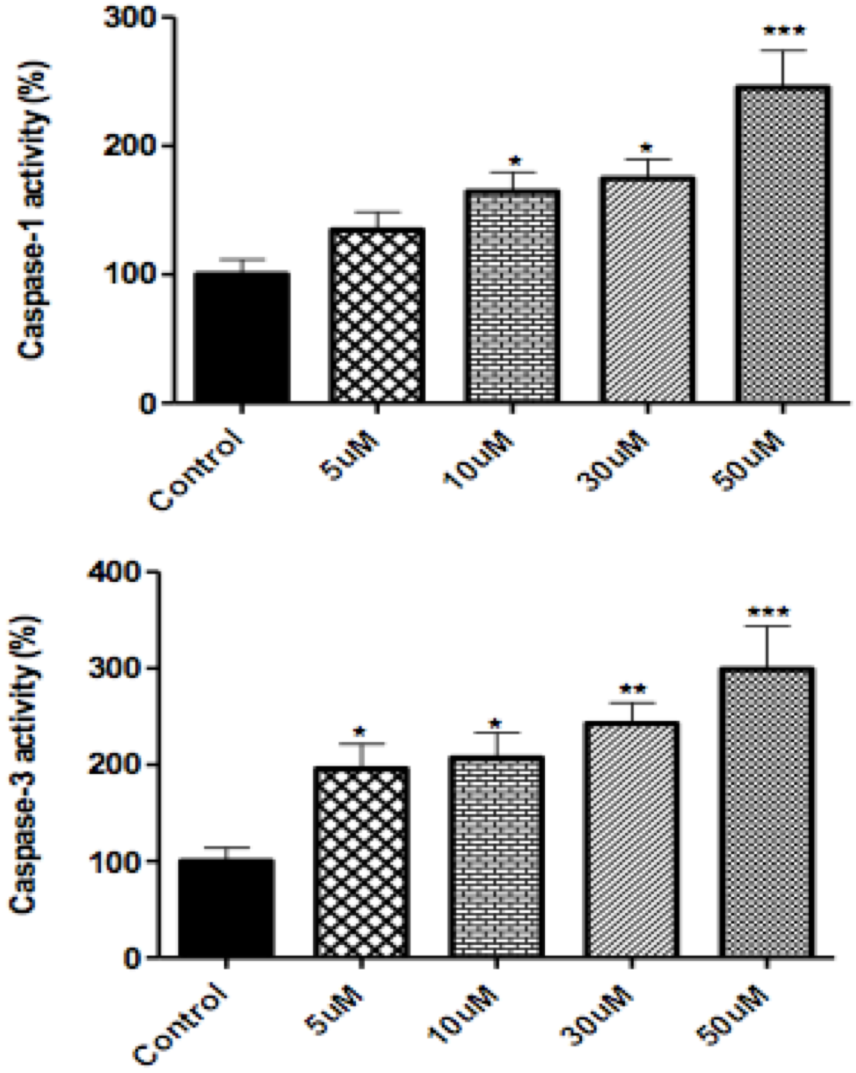

Figure 4-8 Hispolon induced caspase activation in B16BL6 cells. Cells were treated for 24 h with different concentrations of hispolon (0-50 μM). Data are represented. as means ± S.E.M. of n=3 .*p<0.05,**p<0.01, ***p<0.001.

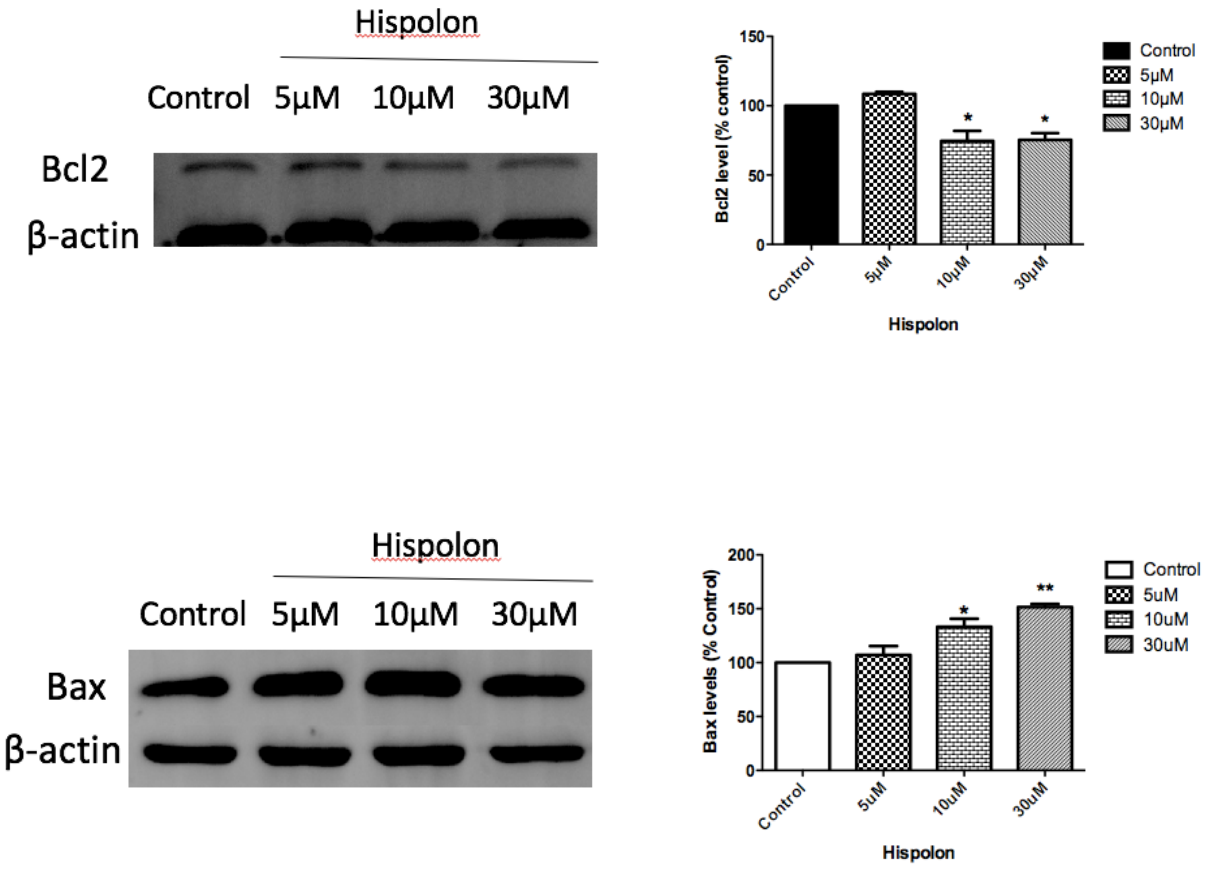

Figure 4-9 Hispolon decreased anti-apoptotic and increased pro-apoptotic expression. Cells were treated for 24 h with different concentrations of hispolon (0-30 μM). Data are means ± S.E.M. of n=3.*p<0.05, **p<0.001.

4.6. References

Birben, E., Sahiner, U. M., Sackesen, C., Erzurum, S., & Kalayci, O. (2012). Oxidative stress and antioxidant defense. *World Allergy Organization Journal, 5*(1), 9-19.

Chen, W., Feng, L., Huang, Z., & Su, H. (2012). Hispidin produced from Phellinus linteus protects against peroxynitrite-mediated DNA damage and hydroxyl radical generation. *Chemico-Biological Interactions, 199*(3), 137-142.

Chen, W., He, F.-Y., & Li, Y.-Q. (2006). The apoptosis effect of hispolon from Phellinus linteus (Berkeley & Curtis) Teng on human epidermoid KB cells. *Journal of Ethnopharmacology, 105*(1-2), 280-285.

Chen, W., Zhao, Z., Li, L., Wu, B., Chen, S.-f., Zhou, H., . . . Li, Y.-Q. (2008). Hispolon induces apoptosis in human gastric cancer cells through a ROS-mediated mitochondrial pathway. *Free Radical Biology and Medicine, 45*(1), 60-72.

Chen, Y.-C., Chang, H.-Y., Deng, J.-S., Chen, J.-J., Huang, S.-S., Lin, I.-H., . . . Huang, G.-J. (2013). Hispolon from phellinus linteus induces G0/G1 cell cycle arrest and apoptosis in NB4 human leukaemia cells. *The American Journal of Chinese Medicine, 41*(06), 1439-1457.

De Gruijl, F. (1999). Skin cancer and solar UV radiation. *European Journal of Cancer, 35*(14), 2003-2009.

He, B., Lu, N., & Zhou, Z. (2009). Cellular and nuclear degradation during apoptosis. *Current Opinion in Cell Biology, 21*(6), 900-912.

Hsiao, P.-C., Hsieh, Y.-H., Chow, J.-M., Yang, S.-F., Hsiao, M., Hua, K.-T., . . . Chien, M.-H. (2013). Hispolon induces apoptosis through JNK1/2-mediated activation of a caspase-8,-9, and-3-dependent pathway in acute myeloid leukemia (AML) cells

and inhibits AML xenograft tumor growth in vivo. *Journal of Agricultural and Food Chemistry, 61*(42), 10063-10073.

Hsieh, M.-J., Chien, S.-Y., Chou, Y.-E., Chen, C.-J., Chen, J., & Chen, M.-K. (2014). Hispolon from Phellinus linteus possesses mediate caspases activation and induces human nasopharyngeal carcinomas cells apoptosis through ERK1/2, JNK1/2 and p38 MAPK pathway. *Phytomedicine, 21*(12), 1746-1752.

Hsin, M.-C., Hsieh, Y.-H., Wang, P.-H., Ko, J.-L., Hsin, I.-L., & Yang, S.-F. (2017). Hispolon suppresses metastasis via autophagic degradation of cathepsin S in cervical cancer cells. *Cell Death & Disease, 8*(10), 3089-3100.

Huang, G.-J., Deng, J.-S., Huang, S.-S., & Hu, M.-L. (2011). Hispolon induces apoptosis and cell cycle arrest of human hepatocellular carcinoma Hep3B cells by modulating ERK phosphorylation. *Journal of Agricultural and Food Chemistry, 59*(13), 7104-7113.

Kim, J. H., Kim, Y. C., & Park, B. (2016). Hispolon from Phellinus linteus induces apoptosis and sensitizes human cancer cells to the tumor necrosis factor-related apoptosis-inducing ligand through upregulation of death receptors. *Oncology Reports, 35*(2), 1020-1026.

Kwong, J. Q., Henning, M. S., Starkov, A. A., & Manfredi, G. (2007). The mitochondrial respiratory chain is a modulator of apoptosis. *The Journal of Cell Biology, 179*(6), 1163-1177.

Looi, C. Y., Moharram, B., Paydar, M., Wong, Y. L., Leong, K. H., Mohamad, K., . . . Mustafa, M. R. (2013). Induction of apoptosis in melanoma A375 cells by a chloroform fraction of Centratherum anthelminticum (L.) seeds involves NF-

kappaB, p53 and Bcl-2-controlled mitochondrial signaling pathways. *BMC Complementary and Alternative Medicine, 13*(1), 166-180.

Lu, T.-L., Huang, G.-J., Lu, T.-J., Wu, J.-B., Wu, C.-H., Yang, T.-C., . . . Chen, Y.-F. (2009). Hispolon from phellinus linteus has antiproliferative effects via MDM2-recruited ERK1/2 activity in breast and bladder cancer cells. *Food and Chemical Toxicology, 47*(8), 2013-2021.

Majrashi, M., Almaghrabi, M., Fadan, M., Fujihashi, A., Lee, W., Deruiter, J., . . . Dhanasekaran, M. (2018). Dopaminergic neurotoxic effects of 3-TFMPP derivatives. *Life Sciences, 209*, 357-369.

McIlwain, D. R., Berger, T., & Mak, T. W. (2013). Caspase functions in cell death and disease. *Cold Spring Harbor Perspectives in Biology, 5*(4),8656-8683.

Ravindran, J., Subbaraju, G. V., Ramani, M. V., Sung, B., & Aggarwal, B. B. (2010). Bisdemethylcurcumin and structurally related hispolon analogues of curcumin exhibit enhanced prooxidant, anti-proliferative and anti-inflammatory activities in vitro. *Biochemical Pharmacology, 79*(11), 1658-1666.

Shamas-Din, A., Kale, J., Leber, B., & Andrews, D. W. (2013). Mechanisms of action of Bcl-2 family proteins. *Cold Spring Harbor perspectives in biology, 5*(4), 8714-8745.

American Cancer Society. (2019). Cancer Facts & Figures 2019. Atlanta: American Cancer Society.

Sprick, M. R., & Walczak, H. (2004). The interplay between the Bcl-2 family and death receptor-mediated apoptosis. *Biochimica et Biophysica Acta (BBA)-Molecular Cell Research, 1644*(2-3), 125-132.

Uttara, B., Singh, A. V., Zamboni, P., & Mahajan, R. (2009). Oxidative stress and neurodegenerative diseases: A review of upstream and downstream antioxidant therapeutic options. *Current Neuropharmacology, 7*(1), 65-74.

Wu, Q., Kang, Y., Zhang, H., Wang, H., Liu, Y., & Wang, J. (2014). The anticancer effects of hispolon on lung cancer cells. *Biochemical and Biophysical Research Communications, 453*(3), 385-391.

Zhao, Z., Sun, Y.-S., Chen, W., Lv, L.-X., & Li, Y.-Q. (2016). Hispolon inhibits breast cancer cell migration by reversal of epithelial-to-mesenchymal transition via suppressing the ROS/ERK/Slug/E-cadherin pathway. *Oncology Reports, 35*(2), 896-904.

Chapter 5 : Design of Hispolon and Doxorubicin Nanoparticles for Melanoma Treatment

5.1. Introduction

Melanoma is the fifth most commonly diagnosed cancer in the United States among both men and women. Approximately 2 million cases of skin cancer were reported in the United States in 2012, of which, 4% were malignant melanoma cases. Malignant melanoma is responsible for more than 79% of deaths from skin cancer (Bharath & Turner, 2009). It is a major global threat to public health with an estimated 96,480 new cases and an estimated 7,230 deaths in 2019 in the United States (American Cancer Society, 2019). Early stage melanoma which has not spread to other organs can be treated by surgery which can yield a high survival rate. However, metastatic malignant melanoma is highly aggressive and difficult to treat with surgical procedures. It needs to be treated by chemotherapy, radiotherapy, immunotherapy or a combination of these (Klefström, Gröhn, Heinonen, Holsti, & Holsti, 1987). Currently used systemic treatment for malignant melanoma is inefficient and malignant melanoma shows high relapse rates. Thus, there is an urgent need to develop new treatment strategies for malignant melanoma that could provide complete remission and prevent future recurrence.

Systemic administration of single chemotherapy to treat cancer has several limitations including fast renal clearance, poor bioavailability and multidrug resistance. In addition, those chemotherapies suffer from systemic adverse effects such as cardiac toxicity, neuropathy, neutropenia, kidney failure, myelosuppression, and alopecia. Furthermore, a high dose of the drug often is required to reach the effective dose due to

low drug accumulation at the tumor site, which makes the side effects severe (Zhang et al., 2016). Thus, a combination of anticancer drugs has been proposed since it might reduce multidrug resistance (MDR) and side effects as a result of lowering the dose (Dong & Mumper, 2010). Further, a combination of two or more anticancer drugs in a delivery system enhances efficacy compared to single therapy, because it might provide additive or synergistic effects.

Doxorubicin is one of the most used drugs for treating a wide range of cancers. It acts by blocking topoisomerase II activity by intercalating between the bases of the DNA double helix, thereby disturbing DNA replication and transcription (Abraham et al., 2005). Like most chemotherapeutic agents, there are often toxic effects on normal tissue which limit the clinical use of doxorubicin. Cardiotoxicity is one of the toxic effects of doxorubicin which might lead to irreversible damage (McGowan et al., 2017). Bone marrow toxicity is another effect of doxorubicin (Harris, Garai, & Valenzuela, 1975). In addition to the narrow therapeutic window of doxorubicin, development of MDR after doxorubicin therapy was one of the issues that hindered its clinical application with several cancers (Nielsen, Maare, & Skovsgaard, 1996). Hence, liposomal doxorubicin has been developed and commercialized (Doxil). Cardiac toxicity is linked to cumulative dose of doxorubicin (> 400-500 mg/cm^2) (Safra, 2003). Therefore, a combination strategy might be helpful to decrease the dose of doxorubicin.

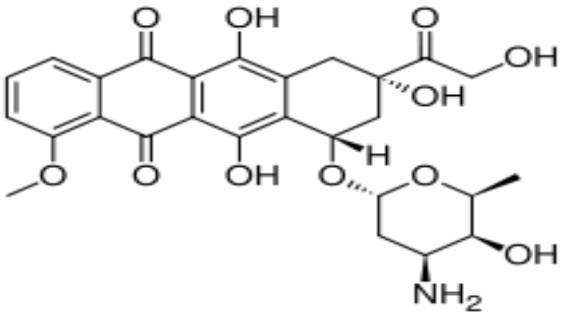

Doxorubicin

A combination of doxorubicin and chemosensitizers has been proposed to inhibit MDR, increase apoptosis of the cancer cells and minimize myocardial damage. Combination therapy produces higher overall and complete remission rates than single therapy. Doxorubicin has been combined with tumor necrosis factor-related apoptosis-inducing ligand (TRAIL), which is known to induce apoptosis by binding to two death receptors DR4 and DR5. This combination liposome formulation induces apoptosis to non-small cell lung cancer both in vitro and in vivo (Wang et al., 2010). Furthermore, Chen Z., et al co- delivered doxorubicin with Bcl-2 siRNA by mesoporous silica nanoparticles to enhance activity of chemotherapy against MDR cancer cells (A. M. Chen et al., 2009). Moreover, the combination of grape seed extract and doxorubicin showed a strong synergistic efficacy on breast cancer (Sharma, Tyagi, Singh, Chan, & Agarwal, 2004).

Hispolon [3,5-Hexadien-2-one, 6-(3,4-dihydroxyphenyl)-4-hydroxy-, (3Z,5E)-] is a polyphenol from *Phellinus linteus,* which has potent antioxidant, anti-inflammatory, anti-proliferative and anti-metastatic activities (Hsieh et al., 2014). Kim, et al. (2016) reported that hispolon showed anticancer effects on colon HCT 116 tumors. Another study demonstrated a hispolon effect in hepatic cancer; it showed that hispolon induces apoptosis by focal adhesion kinase (FAK) and PI3K/Akt signaling pathways (Huang et al.,

2010). In lung cancer, hispolon enhanced cell toxicity, induced G0/G1 cell cycle arrest and apoptosis, and showed that p53 played a critical role in hispolon-mediated antitumor activity (Wu et al., 2014). In addition to its anticancer effect, hispolon has been studied as an antimetastasis agent. Zhao et al. (2016) showed that hispolon inhibited the migration of breast cancer by inhibiting the ROS/ERK/Slug/E-cadherin pathway. Our laboratory studied hispolon anti-melanoma activity using melanoma (B16BL6) cell lines. We established that hispolon is a potent inducer of reactive oxygen species. It inhibits the expression of bcl2 gene, promotes the expression of Bax gene, and caspase enzymes, inhibits complex I and IV, stimulates nitrite content and lipid peroxidation levels, all of which are associated with cell death or apoptosis (Ahmed, Alhowail, Majrashi, Arnold, & Babu, 2019). Therefore, combination of hispolon with doxorubicin might reduce the limitations and challenges associated with doxorubicin treatment mentioned before, and may enhance efficacy of doxorubicin due to the multiple pathways targeted.

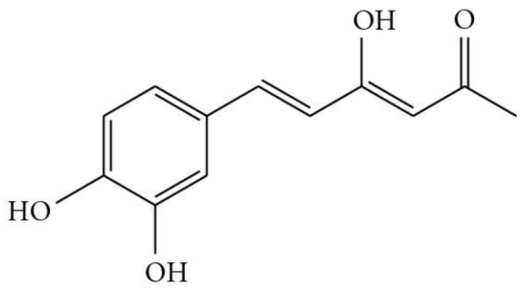

Hispolon

To date, no formulation has been reported for hispolon. However, its low water solubility has impeded its clinical use. Nanocarriers such as liposomes, micelles, polymeric nanoparticles and, hydrogels, have been extensively used in drug delivery. They improve the therapeutic efficacy of many anticancer drugs by enhancing drug accumulation at the tumor site, increasing drug circulation time, enhancing tumor uptake, and minimizing

toxicity (Lila & Ishida, 2017). Furthermore, those nanocarriers can be used to deliver multiple anticancer drugs. Liposomes are considered nontoxic, biodegradable, and non-immunogenic. They consist of a lipid bilayer with a hydrophilic core. Lipophilic molecules can be entrapped in the lipid bilayer membrane and hydrophilic molecules can localize in the aqueous core (Sercombe et al., 2015). It has been well documented that the efficacy of many anticancer drugs is enhanced by using liposomes as a carrier both in vitro and in vivo.

This study investigated the effect of liposomal doxorubicin or hispolon alone or in combination on cell cytotoxicity of B16BL6 melanoma cell death and apoptosis. to assess whether hispolon enhances the therapeutic potential of doxorubicin.

5.2. Materials

1,2-distearoyl-sn-glycero-3-phosphocholine (DSPC) and 1,2-distearoyl-sn-glycero-3-phosphoethanolamine-N-[methoxy(polyethylene glycol)-2000] (ammonium salt) (DSPE-mPEG (2000)) were purchased from Avanti Polar Lipids Inc (Alabaster, AL). Cholesterol and ammonium sulfate were purchased from JT Baker (Phillipsburg, NJ). Fetal bovine serum, Dulbecco's Modified Eagle's Medium (DME) and other reagents for cell culture were purchased from Mediatech (Manassa, VA). Doxorubicin was purchased from AvaChem Scientific (San Antonio, TX). Hispolon was obtained from Natsol Laboratories (Visakhapatnam, India). Tetrazolium bromide (MTT) was purchased from Calbiochem (Darmstadt, Germany). Polycarbonate membrane (0.08 μm) was purchased from Whatman (Maidstone, UK). Melanoma (B16BL6) cancer cells were obtained from American Type Culture Collection (Manassa, VA).

5.3. Methods

5.3.1. Empty liposomes preparation

Liposomes were prepared by thin-film hydration using a rotary evaporator as described by Kang et al (2015). Briefly, lipids were dissolved in chloroform at a lipid molar ratio of 9:5:1 for DSPC/ cholesterol/DSPE-mPEG (2000). The solution was flash evaporated on a rotavapor (Rotavapor, Büchi, Germany) under vacuum (about 25mmHg) at 65 ^{o}C, to form a thin film on the inner wall of the flask. The dry lipid film was then hydrated in 250 mM ammonium sulfate solution (pH 5.5). This mixture was then placed in a water-bath incubator (65 ^{o}C) for 30 min to form coarse liposomes. Seven liquid nitrogen freeze–thaw cycles above the phase transition temperature of the primary lipid prior to extrusion were applied. The liposome mixtures were then passed through 0.08 µm double-stacked polycarbonate filters using Lipex^{TM} 10 ml (Transferra Nanosciences Inc, Burnaby, BC. Canada) at 65 °C. The free ammonium sulfate was removed by dialysis (12, 000-14,000 Daltons molecular weight cut off dialysis tubing) against sucrose solution (10% w/v, 250 ml) at 4 ^{o}C. Sucrose medium was discarded and replaced with fresh medium after 1, 3, 6 h and then left overnight (Kang et al., 2015). Total phospholipid concentration of each formulation was quantified using an assay for inorganic phosphate following acid hydrolysis (Bartlett, 1959). The liposomes contained Coumarin-6 (1%) as a fluorescent dye for imaging.

5.3.2. Hispolon loading in liposomes

The liposomes were prepared according to Sadzuka et al. (2005) with slight modifications. Hispolon was dissolved in ethanol and the solvent was evaporated using

a rotary evaporator to form a hispolon thin film. Empty liposome suspension was added to the thin layer of hispolon to obtain 1:10 molar ratio of hispolon to lipid. Then, mixture was sonicated for 15 min at 65 ^{o} C using a high energy bath type sonicator and left to stand for an hour at room temperature before it was kept at 4^{o}C. The liposomes were then dialyzed against 10% sucrose to remove un-encapsulated drug.

5.3.3. Doxorubicin loading in liposomes

Doxorubicin liposome was prepared by a remote loading method which is based on the encapsulating of drugs using pH and electrochemical gradients (L. Chen, Alrbyawi, Poudel, Arnold, & Babu, 2019). Doxorubicin solution was prepared by dissolving the drug in 10% sucrose and adjusting the pH to 8 by 0.1N NaOH. This solution was added to the empty liposome at 0.2:1 drug-to-lipid ratios. The free drug was removed by dialysis.

5.3.4. Determination of encapsulation efficiency

The amount of encapsulated doxorubicin was determined spectrophotometrically at 480 nm after lysis of the liposomes with Triton X (1%). For hispolon encapsulation, methanol was used to break the liposomes and hispolon was determined spectrophotometrically at 424 nm. All experiments were run in triplicate and mean data were presented. The recovery (%) was calculated as:

$$\text{Recovery}(\%) = \frac{\text{Amount of drug in formulation/lipid}}{\text{Amount of drug used for formulation/lipid}} \times 100$$

5.3.5. Determination of particle size

Particle size and distribution of the liposomal formulations was carried out by dynamic light scattering using Nicomp 380 ZLS particle size analyzer (Particle Sizing Systems, Santa Barbara, CA). Mean particle size and polydispersity index after appropriate dilution were determined.

5.3.6. Determination of osmolality

Osmolality was analyzed by a vapor pressure osmometer (model K-7000 Knauer, Berlin, Germany). Before performing the analyses, the osmometer was calibrated with a solution of NaCl (400 mOsm). The determinations were made in triplicate at room temperature.

5.3.7. Determination of zeta potential

Measurements of liposome zeta potential were carried out by photon correlation spectroscopy (PCS, Zetatrac, Largo, FL, USA). For the analyses, formulations were diluted in an aqueous medium. All determinations were performed in triplicate at room temperature.

5.3.8. In vitro release

The release profile of doxorubicin and hispolon from liposome formulations were determined by dialysis. Liposome formulations (1ml) (1mM hispolon and 0.2 mM doxorubicin) were placed in dialysis tubing and dialyzed against phosphate buffered saline (PBS) pH 7.4 containing 0.05 % tween 80 for achieving sink conditios. All vials were incubated at 37 ^{o}C in a rotary shaker at 150 rpm. Samples were collected at 1, 3,

6,12, and 24 hours and replenished with fresh release medium. The concentration of doxorubicin and hispolon in the release medium were analyzed and the cumulative amount of each released versus time was plotted. All experiments were run in triplicate and mean data with S.E.M. were presented.

5.3.9. Cell culture

Melanoma (B16BL6) cells were cultured in Dulbecco's Modified Eagle's Medium (DMEM). Medium was supplemented with 10% fetal bovine serum (FBS), 100 U/ml penicillin, and 100 µg/ml streptomycin at 37 °C in a humidified atmosphere containing 5% CO_2. All experiments were performed at a confluence of 90 to 95%

5.3.10. Measurement of cytotoxicity by MTT assay

For cytotoxicity assessment, B16BL6 cells were cultured in flat-bottom 96-well plates for 24 hours. Cell density was 5×10^3 cells/well. Serial dilutions of doxorubicin or hispolon formulations were added to the cells with 10% FBS at 37°C in 5 % CO_2 for 48 hours. After 48 hours, 10 µl of 3-[4, 5-dimethylthiazol-2-yl]-2, 5-diphenyl tetrazolium bromide (MTT) was added to each well and the cells were incubated at 37 ^oC for an additional 2 hours. Finally, the medium was aspirated and 200 µl DMSO was added to each well to solubilize the dye remaining in the plates. The absorbance was measured using a microplate reader (spectramax M5, molecular devices, Sunnyvale, CA, USA) at 544 nm. All experiments were run in triplicate and mean data were presented.

5.3.11. Flow cytometric apoptosis analysis

To assess apoptosis, B16BL6 cells were seeded into 6-well plates at a density of 3.5 X 10^5 cells per well and incubated for 24 hours. The culture medium was replaced with medium containing 0.1 μM doxorubicin liposomes, 10 μM hispolon liposomes, or a mixture of both in 2 ml DMEM containing 10% FBS and incubated for 48 hour. Treated and untreated cells were stained as described in Annexin V FITC apoptosis detection Kit TD. Apoptotic cells were quantified by flow cytometry.

5.3.12. Fluorescence microscopy

B16BL6 cells were seeded in a flat bottom 24-well plate for 24 hours. Cells were then treated with coumarin-6 hispolon liposomes (10 μM), doxorubicin liposome (0.1 μM), or a mixture of both for 6 hours. Cells were washed and fixed (15 min in 4% (w/v) paraformaldehyde in PBS). Nuclei were stained with DAPI (4′,6-diamidino-2-phenylindole) for 10 min. All samples were examined with a fluorescence microscope (EVOS fl, ZP-PKGA-0494 REV A, USA) and photographed through a 20 X objective.

5.3.13. Statistical analysis

Doxorubicin and/or hispolon released from liposomes was plotted as a function of time (h). All the data were presented as mean ± S.E.M. Graph Pad Prism software was used to determine the SE and statistical levels of significance. All data were subjected to one-way analysis of variance (ANOVA) to determine the statistical levels of significance. P value less than 0.05 was considered to be statistically significant.

5.4. Results and Discussion:

5.4.1. Preparation of liposomes

The surface of the liposome can be modified and allowed for targeted liposome. Furthermore, long circulation liposome which is obtained by inclusion of PEG in liposome composition, makes the liposome more attractive drug delivery system since it will reduce the side effect and improve the therapeutic efficacy. In this study both hispolon and doxorubicin were loaded in liposome as follows.

5.4.2. Preparation of hispolon liposomes

There are many methods of liposome preparation based on the physical properties of the drugs. For hispolon liposomes, thin film hydration, which is the conventional and most common method for liposomes preparation, was attempted. We observed a very low recovery (26%) when 50% cholesterol, 90% DSPC and 10% DSPE-mPEG(2000) were used. Liposomes with 0% and 20% cholesterol were formulated to improve the EE. Cholesterol did not affect the EE of hispolon. Furthermore, liposomes with 0% and 5% with DSPE-mPEG (2000) were formulated and no effect on the EE was observed. Therefore, remote film loading was chosen to prepare hispolon liposome since it gives high encapsulation efficiency compared to thin film hydration (Sadzuka et al., 2005). Also, this technique increased the entrapment efficiency of several lipophilic drugs like solidus (Haeri et al., 2011), Valspar (Bajelan, Haeri, Vali, Ostad, & Dadashzadeh, 2012), and celecoxib (Perumal, Banerjee, Das, Sen, & Mandal, 2011).

5.4.3. Preparation of doxorubicin liposomes

Active loading is the most used method to encapsulate amphipathic weak basic drugs like doxorubicin. High encapsulation was obtained when doxorubicin was loaded using this method (Haran, Cohen, Bar, & Barenholz, 1993). Doxorubicin has amino groups and is lipophilic at high pH and hydrophilic at low pH. In active loading liposomes are initially prepared in a low pH solution to obtain a low pH within the core (Hood, Vreeland, & DeVoe, 2014). Doxorubicin is uncharged in a basic environment and able to transfer across the membrane. Due to the acid buffer the in core, drug is protonated and can no longer cross the bilayer membrane (Deamer, Prince, & Crofts, 1972). In our study, doxorubicin was actively loaded into core using ammonium sulfate.

5.4.4. Characterization of liposomal formulations

Table 5-1 shows the encapsulation efficiency, particle size, PI and zeta potential for liposomal formulations. Uniform particle size was obtained with high encapsulation efficiency and acceptable osmolality. The particle size and surface charge of the liposome affects liposome pharmacokinetics. Because liposomes have a particle size around 100-200 nm, they can accumulate in tumor sites as a result of enhanced permeability and retention. Immordino et al. (2006) reported that liposomes with particle sizes around 100 nm are preferred for tumor targeting. In our study, the average particle size was less than 100 nm and PI value was less than 0.2. The negative zeta potential for hispolon and doxorubicin liposomes (-44) was due to the presence of PEG-DSPE lipid.

5.4.5. In vitro release

Liposome helps to accumulate the drug at the tumor site and enhances permeability. However, in order for a drug to exert a biological effect, it has to be released from the formulation in a sustained manner (Charrois & Allen, 2004). Figure 5-1 shows the release profile for all formulations. The release profile for hispolon and doxorubicin solution reached ~100% within 3 and 6 hours, respectively. This confirmed that the dialysis membrane did not significantly hinder the release of those drugs. Doxorubicin liposome showed significantly slower release than solution. Doxorubicin released from liposomes after 24 hours was 71% and hispolon was 80.4%. The release profile for hispolon was faster than doxorubicin. Perhaps doxorubicin needed more time to release from the liposome bilayer.

Surface modification of liposomes with PEG reduces the release of drugs and showed a sustained release profile (Nag & Awasthi, 2013). It also forms a protective layer around the liposome which eliminates the faster liposome uptake by reticuloendothelial system (RES) by forming a protective layer around the liposomes (Nag & Awasthi, 2013; Yang et al., 2007; Drummond, Meyer, Hong, Kirpotin, & Papahadjopoulos, 1999). Another advantage of PEGylated liposomes is to reduce toxicity of doxorubicin, such as cardiotoxicity, due to expected low accumulation in cardiac tissue compared to doxorubicin solution (Gabizon, Shmeeda, & Barenholz, 2003).

5.4.6. Cell cytotoxicity

Hispolon is a polyphenolic compound known to induce ROS mediated apoptosis and cell cycle arrest (Y.-C. Chen et al., 2013). MTT assay was used to evaluate the

cytotoxicity effect of hispolon using melanoma cell line. As shown in Figure 5-2A, both hispolon liposome and solution showed similar cell cytotoxicity when cells were incubated with varied concentrations of hispolon (0.5, 1, 5,10, 30, and 50 μM) for 48 hours. The half maximal inhibitory concentration (IC50) for hispolon solution was 5 μM whereas that for hispolon in liposome formulation was 2.5 μM. There was a significant difference observed when cells were treated with the same concentration (5 μM) of hispolon solution and liposome (Figure 5-2B). This showed that loading hispolon in liposome improved drug cytotoxicity. Similar results has been reported for crocin (a carotenoid chemical compound found in the flowers crocus and gardenia) was loaded in liposome (Mousavi et al., 2011). Liposome may help drug enter cells by fusion or endocytosis (Akbarzadeh et al., 2013; Pagano & Weinstein, 1978).

Doxorubicin is an anticancer drug commonly used for treatment of many tumors such as breast cancer (Zheng, Hu, Sui, Ma, & Jiang, 2014), ovarian cancer (Shavit et al., 2014) and melanoma (J.-y. Zhao et al., 2015). Encapsulation of doxorubicin in liposomes reduces side effects and improves therapeutic efficacy. They also affect the pharmacokinetics and tissue distribution of the anti-cancer agent (Olusanya, Haj Ahmad, Ibegbu, Smith, & Elkordy, 2018).

As shown in Figure 5-3A, doxorubicin liposomes showed high cytotoxicity compared to the solution. The IC50 for liposome was 0.1 μM which is three times lower than the IC50 for the solution (0.3 μM). As presented in Figure 5-3B, there was a significant difference in cell cytotoxicity (0.1 μM) between doxorubicin liposome and solution. The liposome delivery system significantly enhanced the delivery of doxorubicin to cells.

The severe toxic side effects associated with conventional anticancer therapies limit the use of high doses of these drugs which might be required to eradicate cancer growth (Nurgali, Jagoe, & Abalo, 2018). Liposomes have been used to reduce the toxic effects and improve therapeutic efficacy. Rivera (2003) reported that PEGylated liposomal doxorubicin has showed similar efficacy to conventional doxorubicin therapy while improving the safety profile in patients with metastatic breast cancer.

Combination therapy is used to improve anticancer efficacy by combining two or more drugs with different mechanism of action and different toxicity profile. PEGylated liposomal doxorubicin in combination with different anticancer agents (cyclophosphamide, paclitaxel, docetaxel and gemcitabine) in breast cancer had a response rate of 33%-75% (Rivera, 2003). We studied the effect of coadminstration of doxorubicin and hispolon on cytotoxicity in B16BL6 cells. There was a significant increase in cell cytotoxicity with doxorubicin and hispolon coadminstration as compared to individual liposomes compounds as presented in Figure 5-4. The cell cytotoxicity of doxorubicin liposome, hispolon liposome and their combination was 54.8%, 29.5% and 14.3%, respectively. Several reports have shown enhanced cell cytotoxicity when two or more drugs were used in combination. There was a synergistic cell inhibition on breast cancer when doxorubicin was combined with lectin compared to either treatment alone (Hong, Park, & Lyu, 2014). Another study showed a significant enhancement of cell cytotoxicity for doxorubicin combined with resveratrol compared to doxorubicin alone (Washington, Kularatne, Biewer, & Stefan, 2018).

5.4.7. Flow cytometric apoptosis analysis

Figure 5-5 shows the apoptosis effect of the hispolon-doxorubicin combination. The percent of apoptotic cells (early and late) treated with hispolon liposome was 26.7% ± 1.67 which was significantly higher than non-treated cells. Our previous results showed that hispolon is a potent inducer of reactive oxygen species, inhibits the expression of B-cell lymphoma-2 protein (Bcl-2) gene, promotes the expression of Bcl-2-associated protein X (Bax) gene, promotes expression of caspase enzymes, inhibits complex I and IV, stimulates nitrite content and lipid peroxidation levels associated in cell death and apoptosis (Ahmed et al., 2019). Furthermore, a significantly higher percent of apoptotic cells were observed with doxorubicin liposome compared with non-treated cells (32.12% ± 7.3). Doxorubicin induces apoptosis in many cell cancers including melanoma (Brouckaert et al., 2004). Doxorubicin induce apoptosis is mainly due to the inhibition of topoisomerase II. Moreover, the percentage of apoptotic cells treated with combination therapy was 48.26% ± 8.4 which was significantly higher than monotherapy. These results indicated the potential enhancement of cancer therapy using a combination of doxorubicin and hispolon.

5.4.8. Cellular uptake

Figure 6 shows the cellular uptake of coumarin-6 liposome that contained hispolon or doxorubicin or mixture of both. The high accumulation of liposome in the cells indicates the efficiency of liposome as delivery system. This result correlates well with the high cytotoxicity of doxorubicin and hispolon when encapsulated in liposomes.

5.5. Conclusion

Co-delivery of doxorubicin and hispolon in a liposome formulation enhanced cell cytotoxicity as well as apoptosis more than individual liposome drug treatment. The combination of hispolon and chemotherapy could lower the toxicity of chemotherapy by allowing lower doses of toxic chemotherapeutic drugs. Our data suggest that the performance of doxorubicin liposomes can be synergistically improved by co-delivering with hispolon as a liposome formulation. As the co-delivery and combination therapy, it offers attractive possibilities for developing treatments that reduce toxic side effects of commonly used chemotherapeutic drugs.

Table 5-1 Characterization of liposomal formulations

Liposome	Particle diameter (nm)	Polydispersity Index (PI)	Zeta potential (mV)	Drug loading	Recovery
Doxorubicin	92 ± 1.6	0.134 ± 0.12	-44.5	1.89%	96.54%
Hispolon	91 ± 2.6	0.101 ± .08	-43.2	8.33%	91.61%

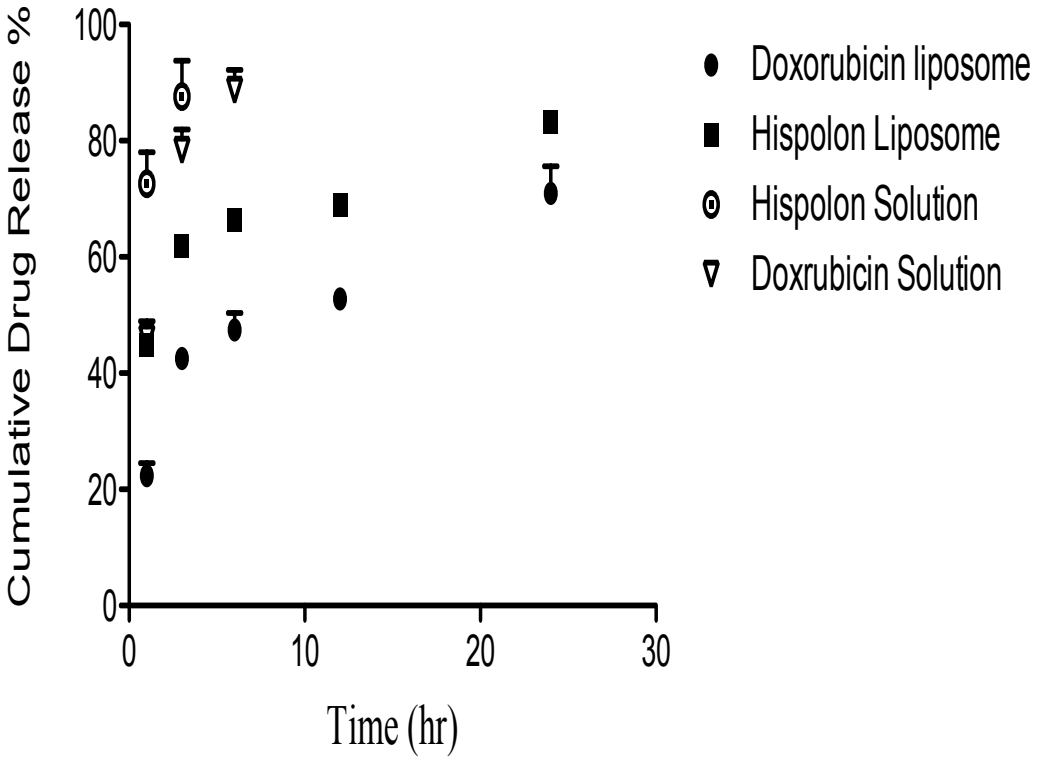

Figure 5-1 In vitro release of doxorubicin and hispolon formulations.

Mean ± S.E.M, n = 3

A

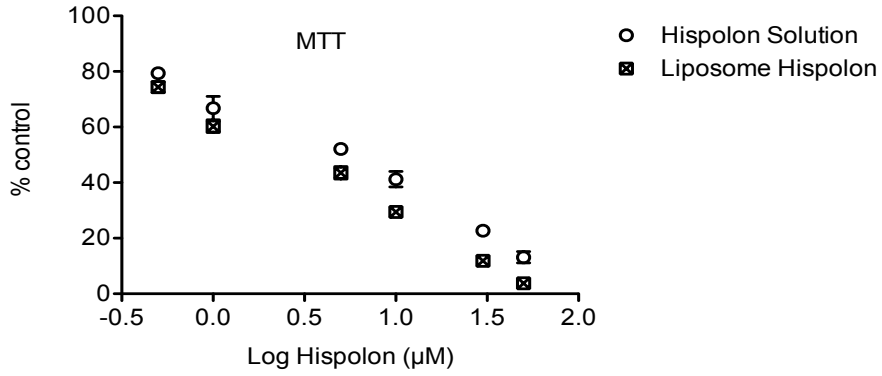

B

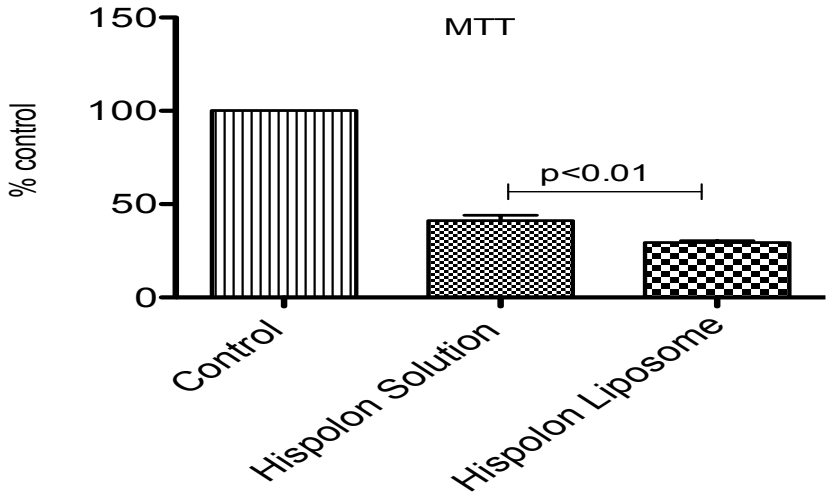

Figure 5-2 Hispolon liposome potentiates the cytotoxic effect in B16BL6 cell line.

Cells were incubated with various concentrations of liposomal formulations (0.5, 1, 5, 10, 30, and 50 μM) for 48 hours (2A). The 10 μM concentration of liposome formulations were compared to a positive control (solution) (2B). All data are expressed as mean percentages ± S.E.M. (n=3)

A

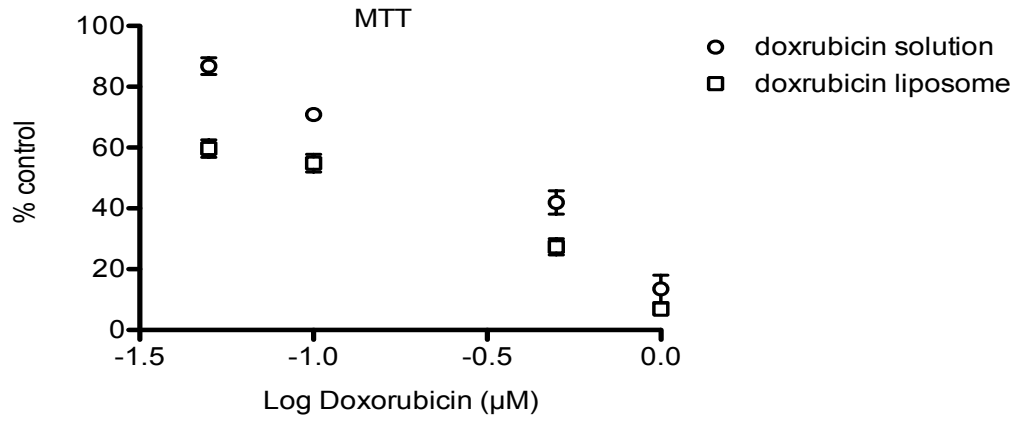

B

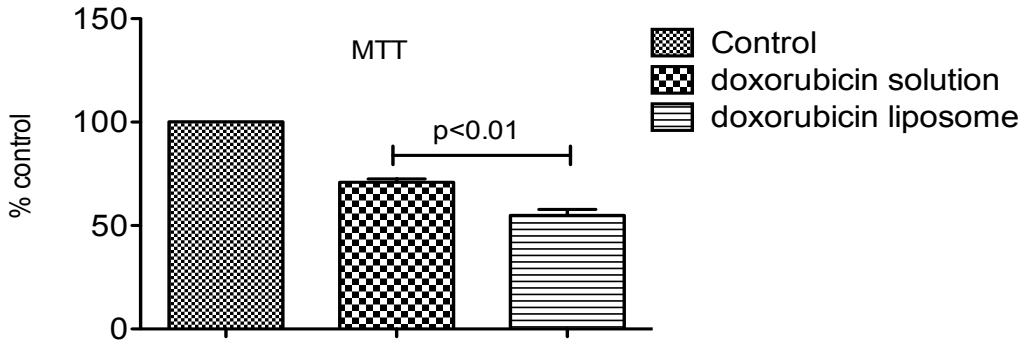

Figure 5-3 Doxorubicin liposome potentiates the cytotoxic effect in B16BL6 cell line. Cells were incubated with various concentrations of different Liposomal formulations (0.05, 0.1, 0.5, 1μM) for 48 hours (3A). The 0.1 μM concentration of liposome formulation was compared to a positive control (solution) (2B). All data are expressed as mean percentages ± S.E.M (n=3).

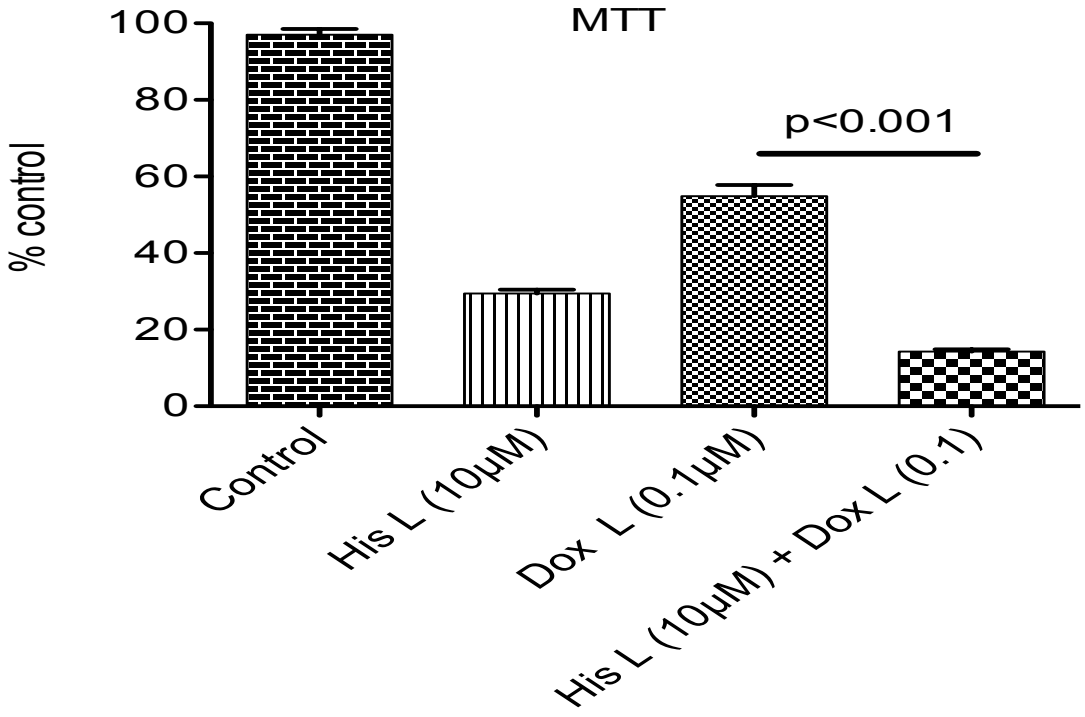

Figure 5-4 The effect of co-administration of doxorubicin liposome (0.1μm) and hispolon liposome (10μm) on B16BL6 cell cytotoxicity. All data are expressed as mean percentages ± S.E.M (n=3).

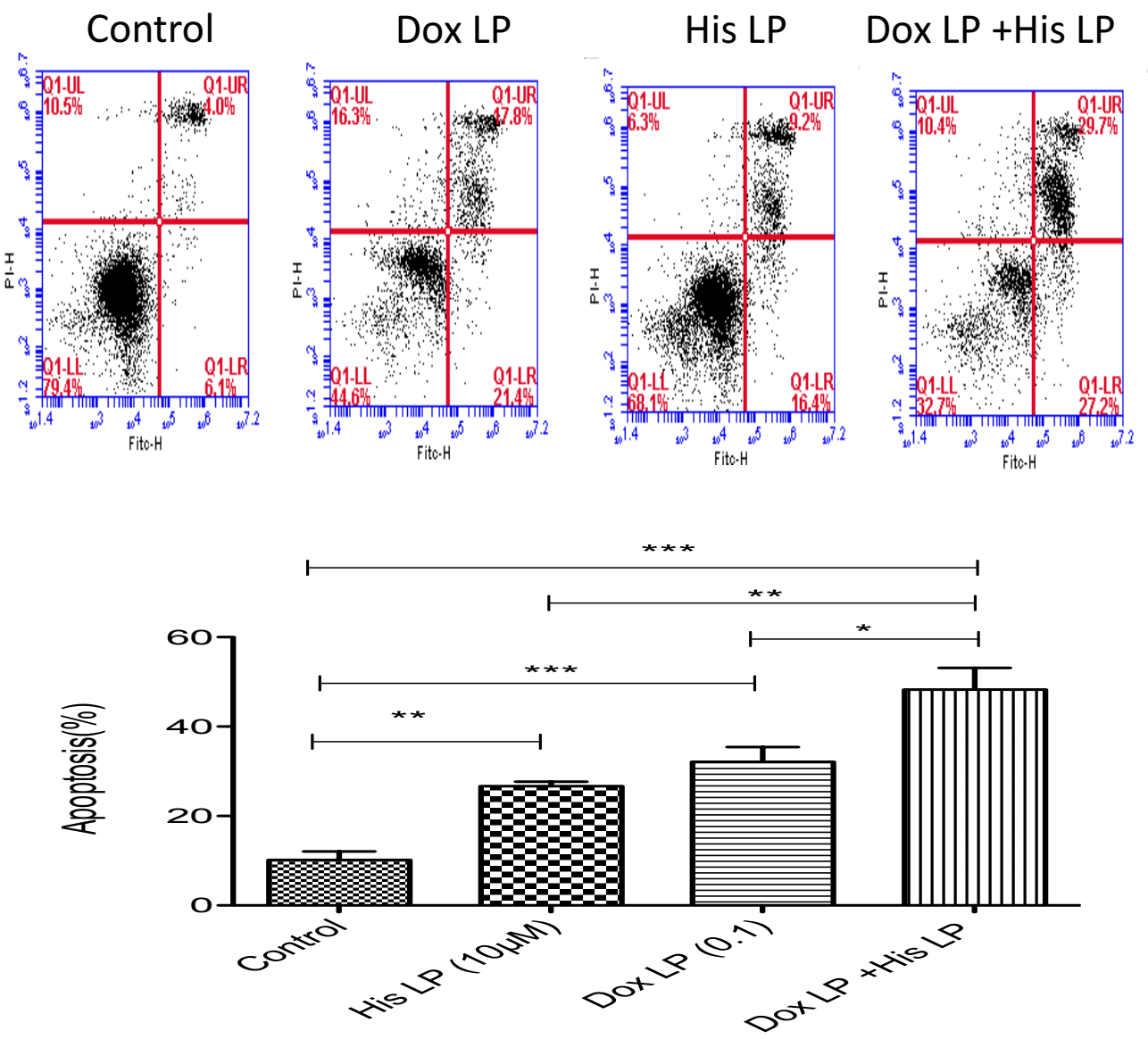

Figure 5-5 Apoptosis analysis of B16BL6 cells after 48 hour exposure to 10 μm hispolon liposome, 0.1 μm doxorubicin liposome and their combination. Cells were grown in 6 well plate and apoptotic cells were measured by flow cytometry after staining with Annexin-V and PI. All data were presented as the mean ±S.E.M (n=3). *p< 0.05, ** p<0.01 *** p<0.001

A

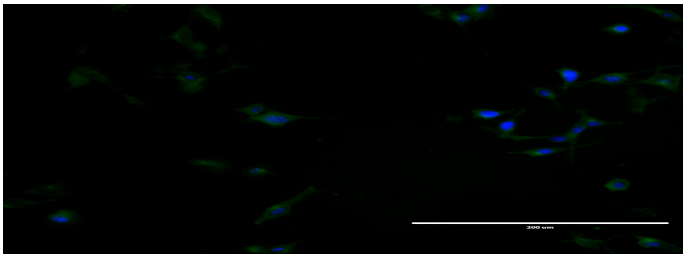

B

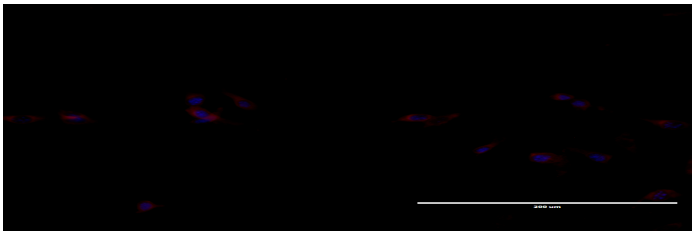

C

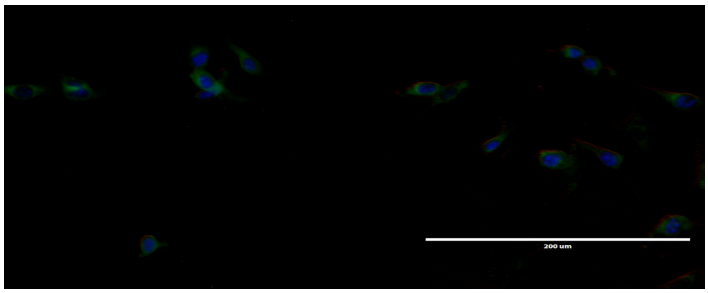

Figure 5-6 Liposome cellular uptake. B16BL6 cells were cultured for 24 hours then treated with (A) Doxorubicin liposome (0.1μM) (B) Coumarin-6-hispolon liposome (10μM) (C), or their combination. To obtain fluorescence images, NPs were visualized with 1% (w/w) coumarin-6.

5.6. References

Abraham, S., Waterhouse, D., Mayer, L., Cullis, P., Madden, T., & Bally, M. (2005). The liposomal formulation of doxorubicin. *Methods in Enzymology, 391*, 71-97.

Ahmed, A., Alhowail, A., Majrashi, M. A., Dhanasekaran, Murali,, Arnold, R., & Babu, R. J. (2019, April 18). *Cytotoxicity of Hispolon in Melanoma (B16BL6) Cell lines*. Poster session presented at Auburn University Symposium, Auburn, AL.

Akbarzadeh, A., Rezaei-Sadabady, R., Davaran, S., Joo, S. W., Zarghami, N., Hanifehpour, Y., . . . Nejati-Koshki, K. (2013). Liposome: classification, preparation, and applications. *Nanoscale Research Letters, 8*(1), 102-111.

Bajelan, E., Haeri, A., Vali, A. M., Ostad, S. N., & Dadashzadeh, S. (2012). Co-delivery of doxorubicin and PSC 833 (valspodar) by stealth nanoliposomes for efficient overcoming of multidrug resistance. *Journal of Pharmacy & Pharmaceutical Sciences, 15*(4), 568-582.

Bartlett, G. R. (1959). Phosphorus assay in column chromatography. *Journal Biological Chemistry, 234*(3), 466-468.

Bharath, A., & Turner, R. (2009). Impact of climate change on skin cancer. *Journal of the Royal Society of Medicine, 102*(6), 215-218.

Birben, E., Sahiner, U. M., Sackesen, C., Erzurum, S., & Kalayci, O. (2012). Oxidative stress and antioxidant defense. *World Allergy Organization Journal, 5*(1), 9-19.

Brouckaert, P., Takahashi, N., van Tiel, S. T., Hostens, J., Eggermont, A. M., Seynhaeve, A. L., . . . ten Hagen, T. L. (2004). Tumor necrosis factor-α augmented tumor response in B16BL6 melanoma-bearing mice treated with stealth liposomal

doxorubicin (Doxil®) correlates with altered Doxil® pharmacokinetics. *International Journal of Cancer, 109*(3), 442-448.

Charrois, G. J., & Allen, T. M. (2004). Drug release rate influences the pharmacokinetics, biodistribution, therapeutic activity, and toxicity of pegylated liposomal doxorubicin formulations in murine breast cancer. *Biochimica Et Biophysica Acta (BBA)-Biomembranes, 1663*(1-2), 167-177.

Chen, A. M., Zhang, M., Wei, D., Stueber, D., Taratula, O., Minko, T., & He, H. (2009). Co-delivery of doxorubicin and Bcl-2 siRNA by mesoporous silica nanoparticles enhances the efficacy of chemotherapy in multidrug-resistant cancer cells. *Small, 5*(23), 2673-2677.

Chen, L., Alrbyawi, H., Poudel, I., Arnold, R. D., & Babu, R. J. (2019). Co-delivery of Doxorubicin and Ceramide in a Liposomal Formulation Enhances Cytotoxicity in Murine B16BL6 Melanoma Cell Lines. *American Association of Pharmceutical Scientists PharmSciTech, 20*(3), 99-109.

Chen, Y.-C., Chang, H.-Y., Deng, J.-S., Chen, J.-J., Huang, S.-S., Lin, I.-H., . . . Huang, G.-J. (2013). Hispolon from Phellinus linteus induces G0/G1 cell cycle arrest and apoptosis in NB4 human leukaemia cells. *The American Journal of Chinese Medicine, 41*(06), 1439-1457.

Deamer, D. W., Prince, R. C., & Crofts, A. R. (1972). The response of fluorescent amines to pH gradients across liposome membranes. *Biochim Biophys Acta, 274*(2), 323-335.

Dong, X., & Mumper, R. J. (2010). Nanomedicinal strategies to treat multidrug-resistant tumors: Current progress. *Nanomedicine, 5*(4), 597-615.

Drummond, D. C., Meyer, O., Hong, K., Kirpotin, D. B., & Papahadjopoulos, D. (1999). Optimizing liposomes for delivery of chemotherapeutic agents to solid tumors. *Pharmacological Reviews, 51*(4), 691-743.

Gabizon, A., Shmeeda, H., & Barenholz, Y. (2003). Pharmacokinetics of pegylated liposomal doxorubicin: review of animal and human studies. *Clinical Pharmacokinetics*, *42*(5), 419-436.

Haeri, A., Sadeghian, S., Rabbani, S., Anvari, M. S., Boroumand, M. A., & Dadashzadeh, S. (2011). Use of remote film loading methodology to entrap sirolimus into liposomes: preparation, characterization and in vivo efficacy for treatment of restenosis. *International Journal of Pharmaceutics, 414*(1-2), 16-27.

Haran, G., Cohen, R., Bar, L. K., & Barenholz, Y. (1993). Transmembrane ammonium sulfate gradients in liposomes produce efficient and stable entrapment of amphipathic weak bases. *Biochimica Et Biophysica Acta (BBA)-Biomembranes, 1151*(2), 201-215.

Harris, P. A., Garai, A. S., & Valenzuela, M. A. (1975). Reduction of doxorubicin (adriamycin) bone marrow toxicity. *Journal of Pharmaceutical Sciences, 64*(9), 1574-1576.

Hong, C.-E., Park, A.-K., & Lyu, S.-Y. (2014). Synergistic anticancer effects of lectin and doxorubicin in breast cancer cells. *Molecular and Cellular Biochemistry, 394*(1-2), 225-235.

Hood, R. R., Vreeland, W. N., & DeVoe, D. L. (2014). Microfluidic remote loading for rapid single-step liposomal drug preparation. *Lab on a Chip*, *14*(17), 3359-3367.

Hsieh, M.-J., Chien, S.-Y., Chou, Y.-E., Chen, C.-J., Chen, J., & Chen, M.-K. (2014). Hispolon from phellinus linteus possesses mediate caspases activation and induces human nasopharyngeal carcinomas cells apoptosis through ERK1/2, JNK1/2 and p38 MAPK pathway. *Phytomedicine, 21*(12), 1746-1752.

Huang, G.-J., Yang, C.-M., Chang, Y.-S., Amagaya, S., Wang, H.-C., Hou, W.-C., . . . Hu, M.-L. (2010). Hispolon suppresses SK-Hep1 human hepatoma cell metastasis by inhibiting matrix metalloproteinase-2/9 and urokinase-plasminogen activator through the PI3K/Akt and ERK signaling pathways. *Journal of Agricultural and Food Chemistry, 58*(17), 9468-9475.

Immordino, M. L., Dosio, F., & Cattel, L. (2006). Stealth liposomes: review of the basic science, rationale, and clinical applications, existing and potential. *International Journal of Nanomedicine, 1*(3), 297-315.

Kang, J. Y., Eggert, M., Mouli, S., Aljuffali, I., Fu, X., Nie, B., . . . May, S. W. (2015). Pharmacokinetics, antitumor and cardioprotective effects of liposome-encapsulated phenylaminoethyl selenide in human prostate cancer rodent models. *Pharmaceutical Research, 32*(3), 852-862.

Kim, J. H., Kim, Y. C., & Park, B. (2016). Hispolon from Phellinus linteus induces apoptosis and sensitizes human cancer cells to the tumor necrosis factor-related apoptosis-inducing ligand through upregulation of death receptors. *Oncology Reports, 35*(2), 1020-1026.

Klefström, P., Gröhn, P., Heinonen, E., Holsti, L., & Holsti, P. (1987). Adjuvant postoperative radiotherapy, chemotherapy, and immunotherapy in stage III breast cancer. II. 5-year results and influence of levamisole. *Cancer, 60*(5), 936-942.

Lila, A. S. A., & Ishida, T. (2017). Liposomal delivery systems: Design optimization and current applications. *Biological and Pharmaceutical Bulletin, 40*(1), 1-10.

McGowan, J. V., Chung, R., Maulik, A., Piotrowska, I., Walker, J. M., & Yellon, D. M. (2017). Anthracycline chemotherapy and cardiotoxicity. *Cardiovascular Drugs and Therapy, 31*(1), 63-75.

Mousavi, S. H., Moallem, S. A., Mehri, S., Shahsavand, S., Nassirli, H., & Malaekeh-Nikouei, B. (2011). Improvement of cytotoxic and apoptogenic properties of crocin in cancer cell lines by its nanoliposomal form. *Pharmaceutical Biology, 49*(10), 1039-1045.

Nag, O. K., & Awasthi, V. (2013). Surface engineering of liposomes for stealth behavior. *Pharmaceutics, 5*(4), 542-569.

Nielsen, D., Maare, C., & Skovsgaard, T. (1996). Cellular resistance to anthracyclines. *General Pharmacology: The Vascular System, 27*(2), 251-255.

Nurgali, K., Jagoe, R. T., & Abalo, R. (2018). Editorial: Adverse effects of cancer chemotherapy: Anything new to improve tolerance and reduce sequelae? *Frontiers in Pharmacology, 9*, 245-248.

Olusanya, T. O. B., Haj Ahmad, R. R., Ibegbu, D. M., Smith, J. R., & Elkordy, A. A. (2018). Liposomal drug delivery systems and anticancer drugs. *Molecules, 23*(4), 907-1024.

Pagano, R. E., & Weinstein, J. N. (1978). Interactions of liposomes with mammalian cells. *Annual Review of Biophysics and Bioengineering, 7*(1), 435-468.

Perumal, V., Banerjee, S., Das, S., Sen, R., & Mandal, M. (2011). Effect of liposomal celecoxib on proliferation of colon cancer cell and inhibition of DMBA-induced tumor in rat model. *Cancer Nanotechnology, 2*(1), 67-79.

Rivera, E. (2003). Liposomal anthracyclines in metastatic breast cancer: Clinical update. *The Oncologist, 8*(Supplement 2), 3-9.

Sadzuka, Y., Takabe, H., & Sonobe, T. (2005). Liposomalization of SN-38 as active metabolite of CPT-11. *Journal of Controlled Release, 108*(2-3), 453-459.

Safra, T. (2003). Cardiac safety of liposomal anthracyclines. *The Oncologist, 8*(Supplement 2), 17-24.

Sercombe, L., Veerati, T., Moheimani, F., Wu, S. Y., Sood, A. K., & Hua, S. (2015). Advances and challenges of liposome assisted drug delivery. *Frontiers in Pharmacology, 6*, 286-299.

Sharma, G., Tyagi, A. K., Singh, R. P., Chan, D. C., & Agarwal, R. (2004). Synergistic anti-cancer effects of grape seed extract and conventional cytotoxic agent doxorubicin against human breast carcinoma cells. *Breast Cancer Research and Treatment, 85*(1), 1-12.

Shavit, L., Lifschitz, M. D., Gabizon, A., Kwa, M., Muggia, F., & Slotki, I. (2014). Pegylated liposomal doxorubicin and renal thrombotic microangiopathy: an under-recognized complication of prolonged treatment for ovarian cancer. *Kidney International, 85*(1), 213.

Wang, S., Ren, W., Liu, J., Lahat, G., Torres, K., Lopez, G., . . . Bankson, J. (2010). TRAIL and doxorubicin combination induces proapoptotic and antiangiogenic effects in soft tissue sarcoma in vivo. *Clinical Cancer Research, 16*(9), 2591-2604.

Washington, K. E., Kularatne, R. N., Biewer, M. C., & Stefan, M. C. (2018). Combination loading of doxorubicin and resveratrol in polymeric micelles for increased loading efficiency and efficacy. *ACS Biomaterials Science & Engineering, 4*(3), 997-1004.

Wu, Q., Kang, Y., Zhang, H., Wang, H., Liu, Y., & Wang, J. (2014). The anticancer effects of hispolon on lung cancer cells. *Biochemical and Biophysical Research Communications, 453*(3), 385-391.

Yang, T., Cui, F. D., Choi, M. K., Cho, J. W., Chung, S. J., Shim, C. K., & Kim, D. D. (2007). Enhanced solubility and stability of PEGylated liposomal paclitaxel: In vitro and in vivo evaluation. *International Journal of Pharmaceutics, 338*(1-2), 317-326.

Zhang, Y., Yang, C., Wang, W., Liu, J., Liu, Q., Huang, F., . . . Kong, D. (2016). Co-delivery of doxorubicin and curcumin by pH-sensitive prodrug nanoparticle for combination therapy of cancer. *Scientific Reports, 6*, 21225-21237.

Zhao, J.-y., Ma, X.-l., Li, Z.-m., Deng, R., Wang, S.-m., Shen, G.-b., . . . Wei, Y.-q. (2015). Down-regulation of MFG-E8 by RNA interference combined with doxorubicin triggers melanoma destruction. *Clinical and Experimental Medicine, 15*(2), 127-135.

Zhao, Z., Sun, Y.-S., Chen, W., Lv, L.-X., & Li, Y.-Q. (2016). Hispolon inhibits breast cancer cell migration by reversal of epithelial-to-mesenchymal transition via suppressing the ROS/ERK/Slug/E-cadherin pathway. *Oncology Reports, 35*(2), 896-904.

Zheng, R.-R., Hu, W., Sui, C.-G., Ma, N., & Jiang, Y.-H. (2014). Effects of doxorubicin and gemcitabine on the induction of apoptosis in breast cancer cells. *Oncology Reports, 32*(6), 2719-2725.

Chapter 6 : Summary and future work

This dissertation developed different lipid based delivery systems, such as microemulsions, proniosomes, and liposomes for treatment of melanoma. Hydroxytyrosol is a well known antioxidant. Formulation development of hydroxytyrosol (HT) has not been studied. Transdermal delivery of hydroxytyrosol is proposed due to extensive hepatic metabolism that after oral delivery. Proniosome was used to enhance the skin permeation for hydroxytyrosol. Various factors affecting skin permeation and skin retention of hydroxytyrosol from proniosomes, such as amount of surfactant and water content, were investigated. The human skin permeation and retention for hydroxytyrosol was improved for all proniosomes formulation. The formulation with 10% water and 45% span 60 exhibited 10-fold higher transdermal flux than the control. Future work will focus on the formulation efficacy in tumor bearing mice and mice with UV damage.

Microemulsions were developed for enhanced transdermal delivery of DAB. Pseudo-ternary phase diagram was used to select the microemulsion formulations. All formulations showed uniform particle size with an acceptable pH value. Skin retention for all the formulations were also higher than the control. All the optimized formulations showed a significant increase in cell cytotoxicity with low IC50 value. For future study, the efficacy of the formulations should be tested in both tumor bearing mice and mice with UV damaged skin.

Hispolon anti-cancer effect has been reported in many types of tumors, but is limited in melanoma. We studied the anti-cancer activity of hispolon against melanoma. Hispolon increase cell cytotoxicity with IC50 around 5 μM. Hispolon is a potent inducer of reactive oxygen species, inhibits the expression of bcl-2 gene, promotes the expression

of Bax gene, promotes expression of caspase enzymes; inhibits complex I and IV, stimulates nitrite content and lipid peroxidation levels. All of these are associated with apoptosis cell death.

The effect of co-administration of doxorubicin liposome and hispolon liposome was investigated. Both liposomes were prepared by dry film hydration and extrusion with subsequent remote loading of doxorubicin or hispolon. Administration of both liposome doxorubicin and liposome hispolon enhanced cell death as well as apoptosis more than liposome loaded with doxorubicin alone. Such co-administration could serve as a promising therapeutic approach to improve clinical outcomes against melanoma. For future work, the efficacy of the formulations will be conducted in tumor bearing mice.